AD_____

Award Number: W81XWH-05-1-0035

TITLE: A Double Selection Approach to Achieve Specific Expression of Toxin Genes for Ovarian Cancer Gene Therapy

PRINCIPAL INVESTIGATOR: David T. Curiel, M.D., Ph.D.
Gene Siegal, M.D., Ph..D.
Minghui Wang, M.D.

CONTRACTING ORGANIZATION: University of Alabama at Birmingham
Birmingham, AL 35294-0111

REPORT DATE: November 2005

TYPE OF REPORT: Annual

PREPARED FOR: U.S. Army Medical Research and Materiel Command
Fort Detrick, Maryland 21702-5012

REPORT DOCUMENTATION PAGE

Form Approved
OMB No. 0704-0188

1. REPORT DATE *(DD-MM-YYYY)*	2. REPORT TYPE	3. DATES COVERED *(From - To)*
01-11-2005	Annual	1 Nov 04 – 31 Oct 05

4. TITLE AND SUBTITLE
A Double Selection Approach to Achieve Specific Expression of Toxin Genes for Ovarian Cancer Gene Therapy

5a. CONTRACT NUMBER

5b. GRANT NUMBER
W81XWH-05-1-0035

5c. PROGRAM ELEMENT NUMBER

6. AUTHOR(S)
David T. Curiel, M.D., Ph.D.
Gene Siegal, M.D., Ph..D.
Minghui Wang, M.D.

E-Mail: david.curiel@ccc.uab.edu

5d. PROJECT NUMBER

5e. TASK NUMBER

5f. WORK UNIT NUMBER

7. PERFORMING ORGANIZATION NAME(S) AND ADDRESS(ES)
University of Alabama at Birmingham
Birmingham, AL 35294-0111

8. PERFORMING ORGANIZATION REPORT NUMBER

9. SPONSORING / MONITORING AGENCY NAME(S) AND ADDRESS(ES)
U.S. Army Medical Research and Materiel Command
Fort Detrick, Maryland 21702-5012

10. SPONSOR/MONITOR'S ACRONYM(S)

11. SPONSOR/MONITOR'S REPORT NUMBER(S)

12. DISTRIBUTION / AVAILABILITY STATEMENT
Approved for Public Release; Distribution Unlimited

13. SUPPLEMENTARY NOTES
Original contains color plates: All DTIC reproductions will be in black and white.

14. ABSTRACT

Gene therapy is a novel treatment modality which offers great potential for the control of carcinoma of the ovary. The efficacy of such approaches, however, is currently limited due to the inability of available gene delivery vehicles (vectors) to achieve efficient and selective gene transfer to target tumor cells. Proposed herein is a strategy to modify one candidate vector, recombinant adenovirus, such that it embodies the requisite properties of efficacy and specificity required for ovarian cancer gene therapy. This approach is based on targeting the delivered anti-cancer gene to tumor via two complimentary approaches. This approach is based upon restricting the expression of the anti-cancer gene exclusively to ovarian cancer tumor cells ("transcriptional targeting") plus directing the binding of the viral vector particle exclusively to tumor cells ("transductional targeting"). This "double targeting" approach is highly novel. We hypothesize that the vector improvements we propose herein will allow an improvement in the therapeutic index achievable by ovarian cancer gent therapy. Further, these strategies, if shown to be efficient efficacious here, have the potential to be rapidly translated into the clinical context. In this regard, our group has gained NIH regulatory approval and support for the employment of targeted vectors for ovarian cancer. We are thus familiar with the upscaling and regulatory aspects of clinical translation of novel gene therapy approaches. The double targeting approach we propose will allow us to illustrate key "proof-of-principle" in a stringent animal model of cancer of the ovary. This data will provide the rationale to endeavor a human clinical trial on this basis. In this event, our experience and infrastructure can function to foster the most rapid possible transitioning of this strategy to the context of Phase I human clinical trials for carcinoma of the ovary.

15. SUBJECT TERMS
Ovarian cancer, targeting, gene therapy

16. SECURITY CLASSIFICATION OF:			17. LIMITATION OF ABSTRACT	18. NUMBER OF PAGES	19a. NAME OF RESPONSIBLE PERSON
a. REPORT	b. ABSTRACT	c. THIS PAGE			USAMRMC
U	U	U	UU	81	19b. TELEPHONE NUMBER *(include area code)*

Table of Contents

Introduction

Ovarian cancer is one of the most common causes of cancer death in women. In large part this is due to the late presentation of the disease. On this basis, it is clear novel therapeutic approaches are warranted. In this regard, gene therapy represents one such novel approach which may be applied in the context of carcinoma of the ovary. For this technique to be successful clinically, highly efficient gene delivery vectors are necessary to deliver therapeutic genes specifically to tumor cells. Tropism-modified adenoviral vectors are the best agent for cell-specific gene delivery. Ovarian cancer-specific markers have been described, such as mesothelin, claudin 4, CD40, which can be exploited as a means to achieve specific infection via "transductional targeting". The specificity of gene expression can be further improved by placing the gene under the control of an ovarian cancer-specific promoter via a "transcriptional targeting" approach. This "double-targeting" strategy achieves a synergistic improvement in specificity, thus enabling a therapeutic result to be obtained.

This project seeks to develop an optimized gene delivery system based on a combination of the best available transductional and transcriptional targeting approaches for ovarian cancer. This system should result in highly efficient and specific expression of toxin encoding genes in tumor cells, enabling these cells to be selectivity eradicated and thus offering a novel technique for the achievement of ovarian cancer gene therapy.

Body

In this initial period of funding we sought to identify candidate ovarian cancer tumor selective promoters (TSP) to achieve transcriptional targeting. The ideal profile of a useful ovarian cancer TSP is inducibility in target tumor cells and non-inducibility in the liver ("tumor on/liver off") (2, 3). This is based on the concept that the intrinsic hepatotropism of Ad requires the means to mitigate expression of vector-induced transgene delivery to that site (1). Our initial survey identified the promoter regions of the genes survivin (4), secretory leukoprotease inhibition (SLPI) (5) and mesothelin (6) as potentially useful in this regard. On this basis, we constructed adenoviral vectors (Ad) containing the candidate ovarian cancer TSPs. Rescued vectors were propagated and validated by molecular analysis.

We next sought to evaluate the candidate targeted Ads *in vitro*. Whereas initial screening could be endeavored via employment of immortalized human tumor cell lines, this analysis was suboptimal in several aspects. First, immortalized cell lines may not reflect with fidelity the gene expression profile of primary tumors (7). In addition, we also sought to determine the "liver off" profile of candidate TSPs to fully establish potential functional utility. On this basis we developed an assay method based on employment of tissue slice material (8, 9). This employment of primary material allowed stringent assessment of promoter function in target and non-target tissues. Employment of this assay has allowed us to characterize the candidate ovarian cancer TSPs with an upredicated level of stringency and to rank their utility for our targeting goals.

We have also begun to employ the defined ovarian cancer TSPs for initial proof-of-principle studies to validate the gains which may accrue via our double targeting strategy. In this regard, we have recently defined a method of transductional targeting based on fiber knob serotype chimerism (10, 11). In this approach, replacement of fiber knob of adenovirus serotype 5 with the corresponding knob region of an alternate adenovirus (human serotype chimera or xenotype adenovirus) allows for target cell infection via non-native cellular entry pathways (12). This is a critical capacity which thereby allows derived Ads to circumvent the deficiency of the Ad5 receptor CAR which is frequently present on ovarian cancer targets (13). Our studies thereby initially employed our candidate ovarian cancer TSPs for transcriptional targeting in combination with knob serotype chimerism for transductional targeting. These studies validated the synergistic gains in tumor selectivity which could be achieved via our double targeting approach (14).

Key Research Accomplishments

- Adenoviral vectors were derived which embody transcriptional targeting via candidate ovarian cancer tumor selective promoters (TSPs)

- Development of a novel substrate assay system for evaluation of ovarian cancer targeting based upon "tissue slice" method

- Validation of utility of candidate ovarian cancer TSPs derived from promoter regions of genes for survivin, secretory leukoprotease inhibitor and mesothelin

- Demonstration of targeting gains via double targeting approach based upon defined ovarian cancer TSP transcriptional targeting and transductional targeting with fiber knob serotype chimerism.

Reportable Outcomes

1. Tsuruta Y, Pereboeva L, Glasgow JN, Luongo CL, Komarova S, Kawakami Y, Curiel DT. Reovirus sigma1 fiber incorporated into adenovirus serotype 5 enhances infectivity via a CAR-independent pathway. Biochem Biophys Res Commun. 2005 Sep 16;335(1):205-14.

2. Stoff-Khalili MA, Rivera AA, Glasgow JN, Le LP, Stoff A, Everts M, Tsuruta Y, Kawakami Y, Bauerschmitz GJ, Mathis JM, Pereboeva L, Seigal GP, Dall P, Curiel DT. A human adenoviral vector with a chimeric fiber from canine adenovirus type 1 results in novel expanded tropism for cancer gene therapy. Gene Ther. 2005 Dec;12(23):1696-706.

3. Nakayama M, Both GW, Banizs B, Tsuruta Y, Yamamoto S, Kawakami Y, Douglas JT, Tani K, Curiel DT, Glasgow JN. An adenovirus serotype 5 vector with fibers derived from ovine atadenovirus demonstrates CAR-independent tropism and unique biodistribution in mice. Virology. 2005. Submitted.

4. Le LP, Le HN, Dmitriev IP, Davydova JG, Gavrikova T, Yamamoto S, Curiell DT, Yamamoto Y. Dynamic monitoring of oncolytkc adenovirus in vivo by genetic capsid labeling. JNCI. 2005. In Press.

Conclusion

Our progress in the first year of this award has validated our central concept – double targeting can improve tumor selective gene delivery to ovarian cancer targets. We have established the utility of several candidate TSPs for ovarian cancer transcriptional targeting via a novel stringent substrate assay method. We have show that these transcriptional targeting methods may be combined with adenoviral transductional targeting strategies to obtain synergistic gains vis à vis selective gene delivery to ovarian cancer tumor cells.

References

1. Stoff-Khalili MA, Dall P, Curiel DT. From gene therapy to virotherapy for ovarian cancer. Minerva Ginecol. 2004 Dec;56(6):503-14. Review.

2. Zhu ZB, Makhija SK, Lu B, Wang M, Kaliberova L, Liu B, Rivera AA, Nettelbeck DM, Mahasreshti PJ, Leath CA 3rd, Yamaoto M, Alvarez RD, Curiel DT. Transcriptional targeting of adenoviral vector through the CXCR4 tumor-specific promoter. Gene Ther. 2004 Apr;11(7):645-8.

3. Casado E, Nettelbeck DM, Gomez-Navarro J, Hemminki A, Gonzalez Baron M, Siegal GP, Barnes MN, Alvarez RD, Curiel DT. Transcriptional targeting for ovarian cancer gene therapy. Gynecol Oncol. 2001 Aug;82(2):229-37. Review.

4. Zhu ZB, Makhija SK, Lu B, Wang M, Kaliberova L, Liu B, Rivera AA, Nettelbeck DM, Mahasreshti PJ, Leath CA, Barker S, Yamaoto M, Li F, Alvarez RD, Curiel DT. Transcriptional targeting of tumors with a novel tumor-specific survivin promoter. Cancer Gene Ther. 2004 Apr;11(4):256-62.

5. Barker SD, Coolidge CJ, Kanerva A, Hakkarainen T, Yamamoto M, Liu B, Rivera AA, Bhoola SM, Barnes MN, Alvarez RD, Curiel DT, Hemminki A. The secretory leukoprotease inhibitor (SLPI) promoter for ovarian cancer gene therapy. J Gene Med. 2003 Apr;5(4):300-10.

6. Breidenbach M, Rein DT, Everts M, Glasgow JN, Wang M, Passineau MJ, Alvarez RD, Korokhov N, Curiel DT. Mesothelin-mediated targeting of adenoviral vectors for ovarian cancer genetherapy. Gene Ther. 2005 Jan;12(2):187-93.

7. Kelly FJ, Miller CR, Buchsbaum DJ, Gomez-Navarro J, Barnes MN, Alvarez RD, Curiel DT. Selectivity of TAG-72-targeted adenovirus gene transfer to primary ovarian carcinoma cells versus autologous mesothelial cells in vitro. Clin Cancer Res. 2000 Nov;6(11):4323-33.

8. Kirby TO, Rivera A, Rein D, Wang M, Ulasov I, Breidenbach M, Kataram M, Contreras JL, Krumdieck C, Yamamoto M, Rots MG, Haisma HJ, Alvarez RD, Mahasreshti PJ, Curiel DT. A novel ex vivo model system for evaluation of conditionally replicative adenoviruses therapeutic efficacy and toxicity. Clin Cancer Res. 2004 Dec 15;10(24):8697-703.

9. Rots MG, Elferink MG, Gommans WM, Oosterhuis D, Schalk JA, Curiel DT, Olinga P, Haisma HJ, Groothuis GM. An ex vivo human model system to evaluate specificity of replicating andnon-replicating gene therapy agents. J Gene Med. 2005 Jul 26;8(1):35-41 [Epub ahead of print]

10. Kanerva A, Mikheeva GV, Krasnykh V, Coolidge CJ, Lam JT, Mahasreshti PJ, Barker SD, Straughn M, Barnes MN, Alvarez RD, Hemminki A, Curiel DT. Targeting adenovirus to the serotype 3 receptor increases gene transfer efficiency to ovarian cancer cells. Clin Cancer Res. 2002 Jan;8(1):275-80.

11. Lam JT, Kanerva A, Bauerschmitz GJ, Takayama K, Suzuki K, Yamamoto M, Bhoola SM, Liu B, Wang M, Barnes MN, Alvarez RD, Siegal GP, Curiel DT, Hemminki A. Inter-patient variation in efficacy of five oncolytic adenovirus candidates for ovarian cancer therapy. J Gene Med. 2004 Dec;6(12):1333-42.

12. Wu H, Han T, Lam JT, Leath CA, Dmitriev I, Kashentseva E, Barnes MN, Alvarez RD, Curiel DT. Preclinical evaluation of a class of infectivity-enhanced adenoviral vectors in ovarian cancer gene therapy. Gene Ther. 2004 May;11(10):874-8.

13. Kim M, Zinn KR, Barnett BG, Sumerel LA, Krasnykh V, Curiel DT, Douglas JT. The therapeutic efficacy of adenoviral vectors for cancer gene therapy is limited by a low level of primary adenovirus receptors on tumour cells. Eur J Cancer. 2002 Sep;38(14):1917-26.

14. Rein DT, Breidenbach M, Kirby TO, Han T, Siegal GP, Bauerschmitz GJ, Wang M, Nettelbeck DM, Tsuruta Y, Yamamoto M, Dall P, Hemminki A, Curiel DT. A fiber-modified, secretory leukoprotease inhibitor promoter-based conditionally replicating adenovirus for treatment of ovarian cancer. Clin Cancer Res. 2005 Feb 1;11(3):1327-35.

Appendices

1. Tsuruta Y, Pereboeva L, Glasgow JN, Luongo CL, Komarova S, Kawakami Y, Curiel DT. Reovirus sigma1 fiber incorporated into adenovirus serotype 5 enhances infectivity via a CAR-independent pathway. Biochem Biophys Res Commun. 2005 Sep 16;335(1):205-14.

2. Stoff-Khalili MA, Rivera AA, Glasgow JN, Le LP, Stoff A, Everts M, Tsuruta Y, Kawakami Y, Bauerschmitz GJ, Mathis JM, Pereboeva L, Seigal GP, Dall P, Curiel DT. A human adenoviral vector with a chimeric fiber from canine adenovirus type 1 results in novel expanded tropism for cancer gene therapy. Gene Ther. 2005 Dec;12(23):1696-706.

3. Nakayama M, Both GW, Banizs B, Tsuruta Y, Yamamoto S, Kawakami Y, Douglas JT, Tani K, Curiel DT, Glasgow JN. An adenovirus serotype 5 vector with fibers derived from ovine atadenovirus demonstrates CAR-independent tropism and unique biodistribution in mice. Virology. 2005. Submitted.

4. Le LP, Le HN, Dmitriev IP, Davydova JG, Gavrikova T, Yamamoto S, Curiell DT, Yamamoto Y. Dynamic monitoring of oncolytkc adenovirus in vivo by genetic capsid labeling. JNCI. 2005. In Press.

APPENDIX 1

Available online at www.sciencedirect.com

SCIENCE DIRECT

ELSEVIER

Biochemical and Biophysical Research Communications 335 (2005) 205–214

BBRC

www.elsevier.com/locate/ybbrc

Reovirus σ1 fiber incorporated into adenovirus serotype 5 enhances infectivity via a CAR-independent pathway

Yuko Tsuruta [a], Larisa Pereboeva [a], Joel N. Glasgow [a], Cindy L. Luongo [b], Svetlana Komarova [a], Yosuke Kawakami [a], David T. Curiel [a,*]

[a] *Division of Human Gene Therapy, Departments of Medicine, Pathology, and Surgery, and The Gene Therapy Center, The University of Alabama at Birmingham, Birmingham, AL 35294, USA*

[b] *Department of Microbiology, The University of Alabama at Birmingham, Birmingham, AL 35294, USA*

Received 23 June 2005

Available online 25 July 2005

Abstract

Adenovirus serotype 5 (Ad5) has been used for gene therapy with limited success because of insufficient infectivity in cells with low expression of the primary receptor, the coxsackie and adenovirus receptor (CAR). To enhance infectivity in tissues with low CAR expression, tropism expansion is required via non-CAR pathways. Serotype 3 Dearing reovirus utilizes a fiber-like σ1 protein to infect cells expressing sialic acid and junction adhesion molecule 1 (JAM1). We hypothesized that replacement of the Ad5 fiber with σ1 would result in an Ad5 vector with CAR-independent tropism. We therefore constructed a fiber mosaic Ad5 vector, designated as Ad5-σ1, encoding two fibers: the σ1 and the wild-type Ad5 fiber. Functionally, Ad5-σ1 utilized CAR, sialic acid, and JAM1 for cell transduction and achieved maximum infectivity enhancement in cells with or without CAR. Thus, we have developed a new type of Ad5 vector with expanded tropism, possessing fibers from Ad5 and reovirus, that exhibits enhanced infectivity via CAR-independent pathway(s).

Keywords: Gene therapy; Adenovirus; Reovirus; σ1 spike protein; Tropism expansion; Coxsackie and adenovirus receptor

Adenoviral vectors, in particular human serotype 5 (Ad5), have been widely employed for cancer gene therapy applications, owing to their unparalleled ability to accomplish in vivo gene transfer [1]. Despite this capacity, the limited efficacies noted in human gene therapy trials have suggested deficiencies of this vector vis-à-vis the achievement of efficient gene delivery. In this regard, it has been observed that human tumor cells frequently manifest a relative deficiency of the primary Ad receptor, coxsackie and adenovirus receptor (CAR) [2]. This CAR deficiency renders many tumor cells resistant to Ad infection, undermining cancer gene therapy strategies that require efficient tumor cell transduction. Thus, this unanticipated aspect of tumor biology potentially confounds direct exploitation of current generation of human Ad-based vectors.

To address this issue, strategies have been proposed to alter the tropism of Ad to accomplish CAR-independent infection of tumor cells [2]. Initial efforts to this end focused on the use of so-called retargeting adaptors that cross-link Ad to non-CAR receptors that are overexpressed on tumor cells [2,3].

Genetic capsid modification has also been endeavored to achieve these same functional ends. This approach has rationally focused on the fiber knob domain, the primary determinant of Ad tropism, to achieve CAR-independent cell entry. Ad fiber pseudotyping, the genetic substitution of either the entire fiber or the fiber knob domain with its structural counterpart from another human Ad serotype, has been realized. Fiber-pseudotyped vectors display CAR-independent

* Corresponding author. Fax: +1 205 975 7476.
E-mail address: curiel@uab.edu (D.T. Curiel).

0006-291X/$ - see front matter © 2005 Elsevier Inc. All rights reserved.
doi:10.1016/j.bbrc.2005.07.054

tropism by virtue of the natural diversity in receptor recognition found in species B and D Ad fibers. This approach has identified vectors with superior infectivity to Ad5 in several clinically relevant cell types [4–6]. These studies clearly established that genetic capsid modification can achieve the goal of enhanced transduction of tumor cells via CAR-independent cell entry.

On this basis, advanced strategies to achieve further infectivity enhancement have been proposed. We previously derived a fiber mosaic Ad5 vector that incorporates two distinct fibers: the Ad5 fiber and a chimeric fiber that incorporates the Ad3 fiber knob domain. This strategy provided viral entry via two different pathways with additive gains in infectivity [7]. We next explored a strategy to expand Ad tropism by means of exploiting the tropism of non-Ad viruses. Specifically, we endeavored the construction and characterization of fiber mosaic Ad5 vectors that contained fibers of Ad5 and reovirus. In particular, the receptor-binding molecule of serotype 3 Dearing (T3D) reovirus, called the σ1 protein, was incorporated into fiber mosaic Ad5 vectors together with the wild-type Ad5 fiber. This fiber-like σ1 attachment protein is known to bind sialic acid [8] and junction adhesion molecule 1 (JAM1) [9], which together determine T3D reovirus tropism. Since T3D reovirus tropism is clearly distinct from that of Ad, the σ1 protein is a promising candidate for incorporation into a fiber mosaic Ad vector, which could bind to neoplastic cells using the widely expressed cell receptors JAM1, sialic acid, and CAR. Our study establishes a novel strategy to achieve infectivity enhancement based on a fiber mosaic Ad5 vector, which contains fibers from different virus families.

Materials and methods

Cell lines. The 293 cells were purchased from Microbix (Toronto, Ontario, Canada). Human embryonic rhabdomyosarcoma RD cells, human glioma cell line U118MG, human head and neck tumor cell line FaDu, human ovarian cancer cell lines ES-2, OV-3, SK-OV-3, and OVCAR-3, Chinese hamster ovary (CHO) cells, and Lec2 cells were obtained from the American Type Culture Collection (ATCC, Manassas, VA). Human ovarian adenocarcinoma cell lines OV-4 and Hey were a kind gift from Dr. Timothy J. Eberlein (Harvard Medical School, Boston, MA) and Dr. Judy Wolf (M.D. Anderson Cancer Center, Houston, TX), respectively. L929 cells, U118MG-hCAR-tailless cells, and 211B cells were maintained as described previously [8,10,11]. Cell lines were cultured in media recommended by suppliers (Mediatech, Herndon, VA, and Irvine Scientific, Santa Ana, CA). FBS was purchased from Hyclone (Logan, UT). All cells were grown at 37 °C in a humidified atmosphere of 5% CO_2. Primary human ovarian carcinoma cells were established in culture from fresh malignant ascites fluid obtained from patients with pathologically confirmed ovarian adenocarcinoma during surgery at the University of Alabama at Birmingham (UAB) Hospital. Approval was obtained from the UAB Institutional Review Board before acquisition of samples. Cancer cells were purified from ascites fluid by a previously described immunomagnetic-based method [12].

Generation of the σ1 chimeric fiber construct. A schematic of the σ1 chimeric fiber structure is shown in Fig. 1A. To design the σ1 chimeric fiber, the fiber tail domain of Ad5 was amplified by PCR from plasmid pNEB.PK.3.6 [5]. The PCR product was cloned into pGEM4ZT3DS1 that encodes T3D reovirus σ1, resulting in pGEM4ZT3DS1delBam-Ad5tail. The Ad5tail and entire σ1 sequence was PCR-amplified from pGEM4ZT3DS1delBamAd5tail, using the primers 5′-GCCATG AAGCGCGCAAGACCGTCTGAA (sense), 5′-TTTACTAGATGA AATGCCCCAGTGCCGC (the first antisense for addition of stop codon and polyadenylation signal), and 5′-GAAATCAATTGTTTAC TAGATGAAATGCCC (the second antisense for addition of *Mun*I restriction site). The resultant PCR product of the σ1 chimeric fiber was cloned into pNEB.PK.3.6, resulting in pNEB.PK.3.6Ad5tail/σ1. The sequence of pNEB.PK.3.6Ad5tail/σ1 was confirmed by DNA sequencing. This σ1 chimeric fiber was designated as F5S1.

To design the expression vector for the σ1 chimeric fiber, we cloned the F5S1 sequence into plasmid pShuttle-CMV (Qbiogene, Carlsbad, CA). The resultant expression plasmid was designated as pShuttle-CMV-AdSig.

Generation of shuttle plasmids for fiber mosaic Ad5 genome. The construct was based on a fiber mosaic Ad genome that encodes two fiber genes (the wild-type Ad5 fiber and Fiber-Fibritin, designated as FF) in the L5 region, which has been described previously [13]. Our strategy was to replace the fibritin part in the chimeric fiber FF with the σ1 sequence and create the σ1 chimeric fiber (F5S1H). Coding sequence of σ1 was amplified from plasmid pNEB.PK.3.6Ad5tail/σ1 with the primers 5′-CAGAACGTTGGGGATCCTCGCCTACG TGAAGAAGTAGTAC and 5′-TCCTCTAGATCCGCCCGTGAAA CTACGCGGGTACGAAAC. The PCR product was cloned into *Acl*I/*Xba*I sites of FF in plasmid pZpTG 5FF3 [13]. We replaced the fibritin sequence with σ1 coding sequence in-frame with a carboxy-terminally encoded 6-histidine (6-His) stretch, resulting in F5S1H. The resulting plasmid was designated as pZpTG5F/S1.6H. An *Age*I/*Age*I fragment of this plasmid was cloned into the *Age*I site of pNEB.PK.FSP [5] to obtain a shuttle plasmid, designated as pNEB.PK.FSPF5S1/F5, which contains tandem fiber genes: the σ1 chimeric fiber, F5S1H, and the wild-type Ad5 fiber.

Generation of recombinant Ad. A schematic of the viruses used in this study is shown in Fig. 1B. Recombinant Ad5 genomes containing the tandem fiber genes were derived by homologous recombination in *Escherichia coli* BJ5183 with *Sna*I-linearized rescue plasmid pVK700 and the tandem fiber-containing *Pac*I and *Kpn*I-fragment of pNEB.PK.FSPF5S1/F5 essentially as described previously [14]. The recombinant region of the genomic clones was sequenced prior to transfection into 293 cells. All vectors were propagated in 293 cells and purified using a standard protocol [15]. The resultant fiber mosaic virus was Ad5-σ1. Viral particle (v.p.) concentration was determined by the method of Maizel et al. [16]. An infectious titer was determined according to the AdEasy Vector System (Qbiogene).

PCR amplification of viral genome fragments. Viral DNA was amplified using the Taq PCR Core Kit (Qiagen, Valencia, CA). The sequences of the primers were as follows: Ad5tail-sense 5′-ATGAAGC GCGCAAGACCGTCTGAAGAT; Ad5knob-antisense 5′-TTATTCT TGGGCAATGTATGAAAAAGT; and σ1head-antisense 5′-ATTCT TGCGTGAAACTACGCGG.

Protein electrophoresis and Western blotting. To detect the incorporation of fibers in virus particles, Ad vectors equal to 5.0×10^9 v.p. were resolved by SDS–PAGE and Western blotting as described previously [13].

To detect trimerization of the σ1 chimeric fiber, F5S1, the expression plasmid pShuttle-CMV-AdSig was transiently transfected into 293 cells using SuperFect Transfection Reagent (Qiagen). Cell lysates were used for SDS–PAGE and Western blotting. For JAM1 detection, a panel of cell lines was harvested for SDS–PAGE and analyzed by Western blotting using anti-JAM1 monoclonal antibody (BD Biosciences Clontech, Palo Alto, CA).

Recombinant proteins. Recombinant T3D σ1 was produced as described in Chandran et al. [17]. Ad5 fiber knob domain recombinant

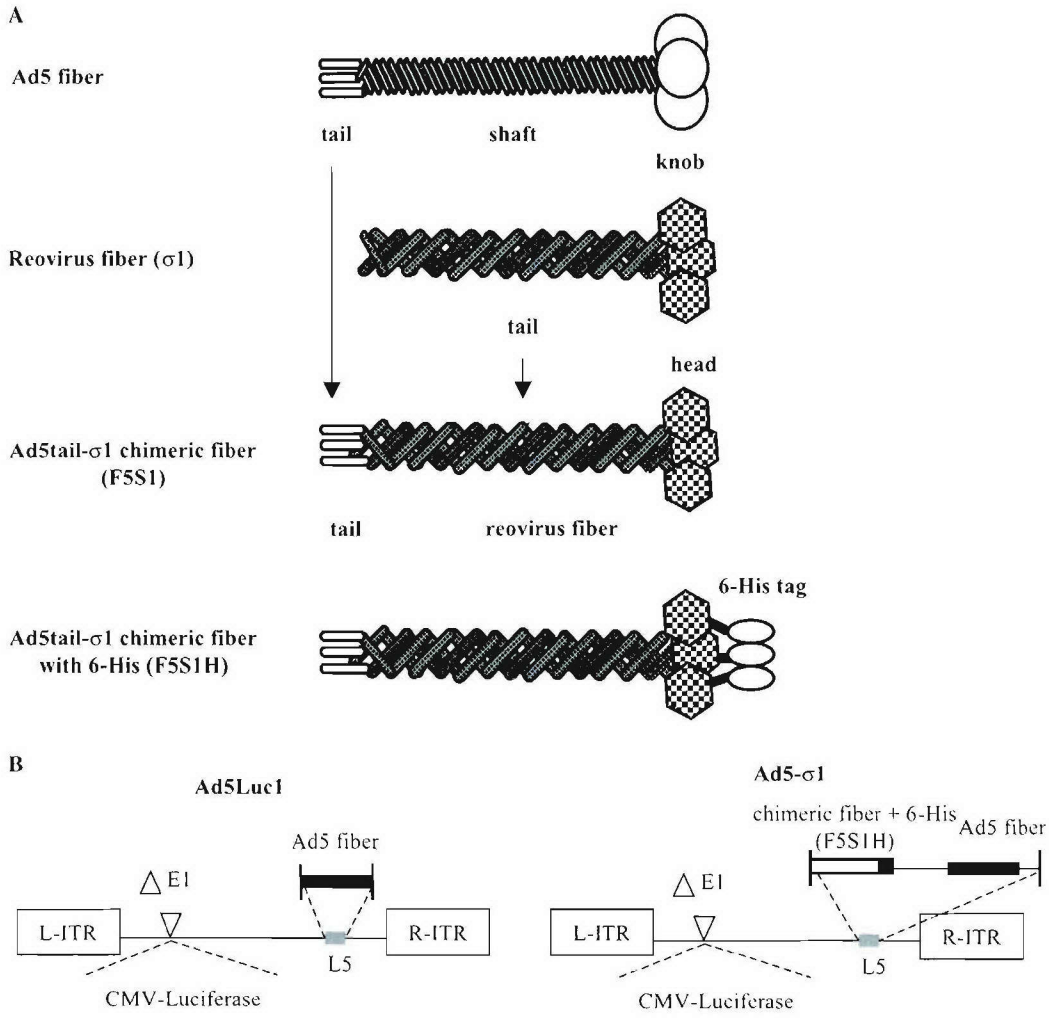

Fig. 1. Schema of fiber mosaic Ad5 genomes. (A) Key components of the σ1 chimeric fiber. In the σ1 chimeric fiber, the tail of Ad5 fiber is fused to the reovirus fiber protein σ1 (designated as F5S1). A six-histidine (6-His) tag is fused to the carboxy-terminus of the σ1 chimeric fiber through a linker (designated as F5S1H). (B) Map of Ad5 genomes with fiber modification. In both vectors, the E1 region is replaced by CMV promoter/luciferase transgene cassette. Ad5Luc1 is a control virus that carries the wild-type Ad5 fiber. Ad5-σ1 is a fiber mosaic vector that carries the σ1 chimeric fiber with a carboxy-terminal 6-His tag (F5S1H) as well as the wild-type Ad5 fiber.

protein was produced and purified as described previously [5]. Concentration of protein in all experiments was determined by the Bradford method (Bio-Rad Laboratories, Hercules, CA).

In vitro gene transfer assays. Cells were infected with virus at 37 °C for 1 h and unbound virus was washed away. After 24 h of incubation at 37 °C, a luciferase assay was performed (Promega, Madison, WI) according to the manufacturer's instructions. Data are presented as mean values ± SD.

Competitive inhibition assay. Recombinant Ad5 fiber knob proteins or anti-JAM1 polyclonal antibody (c-15, Santa Cruz Biotechnology, Santa Cruz, CA) was incubated with the cells at 37 °C for 15 min prior to infection. Alternatively, cells were treated with 333 milliunits/ml of *Clostridium perfringens* neuraminidase type X (Sigma–Aldrich, St. Louis, MO) at 37 °C for 30 min to remove cell-surface sialic acid, followed by two washes with PBS. Cells were then adsorbed with viruses at 37 °C for 1 h. Unbound virus and blocking agents were washed away. After 24 h of incubation at 37 °C, the cells were processed for luciferase assay, as described above. For σ1 blocking experiments, anti-T3D σ1 antibody (9BG5, a gift from Dr. Patrick W.K. Lee, University of Calgary, Calgary, Canada) [18] was incubated with virus at room temperature for 1 h prior to cell infection. Subsequent procedures were same as described above. Data are presented as mean values ± SD.

Flow cytometry. For CAR detection, the cells were incubated with 2 μg/ml of the anti-human CAR monoclonal antibody RmcB (hybridoma was purchased from ATCC) or normal mouse IgG1κ (Sigma–Aldrich) for 1 h on ice. Subsequently, the cells were washed and incubated with FITC-conjugated anti-mouse IgG (Sigma–Aldrich) for an additional 1 h. For sialic acid measurement, cells were incubated with 1 μg/ml FITC-labeled wheat germ agglutinin (WGA; Sigma–Aldrich) on ice for 1 h. After washing with 1% BSA/PBS, the cells were analyzed by flow cytometry at the UAB FACS Core Facility.

Results

Generation of a chimeric fiber (F5S1) containing reovirus σ1

To create a functional chimeric fiber structurally compatible with Ad5 capsid incorporation, we designed the

σ1 chimeric fiber to comprise the amino-terminal tail segment of the Ad5 fiber sequence genetically fused to the entire T3D σ1 protein, with (F5S1H) or without (F5S1) a carboxy-terminal 6-His tag as a detection marker (Fig. 1A).

Prior to Ad5 vector design, we evaluated the trimerization capacity of the σ1 chimeric fiber (F5S1), using pShuttle-CMV-AdSig, a fiber expression plasmid. Following transfection of 293 cells, cell lysates were subjected to SDS–PAGE and Western blot analysis using two primary antibodies, the 4D2 monoclonal antibody (Neomarkers, Fremont, CA) that recognizes the Ad5 fiber tail domain common to both the wild-type Ad5 and the σ1 chimeric fiber, and an anti-T3D σ1 polyclonal antibody (a gift from Dr. Max L. Nibert, Harvard Medical School, Boston, MA) that recognizes σ1. We detected a band for Ad5 fiber from 211B cell lysates [10] at approximately 180 kDa with the 4D2 antibody (Fig. 2, lane 1). This band corresponds to the trimeric fiber molecule, while an approximately 60 kDa band in boiled lysates represents fiber monomers (lane 2). The chimeric fiber was detected with both the 4D2 antibody (lane 3) and an anti-T3D σ1 antibody (data not shown) at an apparent molecular mass of 160–170 kDa. When heat denatured, the monomeric chimeric fiber was detected at an apparent molecular mass of 50 kDa (lane 4). This analysis demonstrates that the σ1 chimeric fiber F5S1 is capable of trimerization, which is required for Ad capsid incorporation.

Construction of fiber mosaic viruses

We sought to create a fiber mosaic Ad5 encoding both the Ad5 fiber and chimeric fibers in the L5 region of the Ad5 genome. We employed a tandem-fiber cassette wherein the F5S1H σ1 chimeric fiber was positioned upstream of the wild-type fiber gene. In this configuration, each fiber was positioned before the untranslated sequences of the wild-type fiber to provide equal transcription, splicing, polyadenylation, and regulation by the major late promoter. We constructed E1-deleted recombinant Ad genomes (Ad5-σ1) containing the wild-type Ad5 fiber, the σ1 chimeric fiber (F5S1H), and a firefly luciferase reporter gene controlled by the CMV immediate early promoter/enhancer. Following virus rescue and large-scale propagation in 293 cells, we obtained Ad5-σ1 vector at concentrations ranging from 1.1×10^{11} v.p./ml to 5.31×10^{12} v.p./ml, depending on the individual preparation. These concentrations compared favorably with that of Ad5Luc1 at 3.74×10^{12} v.p./ml. In addition, the v.p./plaque-forming unit (PFU) ratios determined for Ad5-σ1 and Ad5Luc1 were 22 and 13.3, respectively, indicating excellent virion integrity for both species. Of note, the control vector used throughout this study, Ad5Luc1, is isogenic to Ad5-σ1 in all respects except for the fiber locus.

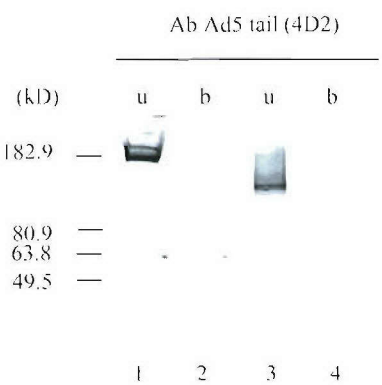

Fig. 2. Western blot analysis of F5S1 chimeric fiber protein in lysates of transiently transfected cells. Fiber proteins were detected by anti-Ad5 fiber tail antibody (4D2). Lanes 1 and 2, 211B cell lysate as a positive control for the wild-type Ad5 fiber; lanes 3 and 4, pShuttle-CMV-AdSig transfected 293 cell lysate for F5S1 chimeric fiber detection (without 6-His). We used cell lysates from 211B cells expressing the wild-type Ad5 fiber as a positive control for detection of Ad5 fiber. The samples in lanes 2 and 4 were heat denatured (b), which resulted in dissociation of trimeric proteins to monomers, while lanes 1 and 3 contain proteins in their native trimeric configuration (unboiled (u)).

Definition of fiber gene configurations for fiber mosaic Ad

We confirmed the fiber genotype of Ad5Luc1 and Ad5-σ1 via diagnostic PCR, using Ad5 fiber or the σ1 chimeric fiber primer pairs and genomes from purified virions as PCR templates (Fig. 3A). To confirm that Ad5-σ1 virions contained both trimerized fibers, we performed SDS PAGE followed by Western blot analysis on viral particles. Using the 4D2 antibody we observed fiber bands at approximately 180 kDa for unboiled samples of Ad5Luc1 and Ad5-σ1 virions, corresponding to fiber trimers (Fig. 3B, lanes 1 and 3). In boiled samples, the 4D2 antibody detected bands of apparent molecular mass of approximately 60 kDa, indicative of fiber monomers (lanes 2 and 4). Due to the near-identical sizes of the σ1 chimeric and the wild-type Ad5 fiber proteins, it was difficult to visualize both fibers simultaneously via Western blot with 4D2.

To confirm the presence of the σ1 chimeric fiber protein in virions, we used the anti-Penta His monoclonal antibody (Qiagen) that recognizes 6-His tags (Fig. 3C) and the anti-T3D σ1 antibody (Fig. 3D). Using the anti-Penta His antibody, we observed the fiber bands corresponding to both trimeric and monomeric σ1 chimeric fiber proteins (Fig. 3C, lanes 2 and 3). The trimeric band of the σ1 chimeric fiber was also detected with the anti-T3D σ1 antibody (Fig. 3D, lane 3), however, the monomeric band of the σ1 chimeric fiber protein was faint because of relatively weak binding affinity of the anti-T3D σ1 antibody (Fig. 3D, lanes 2 and 4). These results confirm that the trimeric F5S1H σ1 chimeric fiber was incorporated into Ad5-σ1 virions.

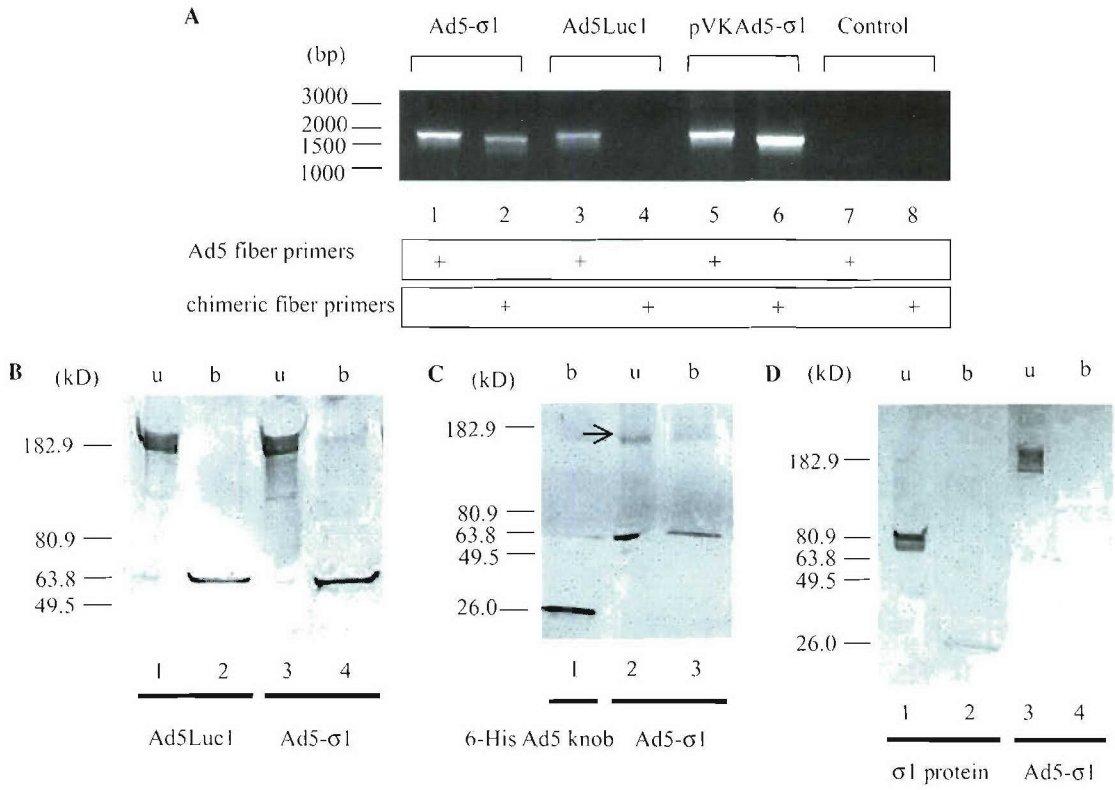

Fig. 3. Analysis of fibers in rescued viral particles. (A) Detection of fiber genes in Ad genome. Rescued viral particles were analyzed with PCR, using pairs of Ad5 fiber primers or σ1 chimeric fiber primers. pVKAd5-σ1 was used as a positive control for both fibers. No PCR template is designated as Control. (B–D) Western blot analysis of fiber proteins in purified virions. (B) A total of 5.0×10^9 v.p. per lane of Ad5Luc1 with the wild-type Ad5 fiber (lanes 1 and 2) or Ad5-σ1 with dual fibers (lanes 3 and 4) were resuspended in Laemmli buffer prior to SDS–PAGE and electrotransfer and detected with the 4D2 anti-Ad5 fiber tail antibody. The samples in lanes 2 and 4 were boiled (b), while lanes 1 and 3 (unboiled (u)) contain proteins in their native trimeric configuration. (C) A total of 5.0×10^9 v.p. per lane of Ad5-σ1 with dual fibers (lanes 2 and 3) was probed with an anti-6-His antibody. Lane 1, recombinant Ad5 knob with a 6-His tag as a positive antibody control; lane 2, unboiled Ad5-σ1 virions; and lane 3, boiled Ad5-σ1 virions. The arrow indicates the position of the trimeric σ1 chimeric fiber protein. (D) A total of 5.0×10^9 v.p. per lane of Ad5-σ1 with dual fibers (lanes 3 and 4) were probed with an anti-T3D σ1 antibody. Lanes 1 and 2, recombinant σ1 protein. The samples in lanes 2 and 4 were boiled, while lanes 1 and 3 contain proteins in their native trimeric configuration (unboiled).

Ad5-σ1 vector exhibits native Ad5 tropism

Our hypothesis was that the inclusion of the σ1 chimeric fiber, F5S1H, into an Ad5 vector would provide infectivity enhancement to Ad-refractory cell types via expanded vector tropism. To test whether this vector retained CAR-dependent tropism, we evaluated Ad5-σ1 infection in a pair of tumor cell lines that vary only in their CAR expression. The human U118MG glioma cell line is CAR-deficient [11]. The U118MG-hCAR-tailless cell is a CAR-positive variant line that artificially expresses the extracellular domain of human CAR [11]. Ad5Luc1 was used as a positive control for CAR binding. As shown in Fig. 4A, Ad5Luc1 exhibited CAR-dependent tropism, as shown by a 40-fold increase in luciferase transgene expression in U118MG-hCAR-tailless cells relative to the parental CAR-deficient U118MG cells. Similarly, Ad5-σ1 exhibited CAR-dependent tropism, as demonstrated by a 53-fold increase in transgene expression in U118MG-hCAR-tailless cells relative to the CAR-deficient U118MG cells (Fig. 4A). Incubation of U118MG-hCAR-tailless cells with recombinant Ad5 knob protein at 50 μg/ml prior to infection efficiently inhibited over 70% of Ad5Luc1 and Ad5-σ1 luciferase activity (Fig. 4B). These data indicate that Ad5-σ1 retains CAR-based tropism, confirming the functionality of the wild-type fiber in our fiber mosaic Ad5.

Ad5-σ1 vector exhibits sialic acid- and JAM1-dependent tropism

To confirm that Ad5-σ1 exploits the non-CAR receptor sialic acid and JAM1 by virtue of the chimeric fiber, we further characterized Ad5-σ1 tropism by performing competitive blocking experiments using 9BG5, a σ1-specific monoclonal antibody that recognizes the T3D σ1 head domain and blocks σ1/JAM1 interaction [18]. Pre-incubation of Ad5-σ1 with 9BG5 prior to infection blocks over 50% of Ad5-σ1 transgene expression in L929 cells, a sialic acid and JAM1-positive cell line commonly used for propagating reovirus (Fig. 4C).

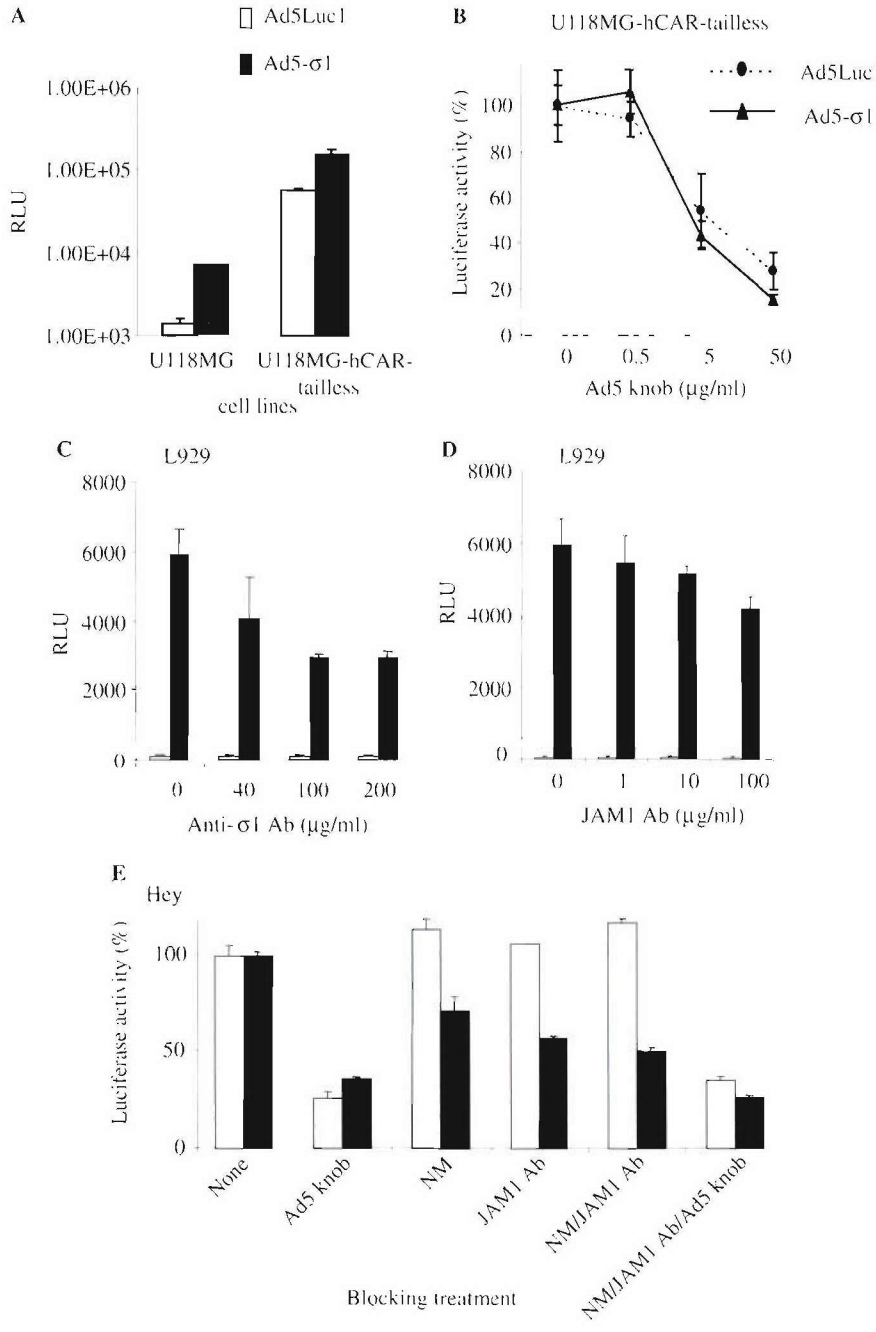

Fig. 4. Evaluation of the efficacy and receptor specificity of Ad5-σ1 mediated gene transfer. (A) Ad5-σ1 infection of a pair of tumor cell lines that vary only in their CAR expression. U118MG is a parental CAR-deficient human glioma cell line, whereas U118MG-hCAR-tailless stably expresses the extracellular domain of human CAR. Cells were infected with Ad5Luc1 (gray bar) and Ad5-σ1 (black bar) at 10 v.p./cell. Luciferase activity was measured 24 h post-infection and is expressed as relative light units (RLU). (B) Recombinant Ad5 fiber knob protein blocks Ad5-σ1 and Ad5Luc1 gene transfer. U118MG-hCAR-tailless cells were incubated with 100 v.p./cell of Ad5-σ1 or Ad5Luc1 with or without recombinant Ad5 fiber knob protein at the indicated concentrations. Luciferase activity was determined 24 h post-infection. All luciferase values were normalized against the activity of controls receiving no knob valued at 100%. (C) σ1 antibody blocks Ad5-σ1 gene transfer. σ1 antibody was incubated with Ad5-σ1 or Ad5Luc1 at 100 v.p./cell for 1 h prior to the infection to L929 cells. Luciferase activity was determined 24 h post-infection. (D) An anti-JAM1 antibody blocks Ad5-σ1 infection. L929 cells were incubated with 100 v.p./cell of Ad5-σ1 or Ad5Luc1 with or without anti-JAM1 antibody (JAM1 Ab) at the indicated concentrations. Luciferase activity was determined 24 h post-infection. (E) Analysis of Ad5-σ1 receptor usage in Hey cells. *C. perfringens* neuraminidase (NM), an anti-JAM1 antibody (JAM1 Ab), and recombinant Ad5 fiber knob protein (Ad5 knob) were employed to block Ad5-σ1 infection. Hey cells were either untreated or treated with 333 milliunits/ml neuraminidase, 100 μg/ml anti-JAM1 antibody, 50 μg/ml recombinant Ad5 fiber knob protein, both neuraminidase and an anti-JAM1 antibody or combined reagents with neuraminidase, anti-JAM1 antibody, and recombinant Ad5 fiber knob protein. Cells were incubated with Ad5-σ1 or Ad5Luc1 at 100 v.p./cell and harvested 24 h later for luciferase activity. All luciferase values were normalized against the activity of controls receiving no blocking treatment valued at 100%. Each data point is an average of four replicates. The error bars indicate standard deviation.

Table 1
Ad5-σ1 luciferase gene expression and co-receptor expression in various cell lines

Cell line	JAM1[a]	Sialic acid[b]	CAR[c]	CAR reference	Activity vs. Ad5Luc1[d]
Fold increase in luciferase					
L929	P	P	L/N	Flow cytometry data	45.3
OV-4	P	P	L/N	Flow cytometry data	5.8
Hey	P	P	L/N	Flow cytometry data	7.0
OV-3	P	P	L/N	Flow cytometry data	4.7
ES-2	P	P	L/N	Flow cytometry data	10.7
SK-OV-3	P	P	L/N	Kashentseva et al. [22]	4.4
OVCAR-3	P	P	M	Kelly et al. [21]	8.5
U118MG	L/N	P	L/N	Kim et al. [11]	6.1
U118MG-hCAR-tailless	L/N	P	P	Kim et al. [11]	5.5
RD	L/N	P	L/N	Cripe et al. [20]	6.4
FaDu	P	P	L/N	Kasono et al. [19]	3.9
CHO	L/N	P	L/N	Flow cytometry data	6.8
Lec2	L/N	N	L/N	Flow cytometry data	2.3

[a] P, highly JAM1-positive; L/N, little or none. As determined by Western blot analysis.
[b] P, highly sialic acid-positive; N, none. As determined by flow cytometric analysis.
[c] P, highly CAR-positive; M, moderate; L/N, little or none.
[d] Multiplicity of infection ranged from 10 to 1000 v.p./cell. Luciferase activity was measured at 24 h post-infection.

The σ1 protein has been reported to utilize the co-receptors JAM1 and sialic acid [8,9]. It has been shown that the σ1 knob-like head domain binds to JAM1 localized on the cell surface and that an anti-JAM1 antibody reduced reovirus replication 10- to 100-fold [9]. Similarly, in the presence of anti-σ1 or anti-JAM1 monoclonal antibodies, a 4-fold decrease in sialic acid-independent σ1 binding has been reported [9]. To further explore the role of JAM1 in Ad5-σ1 infection, we performed competitive blocking experiments using an anti-JAM1 antibody. We used the JAM1-positive L929 cell line for these studies. Exposure of L929 cells to 100 μg/ml anti-JAM1 antibody resulted in approximately 30% inhibition of Ad5-σ1 transgene expression (Fig. 4D). To further clarify Ad5-σ1 tropism, we performed neuraminidase treatment to remove cell-surface sialic acid and competitive blocking experiments using an anti-JAM1 antibody, and Ad5 knob protein. For this analysis, we used the low-CAR human ovarian cancer Hey cell line due to its high sialic acid and JAM1 expression. Transduction by Ad5-σ1 was inhibited 29% by neuraminidase, 42% by an anti-JAM1 antibody, and 50% by combined treatment with neuraminidase and an anti-JAM1 antibody (Fig. 4E). Combined treatment with neuraminidase, an anti-JAM1 antibody, and Ad5 knob protein reduced transduction 74% compared to controls receiving no blocking agent (Fig. 4E), with similar results in U118MG and OV-3 cells (data not shown). Together, these findings confirm that the Ad5-σ1 vector utilizes sialic acid and the JAM1-binding domain of the σ1 chimeric fiber (F5S1H) for cell transduction.

Ad5-σ1 vector exhibits increased transduction of CAR-deficient cells

To demonstrate the contribution of the σ1 chimeric fiber to Ad tropism expansion, we evaluated Ad5-σ1 infectivity in several cell lines. Table 1 shows the co-receptor expression profiles and infectivity of cell lines tested [19–22]. As expected, Ad5-σ1 provided the maximum increase in gene transfer (45-fold) relative to Ad5-Luc1 in L929 cells, which express σ1 receptors sialic acid and JAM1, but no detectable CAR (Table 1, Fig. 5A). In other sialic acid/JAM1-positive and low-CAR cancer cell lines, Ad5-σ1 also provided increased luciferase activity from 3.9-fold (FaDu) to 10.7-fold (ES-2) (Table 1, Fig. 5A). Furthermore, in cancer cells expressing only sialic acid that are JAM1/CAR-negative, Ad5-σ1 provided more than 6-fold higher luciferase activity relative to Ad5Luc1 in RD and U118MG cells (Table 1, Fig. 5A). Thus, we found that the presence of sialic acid and/or JAM1 co-receptors in cell lines contributed to the Ad5-σ1 infection via the usage of the σ1 chimeric fiber. To further demonstrate the σ1 chimeric fiber contribution to Ad5-σ1 infection, we selected a pair of cell lines, JAM1/CAR-negative CHO cells and its sialic acid-negative derivative Lec2 cells (Table 1, Fig. 5B). In CHO cells, Ad5-σ1 provided a 6.8-fold augmentation in luciferase activity versus Ad5Luc1, while infectivity enhancement of Ad5-σ1 on sialic acid-negative Lec2 cells was negligible, suggesting that Ad5-σ1 can exploit sialic acid as a co-receptor.

Many clinically relevant tissues are refractory to Ad infection, including ovarian cancer cells, due to negligible CAR levels [21]. To evaluate the Ad5-σ1 infectivity of patient tissue, we analyzed Ad5-σ1 transduction of primary human ovarian carcinoma cells. Importantly, Ad5-σ1 increased gene transfer to three unpassaged primary ovarian cancer patient samples from 3.9- to 13.5-fold versus Ad5Luc1 (Fig. 5C).

Herein, we have outlined the construction, rescue, purification, and initial tropism characterization of a novel vector containing a non-Ad fiber molecule. Our

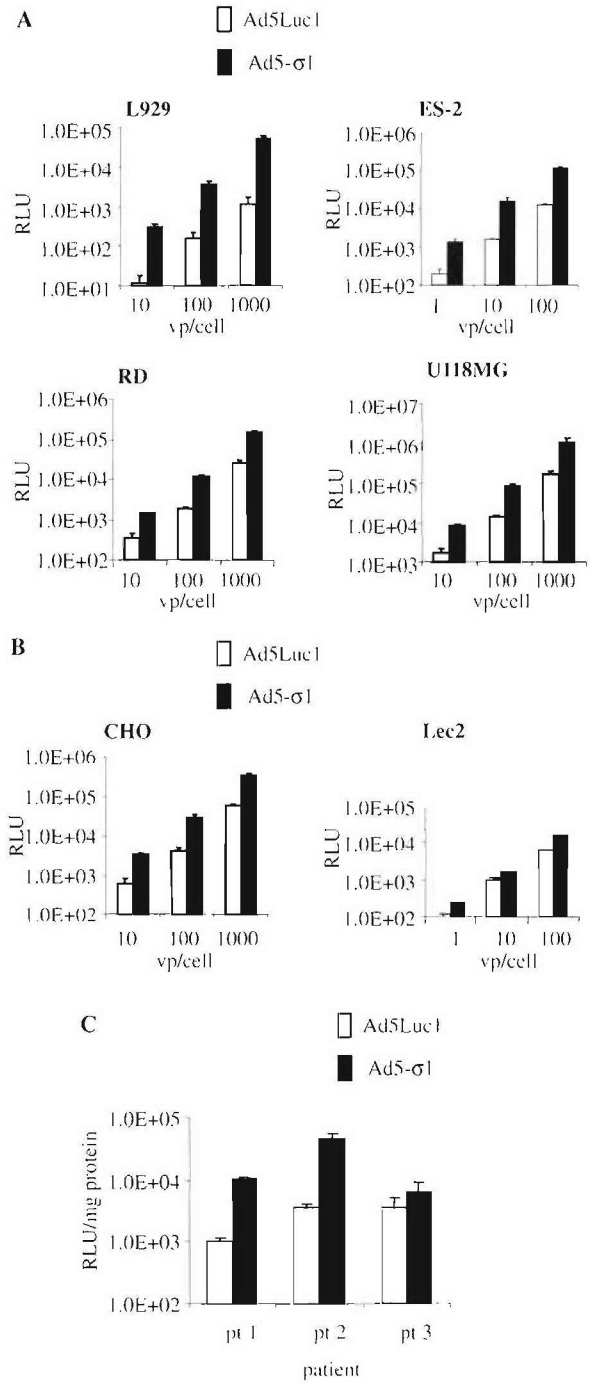

Fig. 5. Infectivity profiles of Ad5-σ1. (A,B) Representative cell lines. (A) Mouse fibroblast cells (L929), ovarian cancer cells (ES-2), human glioma cells (U118MG), and human embryonic rhabdomyosarcoma cells (RD), and (B) sialic acid-positive CHO and sialic acid-negative CHO derivative Lec2 cells were infected with Ad5Luc1 (gray bar) and Ad5-σ1 (black bar) at 1, 10, 100, and 1000 v.p./cell. Luciferase activity was measured 24 h post-infection and is expressed as relative light units (RLU). Each bar represents the mean of three experiments. The error bars indicate standard deviation. (C) Unpassaged primary ovarian cancer cells purified from patient ascites were infected with Ad5Luc1 (gray bar) and Ad5-σ1 (black bar) at 10 v.p./cell. Luciferase activity was measured 24 h post-infection and is expressed as RLU/mg protein. Each bar represents the mean of four experiments. The error bars indicate standard deviation.

results show that in low-CAR cells, Ad5-σ1 provides expanded tropism and increased gene transfer compared to wild-type Ad5 via an alternate infection pathway utilizing the reovirus co-receptors JAM1 and sialic acid. The expanded tropism of this vector represents a crucial attribute for Ad-based gene therapy vectors.

Discussion

A major obstacle to be overcome in Ad5-based cancer gene therapy is the paucity of the primary receptor, CAR, on human primary tumor cells. Variable, but usually low, expression of CAR has been documented in many cancer cell types including glioma, rhabdomyosarcoma, and ovarian cancer [4,11,20]. Thus, Ad gene therapy vectors with CAR-independent and/or expanded tropism may prove valuable for maximal transduction of low-CAR tumors at minimal vector doses.

To achieve expanded tropism by utilizing distinct receptors, we have established a new type of fiber mosaic Ad5 vectors, wherein two fibers derived from different virus families are incorporated in a single virion. This is a novel approach to genetically modify Ad5 vector tropism by means of adding the reovirus receptor-binding spike (σ1) protein to the Ad5 capsid. We selected the spike from reovirus T3D due to its ability to infect numerous tumor cell types that express either JAM1 or sialic acid [23,24].

The main technical feasibility for this new vector is the structural similarity between Ad fiber and the reovirus σ1 protein, which is a trimeric fiber-like molecule protruding from the 12 vertices of the icosahedral reovirus virion [25]. The crystal structure of the reovirus σ1 attachment protein reveals an elongated trimer with two domains: a compact head with a β-barrel fold and a fibrous tail containing a triple β-spiral [25]. The σ1 protein contains two receptor-binding domains: one within the fibrous tail that binds sialic acid [8] and the other in the globular head that binds to JAM1 [9].

In designing a σ1 chimeric fiber, we considered the Ad5 tail portion to be indispensable for incorporation of a σ1 chimeric fiber into the Ad5 penton base. We therefore designed our σ1 chimeric fiber to contain the Ad5 tail and reovirus σ1. The entire σ1 molecule was included since it contains receptor-binding domains in both the tail and head regions [26]. In addition, we engineered a 6-His tag into the C-terminus of σ1 for protein detection. We were initially concerned that the incorporation of the 6-His motif could alter JAM1 recognition, since the C-terminus is proximal to the predicted JAM1-binding motif in the D-E loop of the β-barrel structure [25]. To our knowledge, however, there are no reports suggesting that C-terminal additions are deleterious to normal σ1/JAM1 interaction(s). Indeed, it is unlikely that the 6-His tag interferes significantly with the σ1/JAM1 interaction

since the contribution of JAM1 to the tropism of our mosaic virus was sufficient to result in a 42% decrease in luciferase activity in the presence of an anti-JAM1 antibody (Fig. 5E). Further, we expect that the sialic acid-binding domain localized to the σ1 tail domain would remain unaffected by the C-terminal tag [8,27].

We confirmed the trimerization of the F5S1 σ1 chimeric fiber and constructed an Ad5 genome encoding a tandem fiber cassette, resulting in an Ad5 vector expressing both the Ad5 fiber and a σ1 chimeric fiber. We confirmed that the fiber mosaic Ad5 virions incorporated both fibers by Western blot analysis and by characterizing the functional ability of both fibers to utilize the appropriate receptor(s) for viral transduction.

Consistent with our hypothesis of enhanced infectivity, we observed augmented gene transfer with Ad5-σ1 in all cell lines tested, ranging from 2.3- to 45-fold. This augmentation was variable and often occurred in cell lines with supposedly similar receptor expression profiles. We believe this variation is due to variable receptor expression between cell lines. In this regard, we wish to highlight that the semi-quantitative methodology (Western blot analysis and FACS) used to determine receptor expression in these lines likely masks minor receptor variations between cell lines that accounts for the observed results. Importantly, the observed expanded tropism of Ad5-σ1 extended to a stringent clinical substrate, human primary ovarian tumor tissue, although the augmentation of gene transfer was also variable. While primary ovarian cancer cells are often low in CAR, the specific receptor profiles are unknown. On this basis, the variability in gene transfer very likely reflects natural variability of CAR, JAM1, and sialic acid expression between individual patient samples. These results serve to highlight the utility of Ad vectors that exhibit expanded tropism via utilization of multiple receptors. This vector capacity would be of importance in any future clinical application wherein tissue receptor expression is poorly defined.

During the course of this work, Mercier et al. [28] reported the construction and characterization of an Ad vector containing only the reovirus σ1 fiber. This vector demonstrated JAM1- and SA-dependent tropism that was CAR-independent, resulting in an Ad vector with reovirus tropism only. Mercier demonstrated a 3-fold infectivity enhancement in human dendritic cells relative to Ad5, but did not report any infectivity enhancement in human cancer cells or other substrates. In contrast, we have used the concept of "fiber mosaicism," the use of two separate fibers with distinct receptor recognition, to provide maximum enhanced infectivity via use of multiple receptors. On this basis, we assert that our fiber mosaic Ad5-σ1 vector could offer distinct advantages over Ad vectors with single receptor recognition in the context of an infectivity-enhanced vector for cancer applications.

Our goal was to create a vector with expanded tropism to achieve maximum infectivity enhancement utilizing multiple receptors in CAR and non-CAR cell entry pathways. In this study, the fiber mosaic Ad5-σ1 vector provided enhanced infectivity in low-CAR cancer cell lines resulting from multi-receptor binding properties derived from different virus families. It is our ultimate intent to exploit mosaic adenovirus paradigms in various combinations in order to accomplish additivity or synergism of infectivity enhancements. On this basis, the infectivity gains we demonstrate in this study may contribute to a combinational approach of clinical relevance.

Acknowledgments

This work was supported by the following grants from the National Institute of Health: R01 CA83821, R01 CA94084, and R01 CA93796; Department of Defense W81XWH-05-1-0035; Ovarian Cancer SPORE P50 CA83591 and Breast Cancer SPORE P50 CA89019. We thank Dr. Victor Krasnykh for providing plasmids pVK700 and pNEB.PK.3.6. We also thank Dr. Joanne T. Douglas for providing cell line U118MG-hCAR-tailless, Dr. Dan J. Von Seggern for the cell line 211B, and Dr. Jerry L. Blackwell for the RmcB antibody. We also thank Dr. Maaike Everts for critical reading of the manuscript.

References

[1] J. Gomez-Navarro, D.T. Curiel, J.T. Douglas, Gene therapy for cancer, Eur. J. Cancer 35 (1999) 2039–2057.

[2] V. Krasnykh, I. Dmitriev, J.G. Navarro, N. Belousova, E. Kashentseva, J. Xiang, J.T. Douglas, D.T. Curiel, Advanced generation adenoviral vectors possess augmented gene transfer efficiency based upon coxsackie adenovirus receptor-independent cellular entry capacity, Cancer Res. 60 (2000) 6784–6787.

[3] J.N. Glasgow, G.J. Bauerschmitz, D.T. Curiel, A. Hemminki, Transductional and transcriptional targeting of adenovirus for clinical applications, Curr. Gene Ther. 4 (2004) 1–14.

[4] A. Kanerva, G.V. Mikheeva, V. Krasnykh, C.J. Coolidge, J.T. Lam, P.J. Mahasreshti, S.D. Barker, M. Straughn, M.N. Barnes, R.D. Alvarez, A. Hemminki, D.T. Curiel, Targeting adenovirus to the serotype 3 receptor increases gene transfer efficiency to ovarian cancer cells, Clin. Cancer Res. 8 (2002) 275–280.

[5] V.N. Krasnykh, G.V. Mikheeva, J.T. Douglas, D.T. Curiel, Generation of recombinant adenovirus vectors with modified fibers for altering viral tropism, J. Virol. 70 (1996) 6839–6846.

[6] D.J. Von Seggern, S. Huang, S.K. Fleck, S.C. Stevenson, G.R. Nemerow, Adenovirus vector pseudotyping in fiber-expressing cell lines: improved transduction of Epstein-Barr virus-transformed B cells, J. Virol. 74 (2000) 354–362.

[7] K. Takayama, P.N. Reynolds, J.J. Short, Y. Kawakami, Y. Adachi, J.N. Glasgow, M.G. Rots, V. Krasnykh, J.T. Douglas, D.T. Curiel, A mosaic adenovirus possessing serotype Ad5 and serotype Ad3 knobs exhibits expanded tropism, Virology 309 (2003) 282–293.

[8] J.D. Chappell, V.L. Gunn, J.D. Wetzel, G.S. Baer, T.S. Dermody, Mutations in type 3 reovirus that determine binding to sialic acid

are contained in the fibrous tail domain of viral attachment protein σ1, J. Virol. 71 (1997) 1834–1841.
[9] E.S. Barton, J.C. Forrest, J.L. Connolly, J.D. Chappell, Y. Liu, F.J. Schnell, A. Nusrat, C.A. Parkos, T.S. Dermody, Junction adhesion molecule is a receptor for reovirus, Cell 104 (2001) 441–451.
[10] D.J. Von Seggern, J. Kehler, R.I. Endo, G.R. Nemerow, Complementation of a fibre mutant adenovirus by packaging cell lines stably expressing the adenovirus type5 fibre protein, J. Gen. Virol. 79 (1998) 1461–1468.
[11] M. Kim, L.A. Sumerel, N. Belousova, G.R. Lyons, D.E. Carey, V. Krasnykh, J.T. Douglas, The coxsackievirus and adenovirus receptor acts as a tumour suppressor in malignant glioma cells, Br. J. Cancer 88 (2003) 1411–1416.
[12] S.D. Barker, E. Casado, J. Gomez-Navarro, J. Xiang, W. Arafat, P. Mahasreshti, T.B. Pustilnik, A. Hemminki, G.P. Siegal, R.D. Alvarez, D.T. Curiel, An immunomagnetic-based method for the purification of ovarian cancer cells from patient-derived ascites, Gynecol. Oncol. 82 (2001) 57–63.
[13] L. Pereboeva, S. Komarova, P.J. Mahasreshti, D.T. Curiel, Fiber-mosaic adenovirus as a novel approach to design genetically modified adenoviral vectors, Virus Res. 105 (2004) 35–46.
[14] N. Belousova, V. Krendelchtchikova, D.T. Curiel, V. Krasnykh, Modulation of adenovirus vector tropism via incorporation of polypeptide ligands into the fiber protein, J. Virol. 76 (2002) 8621–8631.
[15] F. Graham, L. Prevec, Manipulation of adenovirus vectors, in: E.J. Murray, J.M. Walker (Eds.), Methods in Molecular Biology, Humana Press, Clifton, NJ, 1991, pp. 109–128.
[16] J.V. Maizel Jr., D.O. White, M.D. Scharff, The polypeptides of adenovirus. I. Evidence for multiple protein components in the virion and a comparison of types 2, 7A, and 12, Virology 36 (1968) 115–125.
[17] K. Chandran, X. Zhang, N.H. Olson, S.B. Walker, J.D. Chappell, T.S. Dermody, T.S. Baker, M.L. Nibert, Complete in vitro assembly of the reovirus outer capsid produces highly infectious particles suitable for genetic studies of the receptor-binding protein, J. Virol. 75 (2001) 5335–5342.
[18] S.J. Burstin, D.R. Spriggs, B.N. Fields, Evidence for functional domains on the reovirus type 3 hemagglutinin, Virology 117 (1982) 146–155.
[19] K. Kasono, J.L. Blackwell, J.T. Douglas, I. Dmitriev, T.V. Strong, P. Reynolds, D.A. Kropf, W.R. Carroll, G.E. Peters, R.P. Bucy, D.T. Curiel, V. Krasnykh, Selective gene delivery to head and neck cancer cells via an integrin targeted adenoviral vector, Clin. Cancer Res. 5 (1999) 2571–2579.
[20] T.P. Cripe, E.J. Dunphy, A.D. Holub, A. Saini, N.H. Vasi, Y.Y. Mahller, M.H. Collins, J.D. Snyder, V. Krasnykh, D.T. Curiel, T.J. Wickham, J. DeGregori, J.M. Bergelson, M.A. Currier, Fiber knob modifications overcome low, heterogeneous expression of the coxsackievirus-adenovirus receptor that limits adenovirus gene transfer and oncolysis for human rhabdomyosarcoma cells, Cancer Res. 61 (2001) 2953–2960.
[21] F.J. Kelly, C.R. Miller, D.J. Buchsbaum, J. Gomez-Navarro, M.N. Barnes, R.D. Alvarez, D.T. Curiel, Selectivity of TAG-72-targeted adenovirus gene transfer to primary ovarian carcinoma cells versus autologous mesothelial cells in vitro, Clin. Cancer Res. 6 (2000) 4323–4333.
[22] E.A. Kashentseva, T. Seki, D.T. Curiel, I.P. Dmitriev, Adenovirus targeting to c-erbB-2 oncoprotein by single-chain antibody fused to trimeric form of adenovirus receptor ectodomain, Cancer Res. 62 (2002) 609–616.
[23] K. Hirasawa, S.G. Nishikawa, K.L. Norman, T. Alain, A. Kossakowska, P.W.K. Lee, Oncolytic reovirus against ovarian and colon cancer, Cancer Res. 62 (2002) 1696–1701.
[24] T. Alain, K. Hirasawa, K.J. Pon, S.G. Nishikawa, S.J. Urbanski, Y. Auer, J. Luider, A. Martin, R.N. Johnston, A. Janowska-Wieczorek, P.W.K. Lee, A.E. Kossakowska, Reovirus therapy of lymphoid malignancies, Blood 100 (2002) 4146–4153.
[25] J.D. Chappell, A.E. Prota, T.S. Dermody, T. Stehle, Crystal structure of reovirus attachment protein σ1 reveals evolutionary relationship to adenovirus fiber, EMBO J. 21 (2002) 1–11.
[26] J.C. Forrest, T.S. Dermody, Reovirus receptors and pathogenesis, J. Virol. 77 (2003) 9109–9115.
[27] E.S. Barton, J.L. Connolly, J.C. Forrest, J.D. Chappell, T.S. Dermody, Utilization of sialic acid as a coreceptor enhances reovirus attachment by multistep adhesion strengthening, J. Biol. Chem. 276 (2001) 2200–2211.
[28] G.T. Mercier, J.A. Campbell, J.D. Chappell, T. Stehle, T.S. Dermody, M.A. Barry, A chimeric adenovirus vector encoding reovirus attachment protein σ1 targets cells expressing junctional adhesion molecule 1, Proc. Natl. Acad. Sci. USA 101 (2004) 6188–6193.

Gene Therapy (2005) 12, 1696–1706

www.nature.com/gt

APPENDIX 2

RESEARCH ARTICLE

A human adenoviral vector with a chimeric fiber from canine adenovirus type 1 results in novel expanded tropism for cancer gene therapy

MA Stoff-Khalili[1,2], AA Rivera[1], JN Glasgow[1], LP Le[1], A Stoff[1,3], M Everts[1], Y Tsuruta[1], Y Kawakami[1], GJ Bauerschmitz[2], JM Mathis[4], L Pereboeva[1], GP Seigal[5], P Dall[2] and DT Curiel[1]

[1]*Departments of Medicine, Surgery, Pathology and the Gene Therapy Center, Division of Human Gene Therapy, University of Alabama at Birmingham, Birmingham, AL, USA;* [2]*Department of Obstetrics and Gynecology, University of Duesseldorf, Medical Center, Duesseldorf, Germany;* [3]*Department of Plastic and Reconstructive Surgery, Dreifaltigkeits-Hospital, Wesseling, Germany;* [4]*Department of Cellular Biology and Anatomy, Louisiana State University Health Sciences Center, Shreveport, LA, USA; and* [5]*Department of Pathology, Cellular Biology and Surgery and the Gene Therapy Center, UAB, Birmingham, AL, USA*

The development of novel therapeutic strategies is imperative for the treatment of advanced cancers like ovarian cancer and glioma, which are resistant to most traditional treatment modalities. In this regard, adenoviral (Ad) cancer gene therapy is a promising approach. However, the gene delivery efficiency of human serotype 5 recombinant adenoviruses (Ad5) in cancer gene therapy clinical trials to date has been limited, mainly due to the paucity of the primary Ad5 receptor, the coxsackie and adenovirus receptor (CAR), on human cancer cells. To circumvent CAR deficiency, Ad5 vectors have been retargeted by creating chimeric fibers possessing the knob domains of alternate human Ad serotypes. Recently, more radical modifications based on 'xenotype' knob switching with non-human adenovirus have been exploited. Herein, we present the characterization of a novel vector derived from a recombinant Ad5 vector containing the canine adenovirus serotype 1 (CAV-1) knob (Ad5Luc1-CK1), the tropism of which has not been previously described. We compared the function of this vector with our other chimeric viruses displaying the CAV-2 knob (Ad5Luc1-CK2) and Ad3 knob (Ad5/3Luc1). Our data demonstrate that the CAV-1 knob can alter Ad5 tropism through the use of a CAR-independent entry pathway distinct from that of both Ad5Luc1-CK2 and Ad5/3-Luc1. In fact, the gene transfer efficiency of this novel vector in ovarian cancer cell lines, and more importantly in patient ovarian cancer primary tissue slice samples, was superior relative to all other vectors applied in this study. Thus, CAV-1 knob xenotype gene transfer represents a viable means to achieve enhanced transduction of low-CAR tumors.
Gene Therapy (2005) **12,** 1696–1706. doi:10.1038/sj.gt.3302588; published online 21 July 2005

Keywords: *canine adenovirus; fiber chimerism; cancer; transductional targeting; gene therapy*

Introduction

Gene therapy is a novel approach for the treatment of malignancies resistant to traditional therapeutic modalities.[1–3] To achieve therapeutic gene delivery, adenoviral vectors (Ad) have been employed owing to their ability to achieve superior levels of *in vivo* gene transfer compared to alternative vector systems.[2] However, despite promising preclinical results obtained in model systems, the major limitation in clinical applications precluding positive outcomes has been inefficient transduction of target tissues by the routinely used human adenovirus serotype 5 vector (Ad5). This problem is mainly due to the insufficient levels of the primary adenoviral receptor, coxsackie-adenovirus receptor (CAR), on target cancer cells.[4,5] In particular, it has been demonstrated that ovarian and breast cancer cells exhibit relative resistance to adenoviral transduction as a result of CAR deficiency.[6,7] This observation predicates the need to develop strategies to alter adenovirus tropism for the goal of efficient gene delivery to cancer cells via 'CAR-independent' pathways.

A general approach to achieve tropism modification is based on genetic modification of certain adenoviral capsid proteins involved in viral binding and target cell entry. Such strategies have largely been directed towards modification of the adenoviral fiber capsid protein, which recognizes the primary receptor CAR. Methods to incorporate heterologeous-binding proteins have exploited locales at the fiber carboxy- terminus and the fiber–knob HI-loop.[8,9] In addition, the approach of fiber–knob serotype chimerism takes advantage of the fact that a subset of human adenovirus serotypes recognize non-CAR primary cellular receptors.[10,11] These various strategies have been successfully employed to achieve a CAR-independent infection capacity for Ad5 vectors. Of note, redirecting the binding of Ad5 to alternate receptors has allowed infectivity enhancement in CAR-deficient, Ad5-refractory tumor targets.[4,12,13]

Correspondence: Dr DT Curiel, Division of Human Gene Therapy, Gene Therapy Center, University of Alabama at Birmingham, 901, 19th Street South, BMR2 502, Birmingham, AL 35294, USA
Received 17 March 2005; accepted 21 June 2005; published online 21 July 2005

Not as rigorously explored, and perhaps more radical, is a recently described approach entailing the development of Ad 'xenotypes'.[14] In this scheme, the fiber–knob of a non-human adenovirus is incorporated into the capsid of a human Ad5 vector to confer novel tropism. Non-human adenoviruses, including those from avian, bovine, porcine, primate, feline, ovine, and canine hosts,[15–17] represent an underused resource in vector design which could offer alternate cellular entry pathways for adenovirus vectors. Although some of these viruses are being developed as gene delivery vectors themselves,[16] the substitution of the Ad5 fiber–knob with these various xenotype fiber–knobs provides an efficient means to analyze their tropism in the context of an Ad5 vector that has been rigourously studied and for which molecular methods have been well established.[2]

Previously, we exploited the unique tropism of canine adenovirus serotype 2 (CAV-2)[18] to generate an Ad5/CAV-2 chimeric vector, which exhibited profound infectivity enhancement of CAR-deficient human tumor cell targets.[14] Another canine adenovirus strain, serotype 1 (CAV-1), has also been partially characterized. Whereas, its cell entry biology has not been described to the extent that has been accomplished for CAV-2, the pathological, structural, biophysical, and serological dissimilarities of CAV1[19–24] in comparison to CAV-2 suggest that a distinct underlying tropism may be operational. In light of these considerations, we explored the potential utilization of an adenoviral xenotype possessing the fiber–knob of CAV-1.

Results

Generation of an Ad5 vector containing a chimeric fiber with the CAV-1 knob domain

Applying structural knowledge of the human Ad5 fiber protein[25] in the context of the CAV-1 fiber indicates that the CAV-1 fiber consists of an N-terminal tail of about 42 amino acids (aa), a shaft of 321 aa, and a remaining C-terminus of 179 aa forming the knob (Figure 1a).[26] A conserved threonine–leucine–tryptophan–threonine (TLWT) motif at the N-terminus of the fiber–knob domain is present in most mammalian Ads including CAV-1. A chimeric fiber was constructed by substitution of the Ad5 fiber–knob with the coding region of the CAV-1 knob domain while preserving the TLWT motif common to both Ad5 and CAV-1 fibers. This procedure was performed by using a two-plasmid rescue system essentially as described by Krasnykh *et al*.[11] We generated an E1-deleted recombinant Ad genome (Ad5Luc1-CK1) incorporating the chimeric Ad5 fiber shaft/CAV-1 knob gene along with a firefly luciferase reporter gene controlled by the CMV immediate early promoter/enhancer in the E1 region. Genomic clones of Ad5Luc1-CK1 were sequenced, and two correct clones

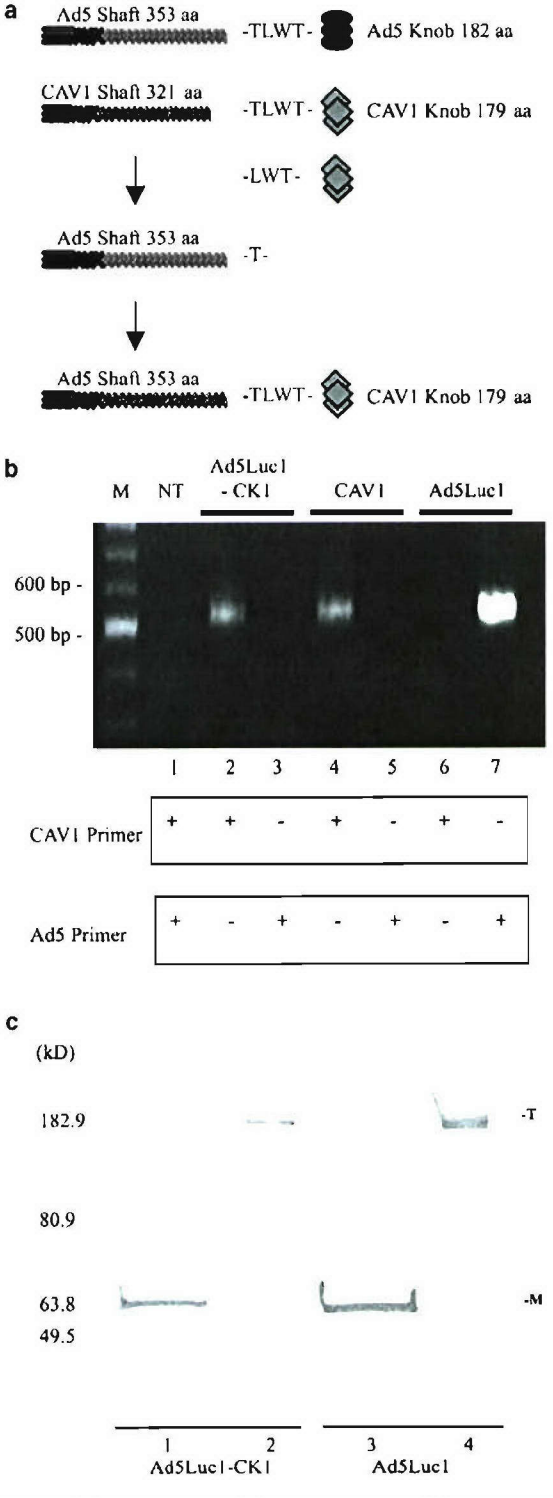

Figure 1 Design and molecular validation of an Ad5 vector containing the CAV-1 fiber–knob domain. (a) Construction of the chimeric fiber of Ad5Luc1-CK1 by incorporating the CAV-1 knob into the Ad5 fiber-shaft protein. The T-L-W-T peptide sequence joining the shaft and knob regions of both fibers is shown in bold. (b) PCR analysis of the fiber genes using Ad genome templates from purified viral particles. CAV-1 virus was used as a positive control. Lanes containing DNA size standards (M) and no PCR template (NT) are designated. Primers used are specific for the CAV-1 or Ad5 fiber gene knob domain. (c) Western blot analysis of fiber protein trimerization. Purified virions (5×10^9 vp) of AdLuc1-CK1 with the chimeric fiber (lanes 1 and 2) and Ad5Luc1 with wild-type Ad5 fiber (lanes 3 and 4) were resuspended in Laemmli buffer before SDS-PAGE and Western analysis with an antitail fiber mAb. The samples in lanes 1 and 3 were heated to 95°C before electrophoresis. Fiber monomers (M) and trimers (T) are indicated. The markers represent molecular mass in kilodaltons.

were chosen. Following transfection into HEK 293 cells, cytopathic effect was observed between 8 and 9 days post-transfection. Large-scale preparations of Ad5Luc1-CK1 and the Ad5Luc1 control vector were produced and purified by double cesium chloride gradient centrifugation. Of note, we applied isogenic vectors in this study based on the Ad5 genome, displaying either the Ad5 knob (Ad5Luc1), CAV1 knob (Ad5Luc1-CK1), or the CAV2 knob (previously named Ad5Luc1-CK but designated here as Ad5Luc1-CK2 for ease of distinction).[14] Using a common scheme would standardize vector-related properties including the reporter gene expression cassette and capsid structure while allowing analysis of gene transfer function as a result of modifying the knob.

The fiber–knob genes of Ad5Luc1 and Ad5Luc1-CK1 were confirmed by PCR using designed primer pairs to specifically amplify the respective knob domains from purified viral genome templates (Figure 1b). Trimerization of the chimeric fiber from viral particles was analyzed by SDS-PAGE followed by Western blot analysis. The monoclonal 4D2 primary antibody which recognizes the Ad5 fiber tail domain common to both wild type Ad5 and chimeric fiber molecules was used. Bands of approximately 200 kDa molecular weight corresponding to the nondenatured trimeric fiber molecule for both Ad5Luc1-CK1 and control virions were observed. On the other hand, bands from boiled samples of the same viruses resolved at an apparent molecular mass of approximately 70 kDa, indicative of the fiber monomer form (Figure 1c). Thus, both the correct sequence integrity and trimerization of Ad5Luc1-CK1 were confirmed.

Distinct binding and gene transfer properties of Ad5Luc1-CK1 and Ad5Luc1-CK2

The rationale for developing our novel Ad5Luc1-CK1 vector was founded on the hypothesis that the CAV-1 knob tropism is distinct from the CAV-2 knob tropism based on differences in the pathobiologies of the viruses during infection in their native canine hosts. To validate this concept, we first evaluated the receptor-binding properties of Ad5Luc1-CK1 (Figure 2a and b) and Ad5Luc1-CK2 (Figure 2c and d) on A549 human lung cancer cells in a recombinant knob competitive inhibition assay employing FACS-based detection of surface-bound virions. As a control, Ad5Luc1 cell binding was also analyzed with Ad5 knob protein blocking (Figure 2e). Interestingly, the data obtained in this competitive inhibition experiment show that the CAV-2 fiber–knob protein cannot effectively block the Ad5Luc1-CK1 cell binding (Figure 2b) whereas the CAV-1 fiber–knob protein can inhibit Ad5Luc1-CK2 cell binding (Figure 2d) to the same extent that each recombinant knob can prevent cell interaction of its respective vector.

To further confirm the distinction between Ad5Luc1-CK1 and Ad5Luc1-CK2-mediated tropism as indicated by the cell-binding assay, we sought to block Ad5Luc1-CK1 and Ad5Luc1-CK2-mediated gene transfer in DK dog kidney and SKOV3.ip1 ovarian cancer cells with the recombinant knob proteins. The data obtained in this competitive inhibition gene transfer experiment show that the CAV-2 knob protein can partially block Ad5-Luc1-CK1 gene transfer in only SKOV3.ip1 cells but not completely (Figure 3a). However, the CAV-1 knob can competitively block Ad5Luc1-CK1 gene transfer with increasing concentrations (Figure 3b). Conversely, the CAV-1 knob protein can totally inhibit Ad5Luc1-CK2 gene transfer in all tested cell lines (Figure 3c) in the same manner that the CAV-2 knob can mediate inhibition of Ad5Luc1-CK2 gene transfer (Figure 3d). These findings are consistent with the results of the cell-binding assay (Figure 2) and suggest the possibility of a common receptor between the CAV-1 and CAV-2 knobs although the Ad5Luc1-CK1 displayed a binding property distinct from the Ad5Luc1-CK2.

Since CAV-2 has been shown to bind to CAR,[14,27] we investigated whether CAR may be a common receptor for the CAV-1 and CAV-2 knobs. For this reason, we performed a blocking experiment of Ad5Luc1-mediated gene transfer in U118-hCAR-tailless cells (a CAR-positive U118 cell line variant that heterelogously expresses the extracellular domain of human CAR[28]) with CAV-1 and CAV-2 fiber–knob proteins. Ad5 fiber–knob protein was used as a control. Ad5Luc1 transduction in U118-hCAR-tailless cells was strongly blocked by all three CAV-1 (95%), CAV-2 (98%), and Ad5 fiber–knob proteins (98%) (data not shown), confirming that all three knobs can interact with the CAR receptor.

Infectivity enhancement of CAV-1 knob xenotype Ad in CAR-deficient cells

Our central goal was to investigate whether the CAV1 'xeno-knob' paradigm would mediate increased transduction in CAR-deficient target cancer cells. To evaluate the CAR-independent receptor-binding properties of our novel Ad5Luc1-CK1 vector in comparison with Ad5-Luc1, CAR-deficient U118MG glioma cell line and its CAR-positive variant U118-hCAR-tailless, which artificially expresses the extracellular domain of human CAR, were used in a cell-binding assay as described above. In CAR-deficient cells U118MG, only a modest level of cell surface-associated Ad5Luc1 (38%) was detected (Figure 4a). In contrast, 81% of the CAR-positive variant line U118-hCAR-tailless cells were positive for Ad5Luc1 binding (Figure 4b). Importantly, our novel vector Ad5Luc1-CK1 exhibited a remarkable 95% cell surface binding in U118 MG (glioma) cells (Figure 4a) and cell interaction comparable to that of Ad5Luc1 in U118-hCAR-tailless cells (Figure 4b).

Successful initial attachment on the cell surface via fiber–knob interaction does not necessarily result in increased gene transfer. To validate effective gene delivery conferred by the binding properties of the CAV-1 knob, we evaluated Ad5Luc1-CK1-mediated gene transfer in the U118MG and U118-hCAR-tailless cell lines (Figure 5). Ad5Luc1 (containing the wild-type Ad5 fiber), Ad5Luc1-CK2, and Ad5/3Luc1, (containing the Ad5 fiber shaft and the Ad3 knob) were used as controls. Ad5Luc1 exhibited clear CAR-dependent tropism as demonstrated by a 100-fold increase in transgene expression in U118-hCAR-tailless cells *versus* the CAR-deficient U118 MG cell line. Conversely, Ad5Luc1-CK1 gene delivery in U118 MG cells was about 100-fold higher than that of Ad5Luc1 while infection of the CAR-positive variant cell line yielded a comparable level of luciferase activity. Although the Ad5 fiber–knob competitively inhibited Ad5Luc1-mediated gene transfer in U118-hCAR-tailless (over 85% at 10 μg/ml), it had no

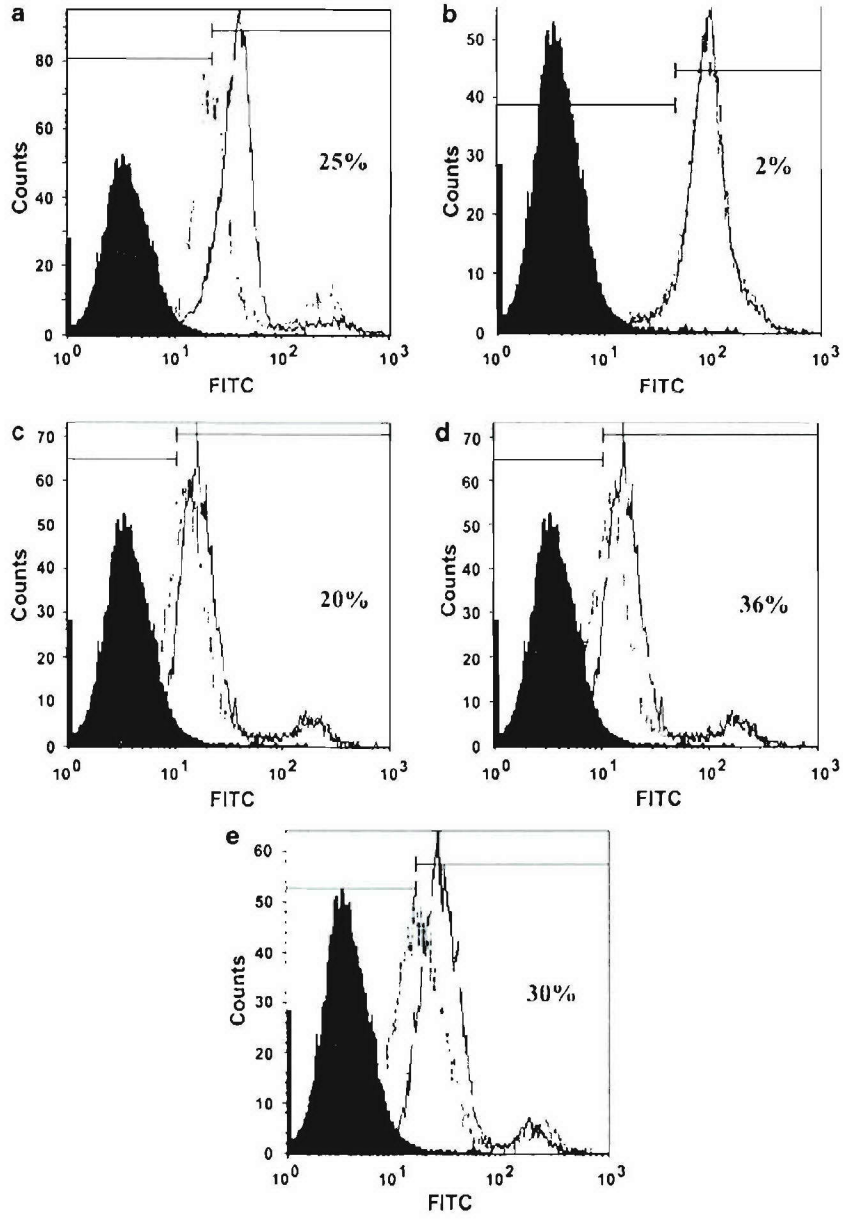

Figure 2 Distinct binding of Ad5Luc1-CK1 and Ad5Luc1-CK2. Flow cytometry-binding assay of Ad5Luc1-CK1 and Ad5Luc1-CK2 on A549 cells in the presence of purified CAV-1 fiber–knob protein and CAV-2 fiber–knob protein (50 μg/ml) (a–d). (a) Ad5Luc1-CK1+CAV-1 knob, (b) Ad5Luc1-CK1+CAV-2 knob, (c) Ad5Luc1-CK2+CAV-2 knob, (d) Ad5Luc1-CK2+CAV-1 knob, (e) Ad5Luc1+Ad5 knob fiber protein. The histograms shown represent unstained cells (gray fill), cells preincubated with PBS and infected with virus (solid line), and cells preincubated with recombinant knob protein and incubated with virus (dashed line). The percent blocking of virus binding represents histogram gating to determine the number of stained cells preincubated in the absence of recombinant knob protein minus the number of stained cells preincubated in the presence of recombinant knob protein.

appreciable effect on Ad5/3Luc1, Ad5Luc1-CK1, and Ad5Luc1-CK2 transduction (Figure 5). Thus, these data suggest that CAV1 knob-mediated gene delivery is CAR independent.

Ad3 receptor independence of CAV1 knob xenotype Ad

To further examine the distinct tropism of the CAV1 knob xenotype vector, interaction of the virus with the Ad3 receptor was indirectly studied with an Ad3 knob-blocking experiment. In this case, the SKOV3.ip1 human ovarian cancer cell line was used because it abundantly expresses the Ad3 receptor.[29] Transgene expression mediated by Ad5/3Luc1 decreased with increasing concentrations of the Ad3 knob protein. In contrast, the purified Ad3 knob exhibited no influence on transduction with Ad5Luc1-CK1 (Figure 6a). Thus, these data show that Ad5Luc1-CK1 also displays an Ad3 receptor-independent tropism.

Enhanced gene transfer of Ad5Luc1-CK1 in cancer cell lines and primary ovarian cancer cells

Finally, we evaluated Ad5Luc1-CK1 transduction in a variety of cancer cells, which are known to be deficient in CAR. In all cases, the Ad5Luc1-CK1 vector achieved

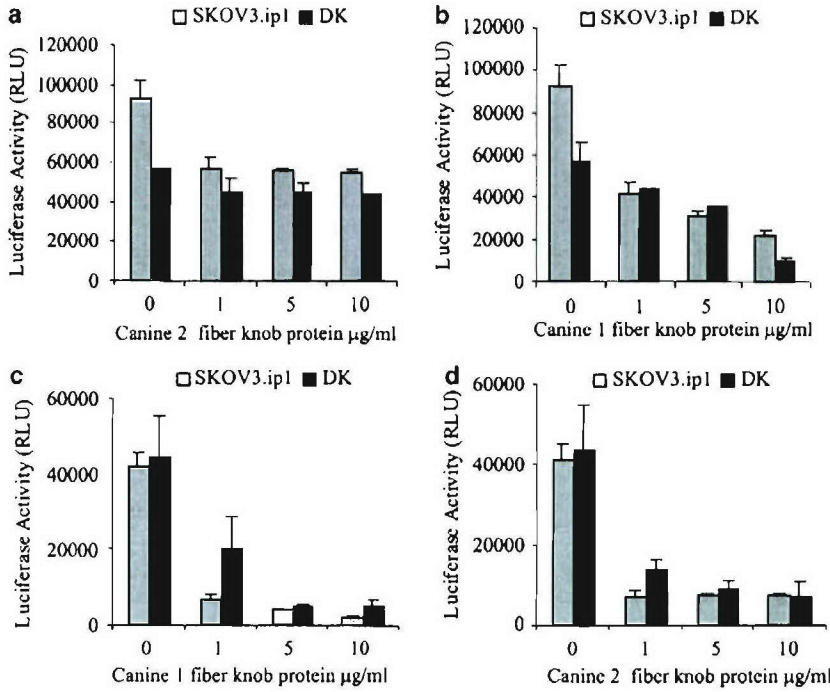

Figure 3 Transduction efficiency of Ad5Luc1-CK1. Luciferase activities following infection of SKOV3.ip1 and DK cells with Ad5Luc1-CK1 (upper panels) and Ad5Luc1-CK2 (lower panels) in the presence of purified CAV-1 fiber–knob protein (b and c) and CAV-2 fiber–knob protein (a and d). Luciferase activity was determined 48 h postinfection and is presented as relative light units (RLU). Each column represents the average of six replicates using 100 vp/cell of each vector and the error bars indicate the s.d.

enhanced transduction above the Ad5 vector, ranging from 11- and 32-fold in SKOV3.ip3 and HEY (ovarian cancer cell lines) to 65- and 100-fold in RD (rhabdomyosarcoma cell line) and U118MG (glioma cell line) (Figure 6b). This gene delivery level was also greatly improved relative to that of Ad5Luc1-CK2, further indicating the distinction between the tropism of the CAV-1 *versus* the CAV-2 knob. More importantly the excellent performance of Ad5Luc1-CK1 was also observed in primary ovarian cancer tissue samples, in which CAR levels are highly variable and often very low.[29] We utilized precision cut tissue slices of patient tumor samples, which represent a highly stringent *ex vivo* model system with three-dimensional characteristics for preclinical screening of adenoviral agents. Ad5Luc1-CK1 demonstrated increased gene transfer capability in ovarian cancer tissue slices (four patients) from 6.2- to 11.4-fold higher than Ad5Luc1 (Figure 6c). Notably, the transduction capacity of Ad5Luc1-CK1 was superior overall compared to our Ad5/3Luc1 and Ad5Luc1-CK2, two chimeric vectors, which themselves have already shown remarkable infectivity enhancements in the same disease context previously.[14,30] Of note, the Ad5Luc1-CK1 and Ad5Luc1-CK2-mediated gene transfer in fibroblasts and keratinocytes was poor.

Evaluation of Ad5Luc1-CK1 transduction in human liver tissue slices

To evaluate liver transduction of Ad5Luc1-CK1 in the most relevant context, the human liver, we infected precision-cut human liver tissue slices of three donors with Ad5Luc1 or Ad5Luc1-CK1. These precision-cut liver slices maintain the tissue architecture and contain the variety of cells normally found in liver.[31] As shown in Figure 7 the luciferase activity in human liver tissue slices infected with Ad5Luc1-CK1 was significantly less than luciferase activity in human liver tissue slices infected with Ad5Luc1 ($P<0.01$).

Discussion

For many target cancer cells it has been noted that low levels of the primary adenoviral receptor CAR may present a limiting factor that compromises the utility of Ad5 as a cancer gene therapy vector. To achieve the levels of efficiency required in the context of cancer gene therapy, it may be necessary to route conventional Ad via CAR-independent pathways. Therefore, achieving CAR-independent and expanded tropism is one of the central tasks in Ad5 vector development for cancer gene therapy. To this end, we endeavored such vector design by genetic capsid engineering to replace the Ad5 fiber–knob with the corresponding structure from a nonhuman 'xenotype' Ad, CAV-1. Interest has recently extended to animal adenoviruses due to the desire to expand the choice of novel gene delivery vectors and thus provide more options for therapeutic strategies and design. In this regard, there are two canine isolates, serotypes 1 and 2, which may offer novel adenovirus infection pathways.[32] CAV-2 is one of the few non-human adenoviruses that have been investigated as a gene transfer vector for human applications. Particularly, a replication-deficient CAV-2 vector has been constructed[14,16,33] and displayed a distinct tropism not exhibited by human

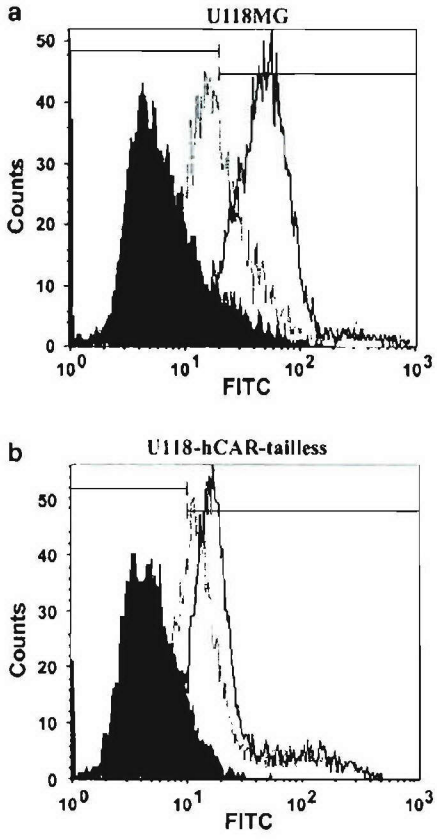

Figure 4 Ad5Luc1-CK1 CAR-independent cell binding. Flow cytometry-binding assay of Ad5Luc1, Ad5Luc1-CK1 on CAR-deficient U118MG (glioma) cells (a) and the CAR-positive variant, U118-hCAR-tailless cells (b). Gray line = cells alone, solid line = cells+Ad5Luc1-CK1, dashed line = cells+Ad5Luc1.

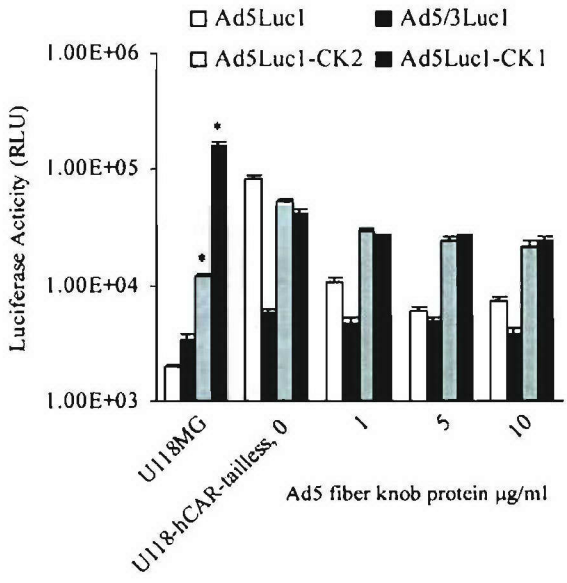

*Figure 5 Ad5Luc1-CK1CAR-independent gene transfer. Luciferase activities following infection of U118MG cells and U118-hCAR-tailless cells with Ad5Luc1, Ad5/3Luc1, and Ad5Luc1-CK1 are presented. The concentration of recombinant Ad5 fiber–knob protein used to block infection is indicated in μg/ml. Luciferase activity was determined 48 h postinfection and is presented as relative light units (RLU). Each column represents the average of three replicates using 100 vp/cell and the error bars indicate the s.d. *P<0.05 versus Ad5.*

Ad5.[18] The tropism of CAV-2 fiber–knob has also been applied in the context of a chimeric Ad5 vector, which provided significant infectivity enhancement over an unmodified Ad5 virus.[14] CAV-1, however, has not been investigated for gene therapy purposes and represents a potential basis for achieving novel adenoviral tropism. In this regard, the data presented in this study represent the first attempt to explore the tropism of the CAV-1 knob.

The rationale of our study to generate a modified Ad5 vector containing the CAV-1 fiber–knob domain was established on the hypothesis that CAV-1 knob-mediated tropism is distinct from that of the CAV-2 knob. The reasons for this speculation include low DNA sequence homology[34,35] and the reported differences in disease manifestations between CAV-1 and CAV-2.[19,36,37] In addition to structural, biophysical, and serological dissimilarities, the two viruses differ greatly in their biological properties. CAV-1 is known to cause allergic uveitis, called the 'blue eye syndrome' and rarely hepatitis,[32] whereas CAV-2 is known to preferentially infect the upper respiratory tract in young dogs, resulting in a mild disease called kennel cough. Neither the CAV-1 nor the CAV-2 receptor(s) have been rigorously identified. Indeed, our blocking experiments employing recombinant fiber–knob proteins revealed that the CAV-1 and CAV-2 fiber–knobs may share a common receptor as evidenced by the ability of the CAV-1 knob to inhibit Ad5Luc1-CK2 function. CAV-2 has been shown to bind directly to soluble recombinant human CAR and can utilize human or murine CAR for cell entry *in vitro*.[27] This finding, combined with our observation that both CAV-1 and CAV-2 knobs can competitively decrease Ad5-mediated gene transfer, suggest that this common receptor may likely be CAR.

Despite the result that both CAV-2 knob-mediated cell binding and gene delivery was competitively inhibited by the CAV-1 knob, the reverse phenomenon of CAV-2 knob blocking CAV-1 knob-mediated gene delivery could not be demonstrated. This observation may be due to a stronger interaction of the CAV-1 knob to the common receptor relative to the CAV-2 knob. However, the data may also be interpreted to support the idea that the CAV-1 knob may possess the ability to bind to a second receptor that is distinct from CAR. Interestingly, the implication that CAV-2 binds to a second receptor has been previously proposed based on gene delivery results both in the context of a CAV-2 vector[27] as well as an Ad5 chimeric vector.[14] If both CAV-1 and CAV-2 knobs have the ability to interact with secondary receptors in addition to CAR, then the secondary receptors for these two knobs may in fact be distinct based on our competitive inhibition results. Certainly, further studies would have to be conducted to validate these hypotheses. In addition, the interplay between these chimeric vectors and other confirmed and putative adenovirus receptors, such as integrins and heparin sulfate, should also be investigated.

Our major goal was to evaluate whether the CAV-1 'xeno-knob' paradigm would mediate expanded CAR-independent tropism in CAR-negative target cancer cells.

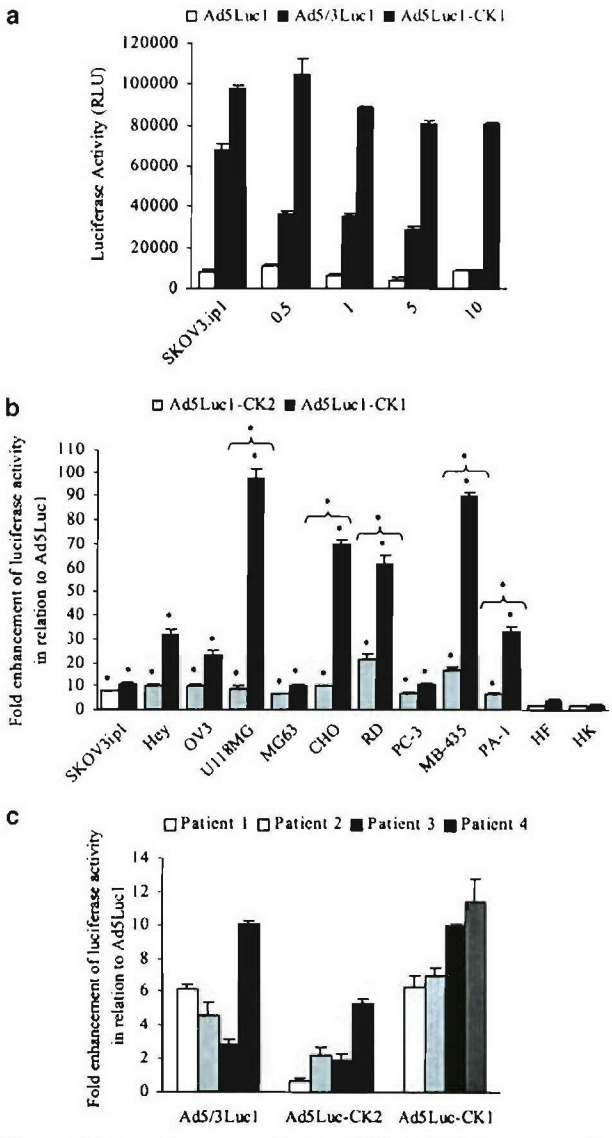

*Figure 6 Enhanced gene transfer by Ad5Luc1-CK1 in cancer cells. Luciferase activities following infection of ovarian cancer cell line SKOV3.ip1 (a), a panel of cancer cell lines (b), and primary ovarian tissue slices (four patients) (c) with the various vectors. Concentration of recombinant Ad3 fiber–knob protein used to block infection (a) is indicated in μg/ml. Luciferase activity was determined 48 h postinfection and is reported in relative units (RLU). Each column represents the average of six replicates using 100 vp/cell of the respective vector and the error bars indicate the s.d. (b) and (c) represent the fold enhancement of luciferase activity in cells infected with various vectors compared to Ad5Luc1. *P < 0.05 versus Ad5. Brackets represent *P < 0.05 Ad5Luc1-CK1 versus Ad5Luc1-CK2 (b).*

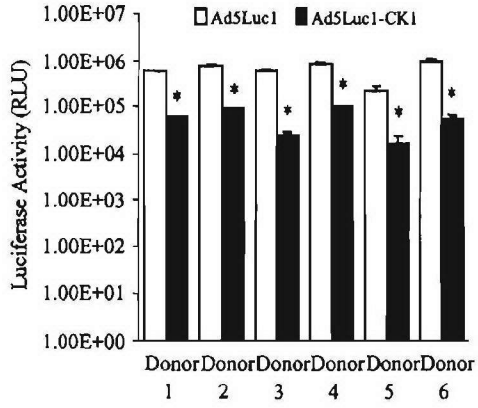

*Figure 7 Ad5Luc1-CK1 displays significant lower infectivity in human liver tissue slices compared to Ad5Luc1. Human liver tissue slices from liver samples of six donors were infected with Ad5Luc1 or Ad5Luc1-CK1 at 500 vp/cell and luciferase activity was measured after 24 h. Luciferase activity was normalized for total protein. Each point represents the mean of three experiments performed in triplicates (three liver tissue slices per donor). Error bars represent s.d. from the mean. *P < 0.05 versus Ad5.*

Even though our data show that the CAV-1 knob may interact with CAR, we were able to achieve enhanced gene transfer with Ad5Luc1-CK1 in a CAR-independent manner. Interestingly, with respect to the CAV-2 knob, this same phenomenon was also observed.[14] Previous studies have utilized other chimeric strategies to attain infectivity enhancement, including the use of the Ad3 knob in the context of an Ad5 vector. The Ad3 receptor appears to be expressed at higher levels than CAR on ovarian cancer cells, therefore allowing 5/3 serotype chimeras to achieve greatly improved gene delivery.[30] Our data revealed the inability of the Ad3 fiber–knob protein to block Ad5luc-CK1 gene transfer, suggesting that this CAV-1 knob chimera, in addition to being CAR independent and distinct from the CAV-2 chimera, does not enter cells via the Ad3 receptor, putatively identified to be CD80, CD86[38] and CD46.[39]

Variable expression of CAR has been documented in many cancer types, such as glioma, melanoma, breast cancer, prostate cancer, and rhabdomyosarcoma.[12,13,40,41] It is known that for entry, viruses often exploit cellular receptors important in conserved pathways. Interestingly, previous studies suggest that CAR may act as a tumor suppressor, which could be linked to its frequent downregulation seen in highly tumorigenic cells.[4] Overcoming this deficiency, both Ad5Luc1-CK1 and Ad5-Luc1-CK2[14] show the ability to bind to and transduce CAR-deficient human glioma cells. Importantly, the transduction by Ad5Luc1-CK1 was augmented by 100-fold *versus* Ad5Luc1 and 75-fold *versus* Ad5Luc1-CK2 in glioma cells and superior to Ad5Luc1 and Ad5Luc1-CK2 in human ovarian cancer, osteosarcoma, and rhabdomyosarcoma cell lines. The significant difference of transduction in the various cancer cell lines between Ad5Luc1-CK1 and Ad5Luc1-CK2 also strongly supports our finding that the CAV-1 knob has a distinct tropism from the CAV-2 knob.

Both Ad5/3Luc1[29,30] and Ad5Luc1-CK2[14] (Ad3 receptor independent) have been reported to exhibit increased infectivity enhancement in ovarian cancer cell lines and primary ovarian cancer cells.[29,30] We endeavored to compare the infectivity enhancement of our seemingly CAR, Ad3 receptor, and CAV2 receptor-independent novel chimeric vector with Ad5/3Luc1 and Ad5Luc1-CK2 in ovarian cancer targets. There is mounting evidence that primary ovarian cancer express highly variable and often low amounts of CAR.[42] Thus, for preclinical evaluation of therapeutic agents, it is crucial to analyze cancer cell substrates that most closely and stringently resemble the patient setting. Gene transfer experiments were performed using primary ovarian

cancer tissue slices obtained by precision cut slice technology, an in *vitro* model representing the architectural features of in *vivo* tissue.[43] In primary ovarian cancer tissue slices, the infectivity enhancement by Ad5Luc1-CK1 was greater than that of Ad5/3Luc1 and Ad5Luc1-CK2. Of note, the gene transfer by Ad5Luc1-CK2 *versus* Ad5Luc1 was only moderate in the primary ovarian cancer tissue slices, further supporting the distinction between the CAV-1 and CAV-2 knobs. The levels of transduction we were able to achieve with Ad5Luc1-CK1 in the primary ovarian cancer samples are one of the highest we have observed in our experience with genetically modified adenoviruses.

Finally, we wished to evaluate the hepatotropism of Ad5Luc1-CK1, since CAV-1 has been reported to rarely cause hepatitis in dogs.[32] Importantly, our data showed that liver transduction of Ad5Luc1-CK1 was significantly lower compared to Ad5Luc1.

Herein, we have constructed a novel Ad5 chimeric xenotype CAV-1 knob vector, which exhibited expanded tropism and displayed superior transduction efficiency in a panel of cancer cells. Importantly, primary tumor tissue slices were also more efficiently transduced with this CAV-1 knob chimeric vector compared to other vectors. The enhanced infectivity appears to be both CAR and Ad3 receptor independent and was also distinct from the transduction pathway of the CAV-2 knob. These results highlight the potential of applying the CAV-1 xeno knob for effective adenovirus cancer gene therapy.

Materials and methods

Cell culture

Human embryonic kidney 293 cells, human embryonic rhabdomyosarcoma RD cells, CAR-negative human glioma U118 MG cells, human osteosarcoma MG63 cells, human ovarian cancer OV3 cells, human lung adenocarcinoma A549 cells, prostate cancer PC-3 cells, breast cancer MB-435 cells, Chinese hamster ovary (CHO) and teratocarcinoma PA-1 cells were obtained from the American Type Culture Collection (ATCC, Manassas, VA, USA). Human ovarian adenocarcinoma cell lines, Hey and SKOV3.ip1, were kind gifts from Drs Judy Wolf and Janet Price (M.D. Anderson Cancer Center, Houston, TX, USA), and Dr Timothy J Eberlein (Harvard Medical School, Boston, MA, USA), respectively. Primary fibroblasts and primary keratinocytes were obtained from Dr NS Banerjee, Department of Biochemistry and Molecular Genetics, University of Alabama at Birmingham, Birnigham, AL, USA). All cells were maintained according to the suppliers' protocols. U118MG-hCAR-tailless cells, which express a truncated form of human CAR (comprising the extracellular domain, transmembrane, and the first two aa from the cytoplasmic domain) have been described previously.[28] These cells were propagated in a 50:50 mixture of Dulbecco's modified Eagle's medium and Ham's F-12 medium (DMEM/F-12) supplemented with 10% (v/v) fetal calf serum (FCS, Gibco-BRL, Grand Island, NY, USA), L-glutamine 2 mM, penicillin (100 U/ml), and streptomycin (100 μg/ml). Stably transfected U118MG-hCAR-tailless cells were maintained in 400 μg/ml G418. Media and supplements were purchased from Mediatech (Herndon, VA, USA).

Human primary ovarian cancer tissue samples

Approval was obtained from the Institutional Review Board prior to initiation of studies on human tissues. Human ovarian primary tumors were obtained from epithelial ovarian carcinoma patients who have undergone debulking as primary therapy and have not had prior chemotherapy (Department of Surgery, University of Alabama at Birmingham (UAB)). Omental samples with extensive tumor infiltration were used to obtain samples since these specimens were the most easily obtained and had large tumor volumes from which adequate slices could be acquired (Krumdieck Tissue Slicer). Time from harvest to slicing was kept to a minimum (<2 h).

Human primary liver tissue samples

Human liver samples were obtained (Department of Surgery, UAB) from six seronegative donor livers that were to be transplanted into waiting recipients. Approval was obtained from the Institutional Review Board prior to initiation of studies on human tissue. All liver samples were flushed with University of Wisconsin (UW) solution (ViaSpan, Barr Laboratories, Inc. Pomona, NY, USA) prior to harvesting and kept on ice in UW solution until slicing. Time from harvest to slicing was kept at an absolute minimum (<2 h).

Krumdieck tissue slicer

The Krumdieck tissue slicing system (Alabama Research & Development[44]) was used in accordance with the manufacturer's instructions and previously published techniques.[45] A coring device was used to create an 8 mm diameter core of ovarian cancer samples and human liver samples. This material was then placed in the slicer filled with ice-cold culture medium. Slice thickness was set at 250 μm using a tissue slice thickness gauge, and slices were cut using the reciprocating blade at 30 revolutions per minute (r.p.m.). Afterwards, the slices were stored in ice-cold culture media prior to culturing. The tissue slices were placed in six-well plates (one slice/well) containing 2 ml of complete media (RPMI with 1% antibiotics, 1% L-glutamine, and 10% FCS for ovarian cancer tissue slices and William's medium E with 1% antibiotics, 1% L-glutamine, and 10% FBS for liver tissue slices). The plates were then incubated at 37°C/5% CO_2 in a humified environment under normal oxygen concentrations for 2 h. A plate rocker set at 60 r.p.m. was used to agitate the slices and to ensure adequate oxygenation and viability.[45,46]

Flow cytometry virus-binding assay

Cells grown in T75 flasks were dislodged with EDTA (0.5 mmol) and resuspended in phosphate buffer solution (PBS) containing 1% bovine serum albumin (BSA). The cells (5×10^5 cells/ml) were incubated with 100 viral particles of the respective vector, or buffer alone, for 1 h at 4°C in 250 μl of PBS–BSA. After three washes with 4 ml of cold PBS–BSA, the cells were incubated with a 1:500 dilution of polyclonal rabbit anti-Ad5 hexon antiserum (Cocalico Biologicals, Reamstown, PA, USA) at 4°C in 250 μl of PBS–BSA. The cells were washed again three times in 4 ml of cold PBS–BSA and incubated with 250 μl of a 1:150 dilution of FITC-labeled goat anti-rabbit IgG secondary antibody (Jackson Immunoresearch Labs,

West Grove, PA, USA) for 1 h in PBS–BSA at 4°C. The cells were analyzed at the UAB FACS Core Facility using a FACScan flow cytometer (Beckton Dickenson, San Jose, CA, USA).

For the recombinant knob competitive inhibition binding assay, A549 cells (5×10^5 cells/ml in 100 µl) were incubated with 100 µl PBS–BSA alone or buffer containing 50 µg/ml recombinant fiber–knob at 4°C for 30 min prior to addition of the viruses, and then antibody staining was performed as described above. To determine the percent blocking of virus binding by the addition of recombinant fiber–knob, histograms representing the staining intensity of cells preincubated in the absence or presence of recombinant knob protein were analyzed. First, the number of cells in the histogram peak representing cells preincubated in the absence of recombinant knob protein was determined by gating the staining to include 99% of the events detected. Then, the percent change in staining intensity was determined by subtracting the number of gated cells in the histogram peak representing cells blocked in virus binding by preincubated in the presence of recombinant knob protein.

Plasmid construction

The CAV-1 fiber–knob (537 bp) domain was amplified from viral DNA isolated from wild-type CAV-1 virus, a kind present from MD Morrison.[32] The following primers were applied: (forward) 5′-TATGGACTGGAC CTGATCCAAACGTT-3′ and (reverse) 5′-TTTATCATTG ATTTTCCCCCACATAGGTGAAGG-3′ (the stop codon TGA and the poly-adenylation signal TAAA are underlined). The plasmid pSHAFT is a cloning vector, which contains the Ad5 fiber gene with the knob region deleted and replaced by a small linker containing *Sma*I and *Eco*ICRI restriction sites.[11] The plasmid was linearized by the enzymes *Sma*I and *Eco*ICRI digestion giving two blunt ends. After gel purification, the PCR product containing the CAV-1 knob was ligated into the linearized pSHAFT resulting in pSHAFT-CK1. This plasmid contains the chimeric fiber gene encoding the complete Ad5 fiber shaft with the CAV-1 knob domain followed by a stop codon and polyadenylation sequence at the 3′ end. The chimeric fiber gene in pSHAFT was digested with *Nco*I and *Mun*I to liberate a 0.75 kb DNA fragment containing the carboxy terminus of the shaft and the CAV-1 knob domain and then ligated into the *Nco*I–*Mun*I-digested shuttle vector PNEB.PK3.6[11] resulting in pNEB.PK.3.6-CK1.

Generation of recombinant adenovirus

Recombinant adenovirus genomes containing the chimeric CAV-1 fiber–knob gene were generated by homologous recombination in BJ5183 *Escherichia coli* with *Swa*I-linearized rescue plasmid PVK700 and the fiber containing *Pac*I-*Kpn*I-fragment of pNEB.PK.3.6-CK1. PVK700 was derived from pTG3602,[47] but contains an almost compete deletion of the fiber gene and a firefly luciferase reporter gene driven by the cytomegalovirus (CMV) immediate early promoter in place of the E1 region. Genomic clones were subjected to sequencing and PCR analysis prior to transfection into 293 cells. Ad5Luc1 is a replication-defective E1-deleted unmodified control Ad5 vector containing a firefly luciferase reporter gene also driven by the CMV promoter.[11] Ad5Luc1-CK2, previously named as Ad5Luc1-CK,[14] is a replication-defective E1-deleted Ad5-based vector containing the CAV-2 knob domain in a chimeric Ad5 fiber molecule. All vectors were propagated in 293 cells and purified by double cesium chloride (CsCl) ultracentrifugation and dialyzed against phoshate-buffered saline with Mg^{2+}, Ca^{2+}, and 10% glycerol. Final virus aliquots were analyzed for viral particle (vp) titer (absorbance at 260 nm) using a conversion factor of 1 OD = 10^{12} vp/ml. All vectors used in this study are essentially isogenic except for the fiber–knob modifications. Using a common vector structure would standardize all conditions including the reporter expression cassette while allowing analysis of gene transfer efficiency as a consequence of varying the knob.

PCR validation of viral genome

Viral DNA was extracted from 1×10^8 vp of Ad5Luc1, Ad5Luc1-CK1, and wild-type CAV-1[32] (Blood Mini Kit, Qiagen) and used as templates for PCR checking. To detect the presence of the Ad5 and CAV-1 fiber–knob genes, each viral genome was amplified in a PCR reaction mixture (Qiagen) containing 50 nM of primer pairs for 30 cycles of denaturation (94°C, 1 min), annealing (54°C, 1 min), and extension (72°C, 1 min). The sequences of the various fiber–knob primer sets are as follows: Ad5 (forward) 5′-AGTGCTCATCTTATTATA AGA-3′, Ad5 (reverse) 5′-CACCACCGCCCTATCCTG AT-3′; CAV-1 (forward) 5′-TATGGACTGGACCTGATC CAAACGTT-3′ and (reverse) 5′-TTTATCATTGATTTTCC CCCACATAGGTGAAGG-3′. PCR products were detected by 1% agarose gel electrophoresis with ethidium bromide staining.

Recombinant fiber–knob proteins

The Ad3, Ad5, and CAV-2 recombinant fiber proteins were produced and purified as described previously.[11,14] The recombinant knob domain of CAV-1 contains an N-terminus 6-histidine tag and was constructed in the pQE-81L expression plasmid (Qiagen, Hilden, Germany). The CAV-1 fiber–knob domain was amplified by PCR using the following primers: (forward) 5′-CAAACACGG ATCCCCTCAAAACAAAA-3′ and (reverse) 5′-TTTAT CATTGATTTTCCCCCACATAGGTGAAGG-3′. The forward primer contains a two-basepair mutation (bold) to create a 5′- end *Bam*HI restriction site (underlined). The PCR product containing the canine 1 fiber–knob region was digested with *Bam*HI, gel purified, and ligated into *Bam*HI-*Sma*I-digested pQE-81L. The resulting plasmid pQE-81L-CAV-1 was analyzed by restriction analysis and sequenced. Expression plasmids were introduced into *E. coli*, and the 6-His-containing fiber–knob proteins from bacterial cultures were purified under native conditions in nickel-nitrilotriacetic acid (Ni-NTA) agarose columns (Qiagen). Concentrations of the final purified knob protein were determined by the Lowry method (Bio-Rad). The trimerization ability of the recombinant CAV-1 fiber–knob was confirmed by Western blot analysis of boiled and unboiled purified knob proteins using a mouse monoclonal Penta-His antibody (Qiagen) and a horseradish peroxidase-conjugated anti-mouse immunoglobulin antibody at a 1:3000 dilution (Dako Corporation, CA, USA), followed by incubation with 3-3′-diaminobenzene peroxidase substrate (DAB; Sigma Company, USA).

Western blot analysis

Aliquots of the Ad vectors equal to 5×10^9 viral particles were diluted into Laemmli buffer and incubated at room temperature or 95°C for 5 min and loaded onto a 4–20% gradient SDS-polyacrylamide gel (Bio-Rad, Hercules, CA, USA). Following electrophoresis protein separation, the protein samples were electroblotted onto a PVDF membrane. The primary 4D2 monoclonal antibody (recognizing the Ad5 fiber tail domain) was diluted 1:3000 (Lab Vision, Freemont, CA, USA) and used to probe the protein blot. Immunoblots were developed by addition of a secondary horseradish peroxidase-conjugated anti-mouse immuno-globulin antibody at a 1:3000 dilution (Dako Corporation, Carpentaria, CA, USA), followed by incubation with 3-3′-diaminobenzene peroxidase substrate for colorimetric development (DAB; Sigma Company, St Louis, MO, USA).

Ad-mediated gene transfer experiments

To determine gene transfer efficiency, 2×10^4 cells were seeded per well in a 24-well plate. The next day, the respective cells were infected for 1 h at 37°C with each vector at 100 vp/cell in 500 µl of infection medium containing 2% FCS. Luciferase activities of cell lysates were measured 48 h later using the Promega luciferase assay system (Madison, WI, USA). Experiments were performed in triplicates or six replicates (where indicated). Error bars represent standard deviations from the mean. For the gene transfer assays involving blocking conditions, recombinant fiber proteins at 0.5 and/or 1, 5, and 10 µg/ml final concentrations were incubated with the cells at 37°C in transduction media 30 min prior to the addition of the virus. Following infection for 1 h, the cells were washed with transduction media to remove unbound virus and the blocking agent. All cells were maintained at 37°C in an atmosphere of 5% CO_2. For gene transfer assays of patient tissue slices, all viral infections were performed with 500 vp/cell in 2% FCS complete culture media.[31] The cell number for the tissue slices was estimated at 1×10^6 cells/slice based on an approximate 10 cell slice thickness (~250 µm) and 8 mm slice diameter. Infections were allowed to proceed for 24 h. The medium was removed and replaced with 10% FCS-complete culture medium. The infected ovarian cancer tissue slices and human liver tissue slices were placed in cell culture lysis buffer (Promega) and homogenized with an ultra sonicator (Fisher Scientific Model 100) at a setting of 15 W for 10 s. The homogenate was centrifuged to pellet the debris, and the luciferase activities were measured using the Promega luciferase assay system (Madison, WI, USA). Experiments were performed in triplicate. Error bars represent s.d. from the mean. Protein concentration of the tissue homogenates was determined using a Bio-Rad DC protein assay kit (Bio-Rad, Hercules, CA, USA) to allow normalization of the gene expression data relative to the number of cells.

Statistics

Data are presented as mean values ± s.d. Statistical differences among groups were assessed with a two-tailed Student's *t*-test. $P(*) < 0.05$ was considered significant.

Acknowledgements

This work was supported by the following grants: Grant of the Deutsche Forschungsgemeinschaft Sto 647/1-1 (to MA Stoff-Khalili); Department of Defense W81XWH-05-1-0035, NIH Grant R01CA083821, R01CA94084 (to DT Curiel); R01CA93796 (to GP Siegal). We thank Lucretia Sumerel for invaluable technical assistance. DNA vectors pSHAFT, pNEB.PK.3.6, and pVK700 were generous gifts from Dr Victor Krasnykh.

References

1 Bauerschmitz GJ, Barker SD, Hemminki A. Adenoviral gene therapy for cancer: from vectors to targeted and replication competent agents (review). *Int J Oncol* 2002; **21**: 1161–1174.
2 Curiel DT, Douglas JT. *Adenoviral Vectors for Gene Therapy.* Academic Press: New York, 2002.
3 Yacoub A *et al.* MDA-7 regulates cell growth and radiosensitivity *in vitro* of primary (non-established) human glioma cells. *Cancer Biol Ther* 2004; **3**: 739–751.
4 Okegawa T *et al.* The dual impact of coxsackie and adenovirus receptor expression on human prostate cancer gene therapy. *Cancer Res* 2000; **60**: 5031–5036.
5 Qin M *et al.* Coxsackievirus adenovirus receptor expression predicts the efficiency of adenoviral gene transfer into non-small cell lung cancer xenografts. *Clin Cancer Res* 2003; **9**: 4992–4999.
6 Anders M *et al.* Inhibition of the Raf/MEK/ERK pathway up-regulates expression of the coxsackie and adenovirus receptor in cancer cells. *Cancer Res* 2003; **63**: 2088–2095.
7 Shayakhmetov DM, Li ZY, Ni S, Lieber A. Targeting of adenovirus vectors to tumor cells does not enable efficient transduction of breast cancer metastases. *Cancer Res* 2002; **62**: 1063–1068.
8 Wickham TJ, Carrion ME, Kovesdi I. Targeting of adenovirus penton base to new receptors through replacement of its RGD motif with other receptor-specific peptide motifs. *Gene Therapy* 1995; **2**: 750–756.
9 Dmitriev I *et al.* An adenovirus vector with genetically modified fibers demonstrates expanded tropism via utilization of a coxsackievirus and adenovirus receptor-independent cell entry mechanism. *J Virol* 1998; **72**: 9706–9713.
10 Shayakhmetov DM, Papayannopoulou T, Stamatoyannopoulos G, Lieber A. Efficient gene transfer into human CD34(+) cells by a retargeted adenovirus vector. *J Virol* 2000; **74**: 2567–2583.
11 Krasnykh VN, Mikheeva GV, Douglas JT, Curiel DT. Generation of recombinant adenovirus vectors with modified fibers for altering viral tropism. *J Virol* 1996; **70**: 6839–6846.
12 Hemmi S *et al.* The presence of human coxsackievirus and adenovirus receptor is associated with efficient adenovirus-mediated transgene expression in human melanoma cell cultures. *Hum Gene Ther* 1998; **9**: 2363–2373.
13 Miller CR *et al.* Differential susceptibility of primary and established human glioma cells to adenovirus infection: targeting via the epidermal growth factor receptor achieves fiber receptor-independent gene transfer. *Cancer Res* 1998; **58**: 5738–5748.
14 Glasgow JN *et al.* An adenovirus vector with a chimeric fiber derived from canine adenovirus type 2 displays novel tropism. *Virology* 2004; **324**: 103–116.
15 Zakhartchouk A, Connors W, van Kessel A, Tikoo SK. Bovine adenovirus type 3 containing heterologous protein in the C-terminus of minor capsid protein IX. *Virology* 2004; **320**: 291–300.
16 Kremer EJ, Boutin S, Chillon M, Danos O. Canine adenovirus vectors: an alternative for adenovirus-mediated gene transfer. *J Virol* 2000; **74**: 505–512.

17 Hess M *et al*. The avian adenovirus penton: two fibres and one base. *J Mol Biol* 1995; **252**: 379–385.
18 Soudais C *et al*. Canine adenovirus type 2 attachment and internalization: coxsackievirus-adenovirus receptor, alternative receptors, and an RGD-independent pathway. *J Virol* 2000; **74**: 10639–10649.
19 Curtis R, Barnett KC. The 'blue eye' phenomenon. *Vet Rec* 1983; **112**: 347–353.
20 Kremer EJ. CAR chasing: canine adenovirus vectors-all bite and no bark? *J Gene Med* 2004; (6 Suppl 1): S139–S151.
21 Marusyk RG, Norrby E, Lundqvist U. Biophysical comparison of two canine adenoviruses. *J Virol* 1970; **5**: 507–512.
22 Marusyk RG, Yamamoto T. Characterization of a canine adenovirus hemagglutinin. *Can J Microbiol* 1971; **17**: 151–155.
23 Marusyk RG. Comparison of the immunological properties of two canine adenoviruses. *Can J Microbiol* 1972; **18**: 817–823.
24 Marusyk RG, Hammarskjold ML. The genetic relationship of two canine adenoviruses as determined by nucleic acid hybridization. *Microbios* 1972; **5**: 259–264.
25 Green NM *et al*. Evidence for a repeating cross-beta sheet structure in the adenovirus fibre. *EMBO J* 1983; **2**: 1357–1365.
26 Rasmussen UB, Schlesinger Y, Pavirani A, Mehtali M. Sequence analysis of the canine adenovirus 2 fiber-encoding gene. *Gene* 1995; **159**: 279–280.
27 Soudais C *et al*. Canine adenovirus type 2 attachment and internalization: coxsackievirus-adenovirus receptor, alternative receptors, and an RGD-independent pathway. *J Virol* 2000; **74**: 10639–10649.
28 Kim M *et al*. The coxsackievirus and adenovirus receptor acts as a tumour suppressor in malignant glioma cells. *Br J Cancer* 2003; **88**: 1411–1416.
29 Kanerva A *et al*. Gene transfer to ovarian cancer *versus* normal tissues with fiber-modified adenoviruses. *Mol Ther* 2002; **5**: 695–704.
30 Kanerva A *et al*. Targeting adenovirus to the serotype 3 receptor increases gene transfer efficiency to ovarian cancer cells. *Clin Cancer Res* 2002; **8**: 275–280.
31 Kirby TO *et al*. A novel *ex vivo* model system for evaluation of conditionally replicative adenoviruses therapeutic efficacy and toxicity. *Clin Cancer Res* 2004; **10**: 8697–8703.
32 Morrison MD, Onions DE, Nicolson L. Complete DNA sequence of canine adenovirus type 1. *J Gen Virol* 1997; **78**: 873–878.
33 Hemminki A *et al*. A canine conditionally replicating adenovirus for evaluating oncolytic virotherapy in a syngeneic animal model. *Mol Ther* 2003; **7**: 163–173.
34 Hu RL *et al*. Detection and differentiation of CAV-1 and CAV-2 by polymerase chain reaction. *Vet Res Commun* 2001; **25**: 77–84.
35 Jouvenne P, Hamelin C. Comparative analysis of the canAV-1 and canAV-2 genomes. *Intervirology* 1986; **26**: 109–114.
36 Willis AM. Canine viral infections. *Vet Clin North Am Small Anim Pract* 2000; **30**: 1119–1133.
37 Erles K, Dubovi EJ, Brooks HW, Brownlie J. Longitudinal study of viruses associated with canine infectious respiratory disease. *J Clin Microbiol* 2004; **42**: 4524–4529.
38 Short JJ *et al*. Adenovirus serotype 3 utilizes CD80 (B7.1) and CD86 (B7.2) as cellular attachment receptors. *Virology* 2004; **322**: 349–359.
39 Sirena D *et al*. The human membrane cofactor CD46 is a receptor for species B adenovirus serotype 3. *J Virol* 2004; **78**: 4454–4462.
40 Li Y *et al*. Loss of adenoviral receptor expression in human bladder cancer cells: a potential impact on the efficacy of gene therapy. *Cancer Res* 1999; **59**: 325–330.
41 Cripe TP *et al*. Fiber knob modifications overcome low, heterogeneous expression of the coxsackievirus-adenovirus receptor that limits adenovirus gene transfer and oncolysis for human rhabdomyosarcoma cells. *Cancer Res* 2001; **61**: 2953–2960.
42 Vanderkwaak TJ *et al*. An advanced generation of adenoviral vectors selectively enhances gene transfer for ovarian cancer gene therapy approaches. *Gynecol Oncol* 1999; **74**: 227–234.
43 Vickers AE *et al*. Organ slice viability extended for pathway characterization: an *in vitro* model to investigate fibrosis. *Toxicol Sci* 2004; **82**: 534–544.
44 Krumdieck CL, dos Santos JE, Ho KJ. A new instrument for the rapid preparation of tissue slices. *Anal Biochem* 1980; **104**: 118–123.
45 Kirby To RA *et al*. A Novel *ex vivo* model system for evaluation of CRAds therapeitic efficacy and toxixity. *Clin Cancer Res* 2004; **10**: 8697–8703.
46 Olinga P *et al*. Comparison of five incubation systems for rat liver slices using functional and viability parameters. *J Pharmacol Toxicol Methods* 1997; **38**: 59–69.
47 Chartier C *et al*. Efficient generation of recombinant adenovirus vectors by homologous recombination in *Escherichia coli*. *J Virol* 1996; **70**: 4805–4810.

SUBMITTED

An Adenovirus Serotype 5 Vector with Fibers Derived from Ovine Atadenovirus Demonstrates CAR-Independent Tropism and Unique Biodistribution in Mice

Masaharu Nakayama[a], Gerald W. Both[c], Boglarka Banizs[a#], Yuko Tsuruta[a], Seiji Yamamoto[a], Yosuke Kawakami[a], Joanne T. Douglas[a,b], Kenzaburo Tani[d], David T. Curiel[a,b] and Joel N. Glasgow[a*]

[a]Division of Human Gene Therapy, Departments of Medicine, Obstetrics and Gynecology, Pathology, Surgery and the [b]Gene Therapy Center, University of Alabama at Birmingham, Birmingham, AL 35294 USA, [c]CSIRO Molecular and Health Technologies, North Ryde, NSW 2113, Australia, [d]Division of Molecular and Clinical Genetics, Medical Institution of Bioregulation, Kyushu University, Fukuoka 812-8582, Japan

M.N. mnakayam@uab.edu
G.W.B. gerry.both@csiro.au
B.B. bbanizs@uab.edu
Y.T yuko.tsuruta@uab.edu
S.Y. yamasei@uab.edu
Y.K. ykawaka@zj9.so-net.ne.jp
J.T.D. jdouglas@uab.edu
K.T. taniken@bioreg.kyushu-u.ac.jp
D.T.C. curiel@uab.edu

* Corresponding Author
Mailing Address:
Division of Human Gene Therapy
University of Alabama at Birmingham
901 19th Street South BMR2-572
Birmingham, AL 35294-2180
Phone: (205) 934-8768
Fax: (205) 975-7949
Email: jng@uab.edu

Current address: Department of Cell Biology, University of Alabama at Birmingham, Birmingham, AL 35294 USA

ABSTRACT

Many clinically important tissues are refractory to adenovirus (Ad) infection due to negligible levels of the primary Ad5 receptor, the coxsackie and adenovirus receptor, CAR. Thus, development of novel CAR-independent Ad vectors should lead to therapeutic gain. Ovine atadenovirus type 7, the prototype member of genus *Atadenovirus*, efficiently transduces CAR-deficient human cells *in vitro* and systemic administration of OAdV is not associated with liver sequestration in mice. The penton base of OAdV7 does not contain an RGD motif, implicating the long-shafted fiber molecule as the sole structural dictate of OAdV tropism. We hypothesized that replacement of the Ad5 fiber with the OAdV7 fiber would result in an Ad5 vector with CAR-independent tropism *in vitro* and liver "detargeting" *in vivo*. An Ad5 vector displaying the OAdV7 fiber was constructed (Ad5Luc1-OvF) and displayed CAR-independent, enhanced transduction of CAR-deficient human cells. When administered systemically to C57BL/6 mice, Ad5Luc1-OvF reporter gene expression was reduced by 80% in the liver compared to Ad5 and exhibited 50-fold higher gene expression in the kidney than the control vector. To our knowledge, this is the first report of a fiber-pseudotyped Ad vector that simultaneously displays decreased liver uptake and a distinct organ tropism *in vivo*. This vector may have future utility in murine models of renal disease.

Key Words: gene therapy, adenovirus, targeting, tropism modification, coxsackie and adenovirus receptor (CAR), liver tropism, kidney tropism

INTRODUCTION

Vectors based on human adenovirus (Ad) serotypes 2 and 5 of species continue to show increasing promise as gene therapy delivery vehicles, especially for cancer gene therapy, due to several key attributes: Ad vectors display *in vivo* stability and excellent gene transfer efficiency to numerous dividing and non-dividing cell targets. In addition, Ad vectors are rarely linked to any severe disease in immunocompetent humans, providing rationale for further development of these vehicles.

The first step in Ad5 infection occurs via high-affinity binding of the virion fiber knob domain to its cognate cellular receptor known as the coxsackie and adenovirus receptor (CAR) (Henry et al., 1994; Xia et al., 1994; Bergelson et al., 1997; Tomko et al., 1997). Following knob-CAR binding, receptor-mediated endocytosis of the virion is dramatically increased by interaction of the penton base Arg-Gly-Asp (RGD) motif with cellular integrins $\alpha v\beta 3$, $\alpha v\beta 5$, $\alpha v\beta 1$, $\alpha 3\beta 1$, or other integrins (Bai et al., 1993; Wickham et al., 1993; Louis et al., 1994; Davison et al., 1997; Li et al., 2001; Salone et al., 2003).

Understanding of this two-step Ad entry pathway explains clinical findings by several groups that have demonstrated that cells expressing low levels of CAR are refractory to Ad infection and gene delivery. Native CAR-dependent tropism results in a scenario wherein non-target but high-CAR cells can be infected while target tissues, if low in CAR, are resistant to Ad infection. Essentially, while Ad delivery is uniquely efficient *in vivo*, the biodistribution of CAR is incompatible with many gene therapy interventions, and *in vivo* co-localization of applied Ad vectors and the receptor is poor (Dmitriev et al., 1998; Miller et al., 1998; Fechner et al., 1999; Li et al., 1999; Cripe et al., 2001).

Based on a clear understanding of native Ad cell recognition, the development of CAR-independent Ad vectors has rationally focused on the fiber protein, the primary determinant of Ad tropism. Ad fiber pseudotyping, the genetic replacement of the knob domain or entire fiber with its structural counterpart from another human Ad serotype, has been employed as a means to derive Ad5-based vectors with CAR-independent tropism by virtue of the natural diversity in receptor recognition found in species B and D Ad fibers, and has identified chimeric vectors with superior infectivity to Ad5 in a variety of clinically relevant

cell types (Gall et al., 1996; Shayakhmetov et al., 2000; Von Seggern et al., 2000; Chiu et al., 2001; Goossens et al., 2001; Havenga et al., 2001; Jakubczak et al., 2001; Havenga et al., 2002; Kanerva et al., 2002).

The development of non-human adenoviruses as gene therapy vehicles has been proposed (Khatri et al., 1997; Rasmussen et al., 1999; Reddy et al., 1999a; Reddy et al., 1999b; Kremer et al., 2000; Löser et al., 2002; Hemminki et al., 2003). The rationale for these efforts has been three-fold: 1) no pre-existing humoral or cellular immunity will exist against "xeno" Ads in the majority of humans (Hofmann et al., 1999; Kremer et al., 2000) 2) several non-human Ads have been demonstrated to efficiently infect human cells without subsequent replication, including canine, bovine and murine mastadenoviruses (Gelhe and Smith, 1969; Nguyen et al., 1999; Rasmussen et al., 1999; Soudais et al., 2000) and ovine atadenovirus (Löser et al., 2000; Kümin et al., 2002) and 3) novel entry biologies of xeno Ads may circumvent CAR deficiency in clinically relevant human target tissues refractory to Ad5-based vectors.

Consistent with these considerations, the 287 isolate of the ovine adenovirus type 7 (OAdV7) has been evaluated as a potential human gene therapy vector (Voeks et al., 2002; Löser et al., 2003; Martiniello-Wilks et al., 2004; Wang et al., 2004). OAdV7 is the prototype isolate of a novel genus of viruses referred to as atadenovirus, due to the high adenine/thymine (A/T) content of its genome (Benko and Harrach, 1998). OAdV7 causes only mild symptoms in sheep and infects numerous human cell types efficiently, although replication in human cells is abortive due to the lack of viral promoter function (Boyle et al., 1994; Khatri et al., 1997; Rothel et al., 1997). OAdV7 displays CAR-independent tropism that is distinct from that of serotype 2 and 5 Ads, utilizing an unknown primary receptor(s) (Xu and Both, 1998). In addition, systemically applied OAdV7 exhibits a distinctive tissue distribution *in vivo* that is less hepatotropic in mice compared to Ad5-based vectors (Hofmann et al., 1999).

OAdV7 tropism is mediated via a 543-residue fiber molecule comprised of a 35 residue N-terminal tail region, a long shaft domain predicted to consists of 25 pseudo-repeats, and a relatively small 121 amino acid C-terminal region comprising the knob domain, (Vrati et al., 1995). In contrast to Ad5, the OAdV7 fiber

does not contain the lysine-rich KKTK sequence found in the third repeat of the Ad5 fiber, a motif suggested to mediate hepatotropism of Ad5 vectors in rodents and primates *in vivo* (Smith et al., 2003a; Smith et al., 2003b). In addition, neither the penton nor fiber of OAdV7 contains an RGD sequence or other identifiable integrin-binding domain, suggesting that interaction with cell-surface integrins may not be required for infection (Vrati et al., 1996; Xu and Both, 1998). Thus, the OAdV7 fiber protein appears to be the sole structural determinant of a unique tropism.

Based on the unique tropism of OAdV7 that combines CAR-independence with a non-hepatotropic biodistribution profile, we hypothesized that an Ad5 vector, containing the OAdV7 fiber as well as its native penton base RGD, would achieve enhanced infectivity of Ad-refractory cell types *in vitro* and liver de-targeted tropism *in vivo*.

RESULTS

Generation of modified Ad5 containing the OAdV7 fiber. The OAdV7 fiber molecule is composed of homotrimers of a 543-amino acid polypeptide. Predicted functional domains within the fiber are the tail domain spanning residues 1 to 35, the shaft domain from 36 to 422 containing approximately 25 pseudorepeats motifs and the 121-amino acid fiber knob domain from 423 to 543 (Vrati et al., 1995). Most mammalian Ads contain a conserved threonine-leucine-tryptophan-threonine (TLWT) motif at the N-terminus of the fiber knob domain, and in human Ad2 and Ad5 a flexible region separating the shaft and the knob domains precedes this motif (van Raaij et al., 1999). The OAdV7 fiber does not contain this motif, thus the start of the knob domain is poorly defined.

Following examination of Ad5 and OAdV7 fiber polypeptide sequences, we identified a common leucine-serine-leucine (LSL) sequence common to both fibers immediately downstream of each tail domain (Fig. 1A). The LSL region was considered a common element in both fibers; therefore we substituted the 44 amino-acid Ad5 tail domain for the native OAdV7 tail domain upstream of the LSL sequence to provide the correct penton base insertion domain for incorporation into the Ad5 capsid. This was accomplished using a two-plasmid rescue system essentially as described (Krasnykh et al., 1996; Glasgow et al., 2004). We constructed an E1-deleted recombinant Ad genome (Ad5Luc1-OvF) containing the chimeric Ad5 tail/OAdV7 fiber gene and a firefly luciferase reporter gene controlled by the CMV immediate early promoter/enhancer in the E1 region. Genomic clones of Ad5Luc1-OvF were sequenced, and two correct clones were chosen. Ad5Luc1-OvF was rescued in 911 cells, and large-scale preparations of Ad5Luc1-OvF were purified by double CsCl gradient centrifugation. The concentration of Ad5Luc1-OvF was 2.7 $x10^{12}$ viral particles (v.p.)/ml while the control vector Ad5Luc1 was 3.74 x 10^{12} v.p./ml. Ad5Luc1 contains the wild type Ad5 fiber and is isogenic to Ad5Luc1-OvF in all respects except for the fiber shaft and knob domains.

We confirmed the fiber knob genotype of Ad5Luc1-OvF via diagnostic PCR, using knob domain-specific primer pairs and genomes from purified virions as PCR templates. Plasmids containing the fiber

sequence of the wild-type OAdV7 fiber (data not shown) or the chimeric fiber gene, were used as positive controls (Fig. 1B). To further confirm that Ad5Luc1-OvF virions contained trimeric fibers, we performed SDS-PAGE followed by Western blot analysis of vector particles. We used the monoclonal 4D2 primary antibody that recognizes the Ad5 fiber tail domain common to both the Ad5 and chimeric OAdV7 fiber molecules. We observed bands at approximately 185 kDa for Ad5Luc1-OvF and control Ad5Luc1 virions, corresponding to trimeric fiber molecules. Bands of boiled samples resolved at an apparent molecular mass of approximately 60-65 kDa, indicative of fiber monomers (Fig. 1C).

Ad5Luc1-OvF vector exhibits expanded tropism and enhanced gene transfer. We hypothesized that the incorporation of the OAdV7 fiber into the Ad5 capsid would provide augmented transduction through expanded Ad vector tropism, including CAR-independent tropism. We therefore evaluated Ad5Luc1-OvF transduction of a panel of cell lines expressing variable levels of CAR (Table 1). As shown in Fig. 2A. Ad5Luc1-OvF provided augmented reporter gene delivery to several CAR-deficient cell lines, with augmentation up to 23-fold compared to Ad5Luc1. Further, Ad5Luc1-OvF increased gene transfer to an unpassaged primary ovarian cancer patient sample as much as 5-fold versus Ad5Luc1 (Fig. 2B). Of interest, Ad5Luc1-OvF gene delivery augmentation to CAR-deficient RD cells (human rhabdomyosarcoma, 1.5-fold), was markedly lower than that to OV-3 cells (human ovarian cancer, 23-fold) and CAR-deficient CHO cells (Chinese hamster ovary, 22-fold), suggesting that RD cells do not express the requisite cell surface molecule(s) for OAdV7 fiber recognition. We also evaluated Ad5Luc1-OvF transduction on a normal human liver epithelial cell line (THLE-3), and observed a 10-fold reduction in gene transfer compared to Ad5Luc1.

Ad5Luc1-OvF exhibits increased cell surface binding in the absence of CAR. To investigate whether Ad5Luc1-OvF mediates increased gene transfer via enhanced cell-surface interaction, we performed cell-binding assays employing FACS-based detection of surface-bound virions. We hypothesized that Ad5Luc1-OvF would display increased attachment to CAR-deficient cells, and possibly CAR-positive cells, compared to Ad5 by virtue of novel virion/cell interaction. For these studies, we selected cell lines that

exhibited distinct gene transfer profiles between Ad5Luc1 and Ad5Luc1-OvF: CAR-deficient CHO cells and the CAR-positive U118-hCAR-tailless cell line that artificially expresses the extracellular domain of human CAR (Kim et al., 2002). Cells were incubated with Ad vectors at 4°C to allow virion attachment, but not internalization, followed by labeling of bound virions with an anti-Ad primary antibody and a FITC-conjugated secondary antibody, with subsequent FACS analysis (see Materials and Methods). As shown in Fig. 3A, surface-bound Ad5Luc1 was detected on 94% of U118-hCAR-tailless cells, while only 8% of these cells were positive for Ad5Luc1-OvF. This observation is consistent with the 100-fold disparity in gene transfer observed for these vectors in the same cell line (Table 1, Fig. 4A). In contrast, only 10% of CAR-negative CHO cells bound Ad5Luc1, while over 60% of CHO cells were positive for Ad5Luc1-OvF (Fig. 3B). These data indicate that a direct positive correlation exists between increased Ad5Luc1-OvF cell-surface interaction and enhanced gene delivery in CAR-deficient cells.

The OAdV7 fiber in Ad5Luc1-OvF dictates CAR-independent tropism. As shown in Table 1 and Fig. 3, Ad5Luc1-OvF gene transfer and cell binding was not dependent on the presence of CAR. To confirm this aspect of Ad5Luc1-OvF tropism, we performed knob-blocking assays using recombinant Ad5 fiber knob protein. As shown in Fig. 4A, Ad5Luc1 exhibited clear CAR-dependent tropism as demonstrated by a 100-fold increase in transgene expression in U118-hCAR-tailless cells versus the CAR-deficient U118MG cell line. Further, preincubation of cells with recombinant Ad5 knob protein at 50μg/ml inhibited 90% and 50% of Ad5 Luc1 gene transfer to U118-hCAR-tailless cells and low-CAR SKOV3.ip1 cells, respectively. (Fig 4B,C). Conversely, Ad5Luc1-OvF gene delivery to U118MG cells was 2-fold higher that that of Ad5Luc1, and transduction of the highly CAR-positive variant line yielded no increase in luciferase values. Further, competitive inhibition with Ad5 knob did not appreciably block Ad5Luc1-OvF-mediated gene transfer in either cell line, confirming the CAR-independent tropism of this vector.

Biodistribution of Ad5Luc1-OvF gene expression in mice. Following confirmation of our first hypothesis that the Ad5Luc1-OvF vector would exhibit enhanced infectivity in low CAR substrates via a novel, non-CAR based tropism, we next addressed the biodistribution profile of Ad5Luc1-OvF. Based on

the biodistribution of intravenously applied OAdV7 in mice (Hofmann et al., 1999) and the lack of the putative heparin sulfate binding motif KKTK in the OAdV7 fiber shaft, we hypothesized that an Ad5 vector containing this fiber would demonstrate decreased hepatotropism *in vivo*. To this end, we evaluated the biodistribution of transgene expression of a panel of Ad vectors including Ad5Luc1-OvF, Ad5Luc1 and Ad5Luc1-ΔKKTK (with the native KKTK sequence deleted from the fiber shaft) as a liver de-targeted control vector, essentially as described (Smith et al., 2003b). For each virus, 8-10 mice per group were injected via the tail vein with 1×10^{11} viral particles. Forty-eight hours post-injection, the liver, spleen, lung, heart and kidney were harvested and homogenized, and luciferase activity and protein concentrations of cleared homogenates were measured. As expected, Ad5Luc1 produced the highest transgene expression in the liver, while Ad5-ΔKKTK vector gene expression in liver was reduced to 1% of control (Fig. 5). In all other organs examined, Ad5-ΔKKTK gene expression was markedly reduced to less than 7% of Ad5Luc1 control levels. Ad5Luc1-OvF gene expression was more evenly distributed among the major organs and was significantly decreased in the liver, to approximately 18% of Ad5Luc1 levels ($p< 0.0028$). Ad5Luc1-OvF gene expression in the heart, spleen and lung was not significantly different from Ad5Luc1. Ad5Luc1-OvF gene expression in the kidney was increased 50-fold versus the Ad5Luc1 control vector ($p<0.042$), resulting in a liver-to-kidney gene expression ratio of 0.59 for Ad5Luc-OvF and 0.002 for Ad5Luc1, a difference of 280-fold.

In the aggregate, Ad5Luc1-OvF, a vector containing fibers from OAdV7 that are unable to bind CAR, demonstrates enhanced gene delivery to CAR-deficient human cells *in vitro* and displays a unique biodistribution characterized by attenuated liver transduction with significant kidney tropism.

DISCUSSION

Despite a variety of avenues explored to improve human adenovirus serotype 5 as a therapeutic agent, this vector exhibits innate drawbacks of CAR-dependency and hepatotropism. Of particular concern is that many clinically important tissues, including several cancer types, are refractory to Ad5 infection due to low CAR expression. Indeed, down regulation of CAR has been reported for several tumor types, including glioma, ovarian, lung, breast and others (Miller et al., 1998; Hemminki and Alvarez, 2002; Bauerschmitz et al., 2002a). As a consequence of limiting CAR levels in many clinically relevant target cells, high Ad vector dosage is often required for *in vivo* efficacy. Given that over 95% of systemically administered Ad particles are sequestered in the liver via hepatic macrophage (Kupffer cell) uptake (Tao et al., 2001) and hepatocyte transduction (Connelly, 1999) of both rodents and primates, therapeutically relevant Ad doses often result in vector-related liver toxicity (Peeters et al., 1996; Lieber et al., 1997; Sullivan et al., 1997; Worgall et al., 1997; Alemany et al., 2000; Shayakhmetov et al., 2004). Thus, Ad vectors exhibiting CAR-independent and/or expanded tropism coupled with low hepatotropism should prove valuable for maximal transduction of low-CAR targets at the lowest possible vector dose.

We sought to achieve this vector design mandate by replacing the Ad5 fiber with the corresponding structure from ovine atadenovirus serotype 7. The fiber of OAdV7 is the only identified structural determinant of native OAdV7 tropism, which is CAR-independent *in vitro* and non-hepatotropic when applied systemically. Genetic incorporation of the OAd7 fiber molecule into the Ad5 virion ablated its CAR-dependence as evidenced by competitive Ad5 knob blocking assays as well as increased cellular attachment to CAR-deficient CHO cells. Our results are consistent with previous findings showing that Ad5 and OAdV7 do not compete with each other for cell entry in cells that both viruses can infect (Xu and Both, 1998). Ad5Luc1-OvF exhibited enhanced infectivity *in vitro*, providing 3- to 23-fold increased gene transfer to several CAR-deficient cell lines and primary ovarian cancer tissue versus Ad5. However, Ad5Luc1-OvF gene transfer to other CAR-deficient human cancer cell lines such as SCC-25, FaDu and LNCaP, as well as the human THLE-3 normal liver cell line, was markedly reduced compared to the Ad5Luc1 control vector.

These findings suggest that the receptor(s) for the OAd7 fiber is not ubiquitously expressed, a biological phenomenon that may provide the basis of a level of cell- or tissue-type selectivity of potential utility.

Intravenous administration of Ad results in accumulation in the liver, spleen, heart, lung, and kidneys of mice, although these tissues may not necessarily be the highest in CAR expression (Reynolds et al., 1999; Wood et al., 1999) This is true with regard to the liver in particular, which sequesters the majority of systemically administered Ad particles via hepatic macrophage (Kupffer cell) uptake (Tao et al., 2001) and hepatocyte transduction, (Connelly, 1999) leading to cytokine release, inflammation and liver toxicity (Peeters et al., 1996; Lieber et al., 1997; Worgall et al., 1997; Shayakhmetov et al., 2004, 2005b). Thus, the nature of adenovirus-host interactions dictating the fate of systemically applied Ad has come under considerable scrutiny.

To this end, attempts to design Ad5 vectors that "detarget" the liver have been based on the assumption that CAR- and integrin-based interactions are required for liver uptake *in vivo*. The majority of attempts to inhibit hepatocyte and/or liver Kupffer cell uptake using Ad5 vectors with ablated CAR- or integrin-binding motifs in the Ad capsid have failed (Alemany and Curiel, 2001; Mizuguchi et al., 2002; Smith et al., 2002; Martin et al., 2003; Smith et al., 2003a), although some mutations of the Ad5 fiber knob have attenuated liver tropism of vectors following systemic administration (Einfeld et al., 2001; Koizumi et al., 2003; Yun et al., 2005). Indeed, recent studies focused on Ad vector biodistribution have demonstrated that Kupffer cell and hepatocyte uptake *in vivo* is largely CAR-independent (Liu et al., 2003; Shayakhmetov et al., 2004), confirming that native Ad5 tropism determinants at work *in vitro* contribute little to vector biodistribution *in vivo*.

The Ad fiber is a major structural determinant of liver tropism *in vivo*, even in the absence of knob/Ad receptor interaction (reviewed by Nicklin et al., 2005). In this regard, Smith and co-workers have examined the role of a putative heparan sulfate proteoglycan (HSPG)-binding motif, KKTK, in the third repeat of the native fiber shaft. Replacement of this motif with an irrelevant GAGA peptide sequence reduced reporter gene expression and Ad DNA in the liver by 90 percent in mice and non-human primates (Smith et al.,

2003a). The authors postulated that removal of the KKTK inhibited Ad5 interaction with heparin sulfate proteoglycans (HSPG) in the liver; however, direct binding of this motif to HSPG has not been demonstrated.

Pseudotyping Ad5 with short-shafted fibers from Ad3, Ad35 or Ad40 that contain no native KKTK results in significant reduction of liver uptake (Table 2) (Nakamura et al.. 2003; Sakurai et al., 2003; Vigne et al., 2003). Further, the use of a shortened Ad5 fiber shaft that retains the native KKTK motif (Vigne et al.. 2003). or replacement of the Ad5 shaft with the short Ad3 shaft domain (Breidenbach et al., 2004) was shown to attenuate liver uptake *in vivo* following intravenous delivery. Indeed, Shayakhmetov and co-workers have recently shown that short-shafted Ad vectors with either CAR- or non-CAR-interacting knob domains do not efficiently interact with hepatocytes *in vivo* and are not taken up by Kupffer cells (Shayakhmetov et al.. 2004).

The Ad5Luc1-OvF fiber contains 25 pseudo-repeats, no KKTK motif, and likely forms a fiber at least as long as the native Ad5 fiber. Long-shafted Ads have been shown to accumulate within liver sinusoids and subsequently infect hepatocytes in a CAR-independent manner (Shayakhmetov et al.. 2004). Thus, our result demonstrating marked reduction of *in vivo* liver gene expression appears to be unique for a long-shafted Ad vector, and is comparable to results obtained with some short-shafted Ads (Table 2). In addition, our findings further support the idea that short-shafted Ad vectors are not liver detargeted due solely to the lack of a KKTK motif.

Recent evidence has highlighted the importance of serum factors in the hepatic uptake of systemically applied Ad vectors. Shayakhmetov and colleagues demonstrated that coagulation factor IX (FIX) and complement component C4-binding protein (C4BP) can direct Ad biodistribution *in vivo* by cross-linking Ad to hepatocellular HSGP and the LDL-receptor related protein. Kupffer cell sequestration of Ad particles was likewise dependent on Ad association with FIX and C4BP (Shayakhmetov et al., 2005a). This work also demonstrated a key vector design approach whereby genetic modification of solvent exposed loop structures in the Ad5 fiber knob attenuated serum factor binding resulting in reduced liver uptake *in vivo*. In

addition to the Ad5Luc1-OvF vector, this serum factor-ablated Ad vector is the only other long shafted liver-detargeted Ad reported to date. Therefore, it is reasonable to posit that reduced liver uptake observed with Ad5Luc1-OvF is the result of the unique structure of the ovine fiber resulting in reduced and/or altered interaction with blood factors that mediate native Ad5 liver uptake.

Gene transfer to the kidney could have significant utility for the treatment of renal disease and in transplantation paradigms (Imai et al., 2004). While Ad, adeno-associated virus (AAV) and retroviral vectors transduce renal cells *in vitro*, systemic delivery of viral vectors has resulted in insufficient gene delivery to the kidney (Moullier et al., 1994; Takeda et al., 2004; Fujishiro et al., 2005). To increase *in vivo* gene transfer to the kidney, perfusion (Heikkila et al., 1996), catheter infusion (Takeda et al., 2004; Fujishiro et al., 2005) and direct interstitial injection (Ortiz et al., 2003) have been employed. Considering the established difficulty of generating Ad-mediated renal gene transfer via systemic injection, our result demonstrating abundant kidney gene expression by Ad5Luc1-OvF is notable. While the mechanism of enhanced kidney gene expression remains under investigation, we interpret this result as a consequence of unique, direct interaction(s) of Ad5Luc1-OvF with kidney and/or renal vasculature, and not solely as a result of decreased liver sequestration, since other Ad vectors exhibiting decreased hepatotropism have not demonstrated appreciable novel tissue tropism (Table 2).

The kidney is a complex organ with numerous specialized compartments including the glomeruli, tubules, interstitium and vasculature. The glomerular capillary endothelium is fenestrated, resulting in the "leaky" vasculature that would allow intravenous Ad vectors to contact the underlying filtration membrane and access to the epithelium of the renal tubule system. Indeed, injection of an Ad vector directly into the renal artery can result in gene transfer to cells of the proximal tubule (Moullier et al., 1994). Given the unique renal localization observed, we are currently extending our studies to determine the precise localization of Ad5Luc1-OvF gene expression within kidney substructures.

To our knowledge, this is the first report of a fiber-pseudotyped Ad vector that simultaneously displays decreased hepatotropism and a distinct organ tropism *in vivo*. Further, this novel redirection of vector

biodistribution is directly attributable to fiber replacement with a non-CAR binding long-shafted fiber, an outcome seemingly at odds with recent fiber pseudotyping reports employing short-shafted vectors. *In vitro*, Ad5Luc1-OvF displays CAR-independent tropism with a positive correlation between increased Ad5Luc1-OvF cell-surface interaction and enhanced gene delivery in CAR-deficient cells, suggesting the use of as-yet unidentified receptor molecule(s). In addition, this vector may prove useful in murine models of renal disease.

MATERIALS AND METHODS

Cell lines

The Ad5 DNA-transformed 293 human embryonic cell line was purchased from Microbix (Toronto, ON, Canada). Human embryonic rhabdomyosarcoma RD cells, CAR-negative human U118 MG glioma cells, PC-3 and LNCaP human prostate cancer cells, MCF7 human breast cancer cells, T24 human bladder cancer cells, Chinese hamster ovary cells (CHO), human squamous cell carcinoma SCC-4 and SCC-25 cells, FaDu human pharynx cancer cells, HeLa and SKOV ovarian cancer cells, LoVo colon cancer cells and OV-3 ovarian cancer cells were obtained from the American Type Culture Collection (ATCC) (Manassas, VA). The human ovarian adenocarcinoma cell lines Hey, SKOV3.ip1, and OV-4 were obtained from Drs. Judy Wolf, Janet Price (both of M.D. Anderson Cancer Center, Houston, TX), and Timothy J. Eberlein, (Harvard Medical School, Boston, MA), respectively. U118-hCAR-tailless cells, which express a truncated form of human CAR comprising the extracellular domain, transmembrane domain, and the first two amino acids from the cytoplasmic domain (Wang and Bergelson, 1999), have been described previously (Kim et al., 2003). All cell lines were cultured at 37°C in 5% CO_2 using culture media recommended by each respective supplier. FCS was purchased from Gibco-BRL (Grand Island, NY) and media and supplements were from Mediatech (Herndon, VA).

Precision-Cut Human Ovarian Cancer Slices

Human ovarian cancer tissue was obtained from livers taken from ovarian cancer patients following institutional review board approval. This procedure has been described previously (Kirby et al., 2004). Briefly, excess material was received from the Department of Obstetrics and Gynecology, the University of Alabama at Birmingham Hospital. Precision-cut ovarian cancer slices (diameter 4 mm, thickness 150 µm) were prepared using a Krumdiek Tissue Slicer (Alabama Research and Development, Munford, AL). Each slice was transferred into a well of a 24-well plate containing 1 ml William's Medium E and placed on a rocker. Liver slices were maintained at 37°C in a 5% CO_2 environment on a rocker and allowed to preincubate for 2 hours before treatment. Ovarian cancer slices were infected with 100 and 1000 vp/cell

with Ad5Luc1 Ad5/OAdV7, or no virus. Ovarian cancer slices were harvested and frozen at 24 hours after infection. Gene transfer was determined using a luciferase activity assay system (Promega, Madison, WI) according to the manufacturer's instructions.

Flow cytometry

Cells grown in T75 flasks were removed by addition of EDTA in PBS and resuspended in PBS containing 1% bovine serum albumin (BSA). Cells (2×10^5) were incubated with 3.5×10^9 viral particles of adenovirus, or buffer only, for 1 hr at 4°C in 250 µl PBS-BSA. Cells were then washed twice in 4 ml cold PBS-BSA and incubated with a 1:500 dilution of polyclonal rabbit anti-Ad5 antiserum (Cocalico Biologicals, Reamstown, PA) at 4°C in 250 µl PBS-BSA. Cells were washed twice in 4 ml cold PBS-BSA and incubated in 250 µl of a 1:150 dilution of FITC-labeled goat anti-rabbit IgG secondary antibody (Jackson Immunoresearch Labs, West Grove, PA) for 1 hr in PBS-BSA at 4°C. Flow cytometry analysis was performed at the UAB FACS Core Facility using FACScan (Beckton Dickenson, San Jose, CA).

Plasmid construction

To create the chimeric fiber used in this study, we fused the Ad5 tail domain to the OAdV7 fiber shaft and knob domains. A 1553-bp PCR product containing a 5' *Sca*I site, the OAdV7 fiber shaft and knob domains and a 3' *Mun*I site was amplified from plasmid pAK containing the right hand *Bam*HI fragment of the OAdV7 genome cloned into Bluescribe M13+ *Bam*HI/*Hin*cII sites. The forward primer designated OAdS*Sca*IF was 5'-AGC GAA GGG TTA GTA CTA TCT TTA AAC-3' and the reverse primer was designated OAd*Mun*I-R2 5'-TCA TAC AAT TGT TTA **TTA** TTG TCT GAA TTG-3'. The underlined bases indicate insertion of restriction sites and the stop codon is shown in bold. Next, a PCR product containing a 5' *Pac*I site, the Ad5 tail domain and a 3' *Sca*I site was amplified from plasmid pNEB.PK.3.6, a pNEB193-based shuttle vector containing the Ad5 fiber (Krasnykh et al., 1996). The forward primer is designated NEB36*Pac*IF 5'-ATT ACG CCA AGC TTG CAT GCC TGC-3' and reverse primer NEB36*Sca*IR 5'-GCA AAG AGA GTA CTC CAG GGG GAC-3'. This PCR product was then digested with *Pac*I and *Sca*I and gel purified. Shuttle vector pNEB.PK.3.6-OvF was created by a 3-piece

ligation of *Pac*I/*Mun*I-digested pNEB.PK.3.6 and the two digested PCR fragments containing the Ad5 tail region and the OAdV7 shaft and knob domains. Direct sequencing confirmed that the coding region for the chimeric fiber was correct.

Generation of recombinant adenovirus.

Recombinant Ad5 genomes containing the chimeric OAdV7 fiber gene were derived by homologous recombination in *E. coli* BJ5183 with *Swa*I-linearized rescue plasmid pVK700 (Belousova et al., 2002) and the fiber-containing *Pac*I-*Kpn*I-fragment of the shuttle vector pNEB.PK.3.6-OvF (described above) essentially as described (Krasnykh et al., 1998). pVK700 is derived from pTG3602 (Chartier et al., 1996), but contains an almost complete deletion of the fiber gene and contains a firefly luciferase reporter gene driven by the cytomegalovirus immediate early promoter in place of the E1 region. Genomic clones were sequenced and analyzed by PCR prior to transfection of 911 cells. Ad5Luc1 is a replication-defective E1-deleted Ad vector containing a firefly luciferase reporter gene in the E1 region driven by the cytomegalovirus immediate early promoter/enhancer (Krasnykh et al., 2001). All vectors were propagated on 911 cells and purified by equilibrium centrifugation in CsCl gradients by a standard protocol. Viral particle (v.p.) concentration was determined at 260 nm by the method of Maizel et al. (Maizel et al., 1968) by using a conversion factor of 1.1×10^{12} v.p./absorbance unit.

Western blot analysis

Aliquots of Ad vectors containing 2.0×10^{10} viral particles were diluted into Laemmli buffer and incubated at room temperature or 99° C for 15 min and loaded onto a 4-20% gradient SDS-polyacrylamide gel (Bio-Rad, Hercules, CA). Following electrophoretic protein separation, proteins were electroblotted onto a PVDF membrane. The primary antibody (monoclonal 4D2 recognizing the Ad5 fiber tail domain) was diluted 1:3000 (Lab Vision, Freemont, CA). Immunoblots were developed by addition of a secondary horseradish peroxidase-conjugated anti-mouse immunoglobulin antibody at a 1:3000 dilution (Dako Corporation, Carpentaria, CA), followed by incubation with 3-3'-diaminobenzene peroxidase substrate (DAB; Sigma Company, St. Louis, MO).

Recombinant fiber knob proteins

The knob domain of Ad5 was expressed in E. coli with an N-terminus 6-histidine tag using the pQE81 expression plasmid (Qiagen, Hilden, Germany). The Ad5 fiber knob domain was PCR amplified using primers that amplified the entire fiber knob domain and the three carboxy-terminal fiber shaft repeats using the following primers: Ad5 (fwd) 5'-CAAACAC***GG***ATCCCCTCAAAACAAAA-3' and (rev) 5'-TTTATTATTCTTGGGCAATGTATGA-3' using plasmid pNEB.PK.3.6 as the template. The forward primer contains a 2-bp mutation (in bold) that creates a 5'-end *Bam*HI restriction site (underlined). The stop codon (TAA) and polyadenylation signal (AATAAA) are underlined in the reverse primer. The PCR products containing the Ad5 fiber knob region was digested with *Bam*HI, gel purified, and ligated into *Bam*HI-*Sma*I-digested pQE81. The resulting plasmid, pQE81-Ad5 was sequenced to identify correct clones. The expression plasmid was introduced into E. coli, and 6-His-containing fiber knob proteins from bacterial cultures were purified on nickel-nitrilotriacetic acid (Ni-NTA) agarose columns (Qiagen). The ability to form trimers was confirmed by Western blot analysis of boiled and unboiled purified knob proteins using a mouse penta-His monoclonal antibody (Qiagen) and a horseradish peroxidase-conjugated anti-mouse immunoglobulin antibody at a 1:3000 dilution (DAKO Corporation), followed by incubation with 3-3'-diaminobenzene peroxidase substrate (DAB; Sigma Company). Concentration of purified knob proteins was determined by the method of Lowry (Bio-Rad).

In Vitro Ad-mediated gene transfer experiments

For virus gene transfer experiments using adherent cell lines, cells were grown in wells of 24-well plates and were incubated for 1 hr at 37°C with each Ad vector diluted to 100 v.p./cell in 500 µl of transduction media containing 2% FCS. Following the incubation, cells were rinsed in transduction media and were maintained at 37°C in an atmosphere of 5% CO_2. Cells were harvested 24 hr post transduction and gene transfer was determined using a luciferase activity assay system (Promega, Madison, WI) according to the manufacturer's instructions.

For experiments containing blocking agents, recombinant fiber knob proteins at 0.5, 5.0 and 50 μg/ml final concentration were incubated with the cells at 37°C in transduction media 15 min before the addition of the virus. Following the transduction, cells were rinsed with transduction media to remove unbound virus and blocking agent, and were maintained at 37°C in an atmosphere of 5% CO_2.

Animals

Mice were obtained at 4 to 6 weeks of age and quarantined at least 1 week before the study. Mice were kept under pathogen-free conditions according to the American Association for Accreditation of Laboratory Animal Care guidelines. Animal protocols were reviewed and approved by the Institutional Animal Care and Use Committee of UAB.

Biodistribution

Female C57BL/6 mice (Charles River Laboratories, Wilmington, MA), aged 6-8 weeks were injected intravenously through the lateral tail vein with 1 x 10^{11} v.p. of Ad5Luc1, Ad5Luc1-OvF, and Ad5-ΔKKTK in 100μl of PBS. After 48 hours mice were sacrificed and livers, lungs, spleens, hearts and kidneys were harvested and representative sections were frozen in the liquid nitrogen immediately. The frozen organ samples were homogenized with a Mini Beadbeater (BioSpec Products, Inc., Bartlesville, OK) in 2 ml micro-tubes (Research Product International Corp., Mt. Prospect, IL) within 100 μl of 1.0 mm zirconia/silica beads (BioSpec Products, Inc.) and 1 ml of Cell Culture Lysis Buffer (Promega), then centrifuged at 14,000 rpm for 2 min. Luciferase activity was measured as before. Mean background luciferase activity was subtracted. All luciferase activities were normalized by protein concentration in the tissue lysates. Protein concentrations were determined using a Bio-Rad DC protein assay kit (Bio-Rad, Hercules, CA).

Statistics

Data were presented as mean values +/- deviation. Statistical differences among groups were assessed by a two-tailed *t*-test assuming unequal variance between groups for increased stringency; $p < 0.05$ was considered significant.

Acknowledgements

This work was supported by grants from the National Institutes of Health: 2R01CA083821 and 1P01HL076540, and from the US Department of Defense: DOD W81XWH-05-1-0035.

REFERENCES

Alemany, R., and Curiel, D. T. 2001. CAR-binding ablation does not change biodistribution and toxicity of adenoviral vectors. Gene Ther 8(17), 1347-53.

Alemany, R., Suzuki, K., and Curiel, D. T. 2000. Blood clearance rates of adenovirus type 5 in mice. J Gen Virol 81(Pt 11), 2605-9.

Bai, M., Harfe, B., and Freimuth, P. 1993. Mutations that alter an Arg-Gly-Asp (RGD) sequence in the adenovirus type 2 penton base protein abolish its cell-rounding activity and delay virus reproduction in flat cells. J Virol 67(9), 5198-205.

Bauerschmitz, G. J., Barker, S. D., and Hemminki, A. 2002a. Adenoviral gene therapy for cancer: From vectors to targeted and replication competent agents (Review). Int J Oncol 21(6), 1161-74.

Belousova, N., Krendelchtchikova, V., Curiel, D. T., and Krasnykh, V. 2002. Modulation of adenovirus vector tropism via incorporation of polypeptide ligands into the fiber protein. J Virol 76(17), 8621-31.

Benko, M., and Harrach, B. 1998. A proposal for a new (third) genus within the family Adenoviridae. Arch Virol 143(4), 829-37.

Bergelson, J. M., Cunningham, J. A., Droguett, G., Kurt-Jones, E. A., Krithivas, A., Hong, J. S., Horwitz, M. S., Crowell, R. L., and Finberg, R. W. 1997. Isolation of a common receptor for Coxsackie B viruses and adenoviruses 2 and 5. Science 275(5304), 1320-3.

Boyle, D. B., Pye, A. D., Kocherhans, R., Adair, B. M., Vrati, S., and Both, G. W. 1994. Characterisation of Australian ovine adenovirus isolates. Vet Microbiol 41(3), 281-91.

Breidenbach, M., Rein, D. T., Wang, M., Nettelbeck, D. M., Hemminki, A., Ulasov, I., Rivera, A. R., Everts, M., Alvarez, R. D., Douglas, J. T., and Curiel, D. T. 2004. Genetic replacement of the adenovirus shaft fiber reduces liver tropism in ovarian cancer gene therapy. Hum Gene Ther 15(5), 509-18.

Chartier, C., Degryse, E., Gantzer, M., Dieterle, A., Pavirani, A., and Mehtali, M. 1996. Efficient generation of recombinant adenovirus vectors by homologous recombination in Escherichia coli. J Virol 70(7), 4805-10.

Chiu, C. Y., Wu, E., Brown, S. L., Von Seggern, D. J., Nemerow, G. R., and Stewart, P. L. 2001. Structural analysis of a fiber-pseudotyped adenovirus with ocular tropism suggests differential modes of cell receptor interactions. J Virol 75(11), 5375-80.

Connelly, S. 1999. Adenoviral vectors for liver-directed gene therapy. Curr Opin Mol Ther 1(5), 565-72.

Cripe, T. P., Dunphy, E. J., Holub, A. D., Saini, A., Vasi, N. H., Mahller, Y. Y., Collins, M. H., Snyder, J. D., Krasnykh, V., Curiel, D. T., Wickham, T. J., DeGregori, J., Bergelson, J. M., and Currier, M. A. 2001. Fiber knob modifications overcome low, heterogeneous expression of the coxsackievirus-adenovirus receptor that limits adenovirus gene transfer and oncolysis for human rhabdomyosarcoma cells. Cancer Res 61(7), 2953-60.

Davison, E., Diaz, R. M., Hart, I. R., Santis, G., and Marshall, J. F. 1997. Integrin alpha5beta1-mediated adenovirus infection is enhanced by the integrin-activating antibody TS2/16. J Virol 71(8), 6204-7.

Dmitriev, I., Krasnykh, V., Miller, C. R., Wang, M., Kashentseva, E., Mikheeva, G., Belousova, N., and Curiel, D. T. 1998. An adenovirus vector with genetically modified fibers demonstrates expanded tropism via utilization of a coxsackievirus and adenovirus receptor-independent cell entry mechanism. J Virol 72(12), 9706-13.

Einfeld, D. A., Schroeder, R., Roelvink, P. W., Lizonova, A., King, C. R., Kovesdi, I., and Wickham, T. J. 2001. Reducing the native tropism of adenovirus vectors requires removal of both CAR and integrin interactions. J Virol 75(23), 11284-91.

Fechner, H., Haack, A., Wang, H., Wang, X., Eizema, K., Pauschinger, M., Schoemaker, R., Veghel, R., Houtsmuller, A., Schultheiss, H. P., Lamers, J., and Poller, W. 1999. Expression of coxsackie adenovirus receptor and alphav-integrin does not correlate with adenovector targeting in vivo indicating anatomical vector barriers. Gene Ther 6(9), 1520-35.

Fujishiro, J., Takeda, S., Takeno, Y., Takeuchi, K., Ogata, Y., Takahashi, M., Hakamata, Y., Kaneko, T., Murakami, T., Okada, T., Ozawa, K., Hashizume, K., and Kobayashi, E. 2005. Gene transfer to the rat kidney in vivo and ex vivo using an adenovirus vector: factors influencing transgene expression. Nephrol Dial Transplant 20(7), 1385-91.

Gall, J., Kass-Eisler, A., Leinwand, L., and Falck-Pedersen, E. 1996. Adenovirus type 5 and 7 capsid chimera: fiber replacement alters receptor tropism without affecting primary immune neutralization epitopes. J Virol 70(4), 2116-23.

Gelhe, W. D., and Smith, K. O. 1969. Abortive infection of human cell cultures by a canine adenovirus. Proc Soc Exp Biol Med 131, 87-93.

Glasgow, J. N., Kremer, E. J., Hemminki, A., Siegal, G. P., Douglas, J. T., and Curiel, D. T. 2004. An adenovirus vector with a chimeric fiber derived from canine adenovirus type 2 displays novel tropism. Virology 324(1), 103-16.

Goossens, P. H., Havenga, M. J., Pieterman, E., Lemckert, A. A., Breedveld, F. C., Bout, A., and Huizinga, T. W. 2001. Infection efficiency of type 5 adenoviral vectors in synovial tissue can be enhanced with a type 16 fiber. Arthritis Rheum 44(3), 570-7.

Havenga, M. J., Lemckert, A. A., Grimbergen, J. M., Vogels, R., Huisman, L. G., Valerio, D., Bout, A., and Quax, P. H. 2001. Improved adenovirus vectors for infection of cardiovascular tissues. J Virol 75(7), 3335-42.

Havenga, M. J., Lemckert, A. A., Ophorst, O. J., van Meijer, M., Germeraad, W. T., Grimbergen, J., van Den Doel, M. A., Vogels, R., van Deutekom, J., Janson, A. A., de Bruijn, J. D., Uytdehaag, F., Quax, P. H., Logtenberg, T., Mehtali, M., and Bout, A. 2002. Exploiting the natural diversity in adenovirus tropism for therapy and prevention of disease. J Virol 76(9), 4612-20.

Heikkila, P., Parpala, T., Lukkarinen, O., Weber, M., and Tryggvason, K. 1996. Adenovirus-mediated gene transfer into kidney glomeruli using an ex vivo and in vivo kidney perfusion system - first steps towards gene therapy of Alport syndrome. Gene Ther 3(1), 21-7.

Hemminki, A., and Alvarez, R. D. 2002. Adenoviruses in oncology: a viable option? BioDrugs 16(2), 77-87.

Hemminki, A., Kanerva, A., Kremer, E. J., Bauerschmitz, G. J., Smith, B. F., Conductier, G., Liu, B., Wang, M., Desmond, R. A., Barnett, B. G., Baker, H. J., Siegal, G., and Curiel, D. 2003. A canine conditionally replicating adenovirus for evaluating oncolytic virotherapy in a syngeneic animal model. Mol. Ther. 7(2), 163-173.

Henry, L. J., Xia, D., Wilke, M. E., Deisenhofer, J., and Gerard, R. D. 1994. Characterization of the knob domain of the adenovirus type 5 fiber protein expressed in Escherichia coli. J Virol 68(8), 5239-46.

Hofmann, C., Löser, P., Cichon, G., Arnold, W., Both, G. W., and Strauss, M. 1999. Ovine adenovirus vectors overcome preexisting humoral immunity against human adenoviruses in vivo. J Virol 73(8), 6930-6.

Imai, E., Takabatake, Y., Mizui, M., and Isaka, Y. 2004. Gene therapy in renal diseases. Kidney Int 65(5), 1551-5.

Jakubczak, J. L., Rollence, M. L., Stewart, D. A., Jafari, J. D., Von Seggern, D. J., Nemerow, G. R., Stevenson, S. C., and Hallenbeck, P. L. 2001. Adenovirus type 5 viral particles pseudotyped with mutagenized fiber proteins show diminished infectivity of coxsackie B-adenovirus receptor-bearing cells. J Virol 75(6), 2972-81.

Kanerva, A., Mikheeva, G. V., Krasnykh, V., Coolidge, C. J., Lam, J. T., Mahasreshti, P. J., Barker, S. D., Straughn, M., Barnes, M. N., Alvarez, R. D., Hemminki, A., and Curiel, D. T. 2002. Targeting adenovirus to the serotype 3 receptor increases gene transfer efficiency to ovarian cancer cells. Clin Cancer Res 8(1), 275-80.

Khatri, A., Xu, Z. Z., and Both, G. W. 1997. Gene expression by atypical recombinant ovine adenovirus vectors during abortive infection of human and animal cells in vitro. Virology 239(1), 226-37.

Kim, M., Zinn, K. R., Barnett, B. G., Sumerel, L. A., Krasnykh, V., Curiel, D. T., and Douglas, J. T. 2002. The therapeutic efficacy of adenoviral vectors for cancer gene therapy is limited by a low level of primary adenovirus receptors on tumour cells. Eur J Cancer 38(14), 1917-26.

Kirby, T. O., Rivera, A., Rein, D., Wang, M., Ulasov, I., Breidenbach, M., Kataram, M., Contreras, J. L., Krumdieck, C., Yamamoto, M., Rots, M. G., Haisma, H. J., Alvarez, R. D., Mahasreshti, P. J., and Curiel, D. T. 2004. A novel ex vivo model system for evaluation of conditionally replicative adenoviruses therapeutic efficacy and toxicity. Clin Cancer Res 10(24), 8697-703.

Koizumi, N., Mizuguchi, H., Sakurai, F., Yamaguchi, T., Watanabe, Y., and Hayakawa, T. 2003. Reduction of natural adenovirus tropism to mouse liver by fiber-shaft exchange in combination with both CAR- and alphav integrin-binding ablation. J Virol 77(24), 13062-72.

Krasnykh, V., Belousova, N., Korokhov, N., Mikheeva, G., and Curiel, D. T. 2001. Genetic targeting of an adenovirus vector via replacement of the fiber protein with the phage T4 fibritin. J Virol 75(9), 4176-83.

Krasnykh, V., Dmitriev, I., Mikheeva, G., Miller, C. R., Belousova, N., and Curiel, D. T. 1998. Characterization of an adenovirus vector containing a heterologous peptide epitope in the HI loop of the fiber knob. J Virol 72(3), 1844-52.

Krasnykh, V. N., Mikheeva, G. V., Douglas, J. T., and Curiel, D. T. 1996. Generation of recombinant adenovirus vectors with modified fibers for altering viral tropism. J Virol 70(10), 6839-46.

Kremer, E. J., Boutin, S., Chillon, M., and Danos, O. 2000. Canine adenovirus vectors: an alternative for adenovirus-mediated gene transfer. J Virol 74(1), 505-12.

Kümin, D., Hofmann, C., Rudolph, M., Both, G. W., and Löser, P. 2002. Biology of ovine adenovirus infection of nonpermissive cells. J Virol 76(21), 10882-93.

Li, E., Brown, S. L., Stupack, D. G., Puente, X. S., Cheresh, D. A., and Nemerow, G. R. 2001. Integrin alpha(v)beta1 is an adenovirus coreceptor. J Virol 75(11), 5405-9.

Li, Y., Pong, R. C., Bergelson, J. M., Hall, M. C., Sagalowsky, A. I., Tseng, C. P., Wang, Z., and Hsieh, J. T. 1999. Loss of adenoviral receptor expression in human bladder cancer cells: a potential impact on the efficacy of gene therapy. Cancer Res 59(2), 325-30.

Lieber, A., He, C. Y., Meuse, L., Schowalter, D., Kirillova, I., Winther, B., and Kay, M. A. 1997. The role of Kupffer cell activation and viral gene expression in early liver toxicity after infusion of recombinant adenovirus vectors. J Virol 71(11), 8798-807.

Liu, Q., Zaiss, A. K., Colarusso, P., Patel, K., Haljan, G., Wickham, T. J., and Muruve, D. A. 2003. The role of capsid-endothelial interactions in the innate immune response to adenovirus vectors. Hum Gene Ther 14(7), 627-43.

Löser, P., Hillgenberg, M., Arnold, W., Both, G. W., and Hofmann, C. 2000. Ovine adenovirus vectors mediate efficient gene transfer to skeletal muscle. Gene Ther 7(17), 1491-8.

Löser, P., Hofmann, C., Both, G. W., Uckert, W., and Hillgenberg, M. 2003. Construction, rescue, and characterization of vectors derived from ovine atadenovirus. J Virol 77(22), 11941-51.

Löser, P., Huser, A., Hillgenberg, M., Kümin, D., Both, G. W., and Hofmann, C. 2002. Advances in the development of non-human viral DNA-vectors for gene delivery. Curr Gene Ther 2(2), 161-71.

Louis, N., Fender, P., Barge, A., Kitts, P., and Chroboczek, J. 1994. Cell-binding domain of adenovirus serotype 2 fiber. J Virol 68(6), 4104-6.

Maizel, J. V., Jr., White, D. O., and Scharff, M. D. 1968. The polypeptides of adenovirus. I. Evidence for multiple protein components in the virion and a comparison of types 2, 7A, and 12. Virology 36(1), 115-25.

Martin, K., Brie, A., Saulnier, P., Perricaudet, M., Yeh, P., and Vigne, E. 2003. Simultaneous CAR- and alpha V integrin-binding ablation fails to reduce Ad5 liver tropism. Mol Ther 8(3), 485-94.

Martiniello-Wilks, R., Wang, X. Y., Voeks, D. J., Dane, A., Shaw, J. M., Mortensen, E., Both, G. W., and Russell, P. J. 2004. Purine nucleoside phosphorylase and fludarabine phosphate gene-directed enzyme prodrug therapy suppresses primary tumour growth and pseudo-metastases in a mouse model of prostate cancer. J Gene Med 6(12), 1343-57.

Miller, C. R., Buchsbaum, D. J., Reynolds, P. N., Douglas, J. T., Gillespie, G. Y., Mayo, M. S., Raben, D., and Curiel, D. T. 1998. Differential susceptibility of primary and established human glioma cells to adenovirus infection: targeting via the epidermal growth factor receptor achieves fiber receptor-independent gene transfer. Cancer Res 58(24), 5738-48.

Mizuguchi, H., Koizumi, N., Hosono, T., Ishii-Watabe, A., Uchida, E., Utoguchi, N., Watanabe, Y., and Hayakawa, T. 2002. CAR- or alphav integrin-binding ablated adenovirus vectors, but not fiber-modified vectors containing RGD peptide, do not change the systemic gene transfer properties in mice. Gene Ther 9(12), 769-76.

Moullier, P., Friedlander, G., Calise, D., Ronco, P., Perricaudet, M., and Ferry, N. 1994. Adenoviral-mediated gene transfer to renal tubular cells in vivo. Kidney Int 45(4), 1220-5.

Nakamura, T., Sato, K., and Hamada, H. 2003. Reduction of natural adenovirus tropism to the liver by both ablation of fiber-coxsackievirus and adenovirus receptor interaction and use of replaceable short fiber. J Virol 77(4), 2512-21.

Nguyen, T., Nery, J., Joseph, S., Rocha, C., Carney, G., Spindler, K., and Villarreal, L. 1999. Mouse adenovirus (MAV-1) expression in primary human endothelial cells and generation of a full-length infectious plasmid. Gene Ther 6(7), 1291-7.

Nicklin, S. A., Wu, E., Nemerow, G. R., and Baker, A. H. 2005. The influence of adenovirus fiber structure and function on vector development for gene therapy. Mol Ther 12(3), 384-93.

Ortiz, P. A., Hong, N. J., Plato, C. F., Varela, M., and Garvin, J. L. 2003. An in vivo method for adenovirus-mediated transduction of thick ascending limbs. Kidney Int 63(3), 1141-9.

Peeters, M. J., Patijn, G. A., Lieber, A., Meuse, L., and Kay, M. A. 1996. Adenovirus-mediated hepatic gene transfer in mice: comparison of intravascular and biliary administration. Hum Gene Ther 7(14), 1693-9.

Rasmussen, U. B., Benchaibi, M., Meyer, V., Schlesinger, Y., and Schughart, K. 1999. Novel human gene transfer vectors: evaluation of wild-type and recombinant animal adenoviruses in human-derived cells. Hum Gene Ther 10(16), 2587-99.

Reddy, P. S., Idamakanti, N., Chen, Y., Whale, T., Babiuk, L. A., Mehtali, M., and Tikoo, S. K. 1999a. Replication-defective bovine adenovirus type 3 as an expression vector. J Virol 73(11), 9137-44.

Reddy, P. S., Idamakanti, N., Hyun, B. H., Tikoo, S. K., and Babiuk, L. A. 1999b. Development of porcine adenovirus-3 as an expression vector. J Gen Virol 80 (Pt 3), 563-70.

Reynolds, P., Dmitriev, I., and Curiel, D. 1999. Insertion of an RGD motif into the HI loop of adenovirus fiber protein alters the distribution of transgene expression of the systemically administered vector. Gene Ther 6(7), 1336-9.

Rothel, J. S., Boyle, D. B., Both, G. W., Pye, A. D., Waterkeyn, J. G., Wood, P. R., and Lightowlers, M. W. 1997. Sequential nucleic acid and recombinant adenovirus vaccination induces host-protective immune responses against Taenia ovis infection in sheep. Parasite Immunol 19(5), 221-7.

Sakurai, F., Mizuguchi, H., Yamaguchi, T., and Hayakawa, T. 2003. Characterization of in vitro and in vivo gene transfer properties of adenovirus serotype 35 vector. Mol Ther 8(5), 813-21.

Salone, B., Martina, Y., Piersanti, S., Cundari, E., Cherubini, G., Franqueville, L., Failla, C. M., Boulanger, P., and Saggio, I. 2003. Integrin alpha3beta1 is an alternative cellular receptor for adenovirus serotype 5. J Virol 77(24), 13448-54.

Shayakhmetov, D. M., Gaggar, A., Ni, S., Li, Z. Y., and Lieber, A. 2005a. Adenovirus binding to blood factors results in liver cell infection and hepatotoxicity. J Virol 79(12), 7478-91.

Shayakhmetov, D. M., Li, Z. Y., Ni, S., and Lieber, A. 2004. Analysis of adenovirus sequestration in the liver, transduction of hepatic cells, and innate toxicity after injection of fiber-modified vectors. J Virol 78(10), 5368-81.

Shayakhmetov, D. M., Li, Z. Y., Ni, S., and Lieber, A. 2005b. Interference with the IL-1-signaling pathway improves the toxicity profile of systemically applied adenovirus vectors. J Immunol 174(11), 7310-9.

Shayakhmetov, D. M., Papayannopoulou, T., Stamatoyannopoulos, G., and Lieber, A. 2000. Efficient gene transfer into human CD34(+) cells by a retargeted adenovirus vector. J Virol 74(6), 2567-83.

Smith, T., Idamakanti, N., Kylefjord, H., Rollence, M., King, L., Kaloss, M., Kaleko, M., and Stevenson, S. C. 2002. In vivo hepatic adenoviral gene delivery occurs independently of the coxsackievirus-adenovirus receptor. Mol Ther 5(6), 770-9.

Smith, T. A., Idamakanti, N., Marshall-Neff, J., Rollence, M. L., Wright, P., Kaloss, M., King, L., Mech, C., Dinges, L., Iverson, W. O., Sherer, A. D., Markovits, J. E., Lyons, R. M., Kaleko, M., and Stevenson, S. C. 2003a. Receptor interactions involved in adenoviral-mediated gene delivery after systemic administration in non-human primates. Hum Gene Ther 14(17), 1595-604.

Smith, T. A., Idamakanti, N., Rollence, M. L., Marshall-Neff, J., Kim, J., Mulgrew, K., Nemerow, G. R., Kaleko, M., and Stevenson, S. C. 2003b. Adenovirus serotype 5 fiber shaft influences in vivo gene transfer in mice. Hum Gene Ther 14(8), 777-87.

Soudais, C., Boutin, S., Hong, S. S., Chillon, M., Danos, O., Bergelson, J. M., Boulanger, P., and Kremer, E. J. 2000. Canine adenovirus type 2 attachment and internalization: coxsackievirus-adenovirus receptor, alternative receptors, and an RGD-independent pathway. J Virol 74(22), 10639-49.

Sullivan, D. E., Dash, S., Du, H., Hiramatsu, N., Aydin, F., Kolls, J., Blanchard, J., Baskin, G., and Gerber, M. A. 1997. Liver-directed gene transfer in non-human primates. Hum Gene Ther 8(10), 1195-206.

Takeda, S., Takahashi, M., Mizukami, H., Kobayashi, E., Takeuchi, K., Hakamata, Y., Kaneko, T., Yamamoto, H., Ito, C., Ozawa, K., Ishibashi, K., Matsuzaki, T., Takata, K., Asano, Y., and Kusano, E. 2004. Successful gene transfer using adeno-associated virus vectors into the kidney: comparison among adeno-associated virus serotype 1-5 vectors in vitro and in vivo. Nephron Exp Nephrol 96(4), e119-26.

Tao, N., Gao, G. P., Parr, M., Johnston, J., Baradet, T., Wilson, J. M., Barsoum, J., and Fawell, S. E. 2001. Sequestration of adenoviral vector by Kupffer cells leads to a nonlinear dose response of transduction in liver. Mol Ther 3(1), 28-35.

Tomko, R. P., Xu, R., and Philipson, L. 1997. HCAR and MCAR: the human and mouse cellular receptors for subgroup C adenoviruses and group B coxsackieviruses. Proc Natl Acad Sci U S A 94(7), 3352-6.

van Raaij, M. J., Mitraki, A., Lavigne, G., and Cusack, S. 1999. A triple beta-spiral in the adenovirus fibre shaft reveals a new structural motif for a fibrous protein. Nature 401(6756), 935-8.

Vigne, E., Dedieu, J. F., Brie, A., Gillardeaux, A., Briot, D., Benihoud, K., Latta-Mahieu, M., Saulnier, P., Perricaudet, M., and Yeh, P. 2003. Genetic manipulations of adenovirus type 5 fiber resulting in liver tropism attenuation. Gene Ther 10(2), 153-62.

Voeks, D., Martiniello-Wilks, R., Madden, V., Smith, K., Bennetts, E., Both, G. W., and Russell, P. J. 2002. Gene therapy for prostate cancer delivered by ovine adenovirus and mediated by purine nucleoside phosphorylase and fludarabine in mouse models. Gene Ther 9(12), 759-68.

Von Seggern, D. J., Huang, S., Fleck, S. K., Stevenson, S. C., and Nemerow, G. R. 2000. Adenovirus vector pseudotyping in fiber-expressing cell lines: improved transduction of Epstein-Barr virus-transformed B cells. J Virol 74(1), 354-62.

Vrati, S., Boyle, D., Kocherhans, R., and Both, G. W. 1995. Sequence of ovine adenovirus homologs for 100K hexon assembly, 33K, pVIII, and fiber genes: early region E3 is not in the expected location. Virology 209(2), 400-8.

Vrati, S., Brookes, D. E., Strike, P., Khatri, A., Boyle, D. B., and Both, G. W. 1996. Unique genome arrangement of an ovine adenovirus: identification of new proteins and proteinase cleavage sites. Virology 220(1), 186-99.

Wang, X. Y., Martiniello-Wilks, R., Shaw, J. M., Ho, T., Coulston, N., Cooke-Yarborough, C., Molloy, P. L., Cameron, F., Moghaddam, M., Lockett, T. J., Webster, L. K., Smith, I. K., Both, G. W., and Russell, P. J. 2004. Preclinical evaluation of a prostate-targeted gene-directed enzyme prodrug therapy delivered by ovine atadenovirus. Gene Ther 11(21), 1559-67.

Wickham, T. J., Mathias, P., Cheresh, D. A., and Nemerow, G. R. 1993. Integrins alpha v beta 3 and alpha v beta 5 promote adenovirus internalization but not virus attachment. Cell 73(2), 309-19.

Wood, M., Perrotte, P., Onishi, E., Harper, M. E., Dinney, C., Pagliaro, L., and Wilson, D. R. 1999. Biodistribution of an adenoviral vector carrying the luciferase reporter gene following intravesical or intravenous administration to a mouse. Cancer Gene Ther 6(4), 367-72.

Worgall, S., Wolff, G., Falck-Pedersen, E., and Crystal, R. G. 1997. Innate immune mechanisms dominate elimination of adenoviral vectors following in vivo administration. Hum Gene Ther 8(1), 37-44.

Xia, D., Henry, L. J., Gerard, R. D., and Deisenhofer, J. 1994. Crystal structure of the receptor-binding domain of adenovirus type 5 fiber protein at 1.7 A resolution. Structure 2(12), 1259-70.

Xu, Z. Z., and Both, G. W. 1998. Altered tropism of an ovine adenovirus carrying the fiber protein cell binding domain of human adenovirus type 5. Virology 248(1), 156-63.

Yun, C. O., Yoon, A. R., Yoo, J. Y., Kim, H., Kim, M., Ha, T., Kim, G. E., and Kim, J. H. 2005. Coxsackie and adenovirus receptor binding ablation reduces adenovirus liver tropism and toxicity. Hum Gene Ther 16(2), 248-61.

FIGURE LEGENDS

FIG. 1. Diagram depicting the design of the chimeric fiber and molecular validation of Ad5Luc1-OvF. (A) Construction of the 553 amino acid chimeric fiber of Ad5Luc1-OvF, including the N-terminal amino acid sequences of the OAdV7 and human Ad5 fiber proteins. The LSL sequence common to both fibers that served as the junction for the replacement of the OAdV7 tail domain, as well as other common sequences, are highlighted. The final Ad5Luc1-OvF fiber sequence is underlined, and the arrow highlights that Val^{46} of the Ad5 tail domain is followed by Leu^{37} in the OAdV7 fiber. (B) PCR analysis of fiber genes using Ad genomes from rescued viral particles as the PCR templates. Ad5Luc1 virions and fiber shuttle plasmid pNEB.PK3.6-OvF (designated as pNEB-OvF in the figure) were used as controls. Lanes containing DNA size standards (M) and no PCR template (NT) are designated. Primers used are specific for the OAdV7 or Ad5 fiber gene knob domain. PCR products indicating the presence of the Ad5 or OAdV7 fiber knob domains are 540bp and 366bp, respectively. (C) Western blot analysis of fiber proteins from purified virions. 1×10^{10} v.p. of Ad5Luc1 with wild type Ad5 fiber (lanes 3,4) or Ad5Luc1-OvF with chimeric OAdV7 fiber (lanes 1,2) were resuspended in Laemmli buffer prior to SDS-PAGE and Western analysis with an anti-tail Ad5 fiber mAb. Samples in lanes 1 and 3 were heated to 95°C prior to electrophoresis. Fiber monomers (M) and trimers (T) are indicated. Molecular mass markers indicate kilodaltons.

FIG. 2. Ad5Luc1-OvF-mediated gene transfer. Luciferase activities following transduction of a panel of CAR-deficient cell lines (A), and unpassaged primary ovarian cancer cells purified from patient ascites (B). Luciferase activity was determined 24 hours post-transduction and is reported in relative light units (RLU) in panel A and RLU/mg cellular protein in panel B. Each column is average of 4 replicates using 100 v.p./cell, and the error bar indicates the standard deviation.

FIG. 3. FACS analysis of Ad5Luc1 and Ad5Luc1-OvF binding to U118-hCAR-tailless (upper panel), or CHO cells (lower panel). Aliquots of 2×10^5 cells were incubated with polyclonal rabbit anti-Ad5

antiserum following binding of virus to the cells at 4°C (to block internalization). Cells were incubated in the presence of anti-rabbit FITC-labeled secondary antibody and subjected to flow cytometry analysis. The gray peaks in the histograms represent negative control cells incubated with primary and secondary antibodies only. The thin line indicates Ad5 cellular attachment, and the heavy line indicates Ad5Luc1-OvF attachment. In U118-hCAR-tailless cells, approximately 94% of cells were positive for Ad5Luc1 surface attachment (thin line), while only 8% of cells were positive for Ad5Luc1-OvF (heavy line) versus control cells receiving primary and secondary antibodies (gray peak). In CHO cells, 10% of cells were positive for Ad5Luc1 attachment compared to 60% positive cells for Ad5Luc1-OvF.

FIG. 4. Ad5Luc1 and Ad5Luc1-OvF mediated gene transfer with Ad5 knob blocking. Luciferase activities following transduction of low-CAR U118 MG cells and CAR-expressing U118-hCAR-tailless cells (A), transduction of U118-hCAR-tailless with Ad5Luc1 (white squares) or Ad5Luc1-OvF (black squares) with Ad5 knob block (B) and low-CAR SKOV3.ip1 cells with Ad5 knob block (C). Concentration of recombinant Ad5 fiber knob protein used to block transduction is indicated in μg/ml. Luciferase activity was determined 24 hours post-transduction and is reported in relative light units (RLU) in (A) or in percent total of unblocked luciferase activity for ease of comparison (B,C). Each column is average of 4 replicates using 100 v.p./cell, and error bar indicates standard deviation.

FIG. 5. *In vivo* biodistribution of Ad5-based vectors after intravenous injection into female C57BL/6 mice. Mice 6-8 weeks of age were injected with 1×10^{11} vp of Ad5Luc1 (open bars), Ad5Luc1-OvF (black bars), or Ad5-ΔdKKTK (cross-hatched bars). Luciferase activity was determined 48 hours post-injection. Results from two individual experiments using different preparations of Ad5Luc1-OvF were combined and are presented as relative light units (RLU) normalized for total protein concentration for each individual organ. Each data point is an average of 8-10 mice (Ad5Luc1, n=10; Ad5Luc1-OvF, n=8; Ad5-ΔKKTK, n=10) and error bars indicate standard deviation. *$p < 0.0028$ versus Ad5Luc1 in liver, #$p < 0.042$ versus Ad5Luc1 in

kidney. For all tissues except heart, Ad5ΔKKTK luciferase values were significantly lower than Ad5Luc1, $p < 0.017$. In all cases a two-tailed t-test assuming unequal variance between groups was used for increased stringency.

Figure 1

A.

OAdV7 **MKRAR..... WDPVYPFSEER.....LVP...L. .PPFIEAGKGLK.SEGLILSLNFDPI-**

Ad5 **MKRARPSEDTFNPVYPYDTETGPPTVPFLTPPFVSPNGFQESPPGVLSLRLSEP-**

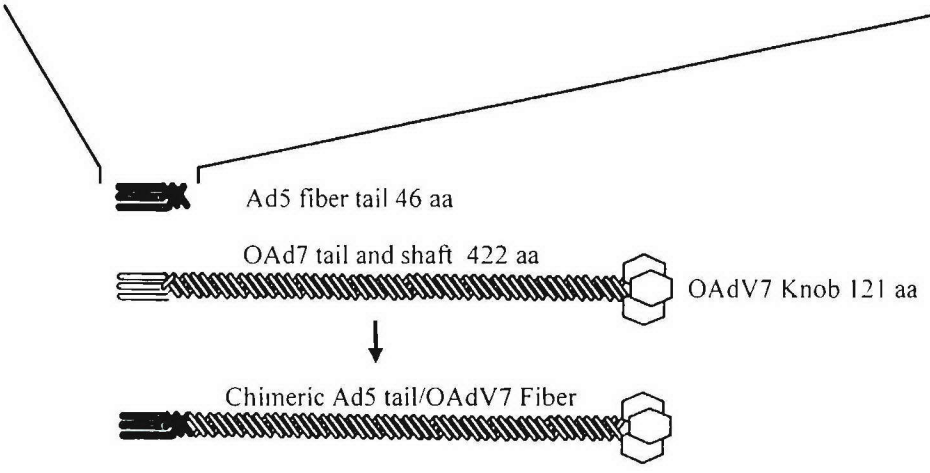

B.

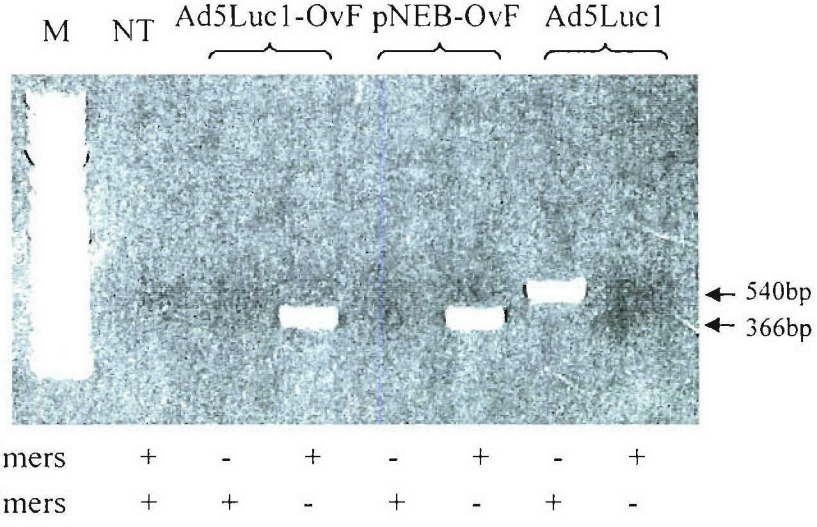

C.

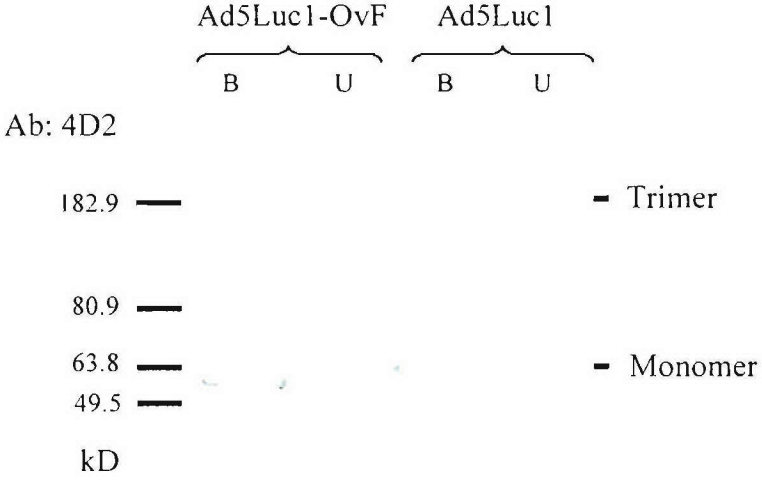

Figure 2

A.

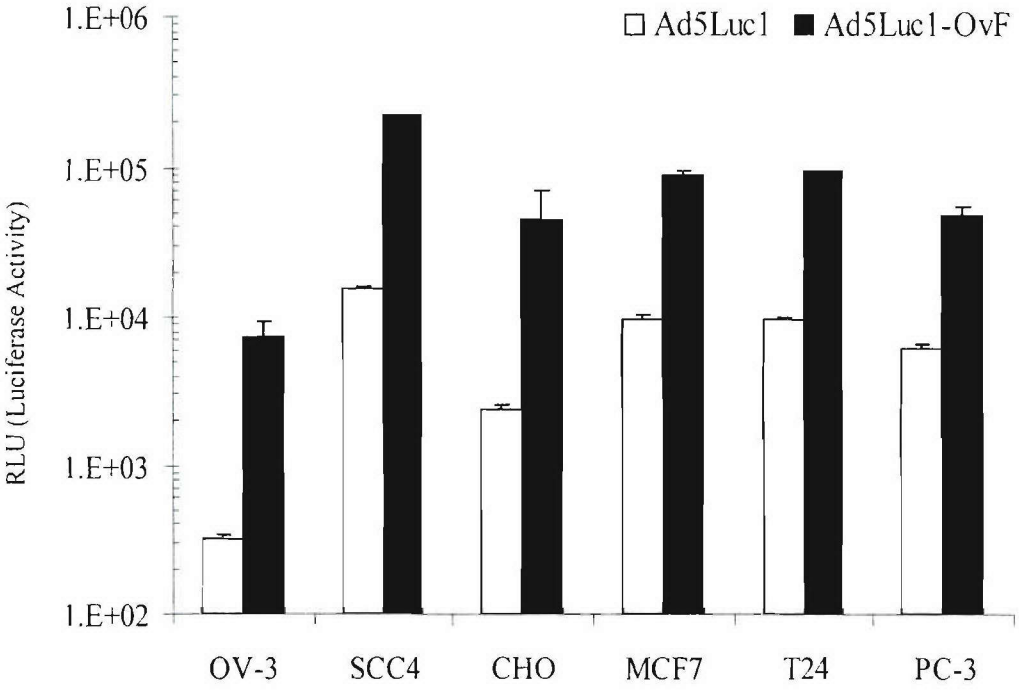
Ad5Luc1
Ad5Luc1-OvF
RLU (Luciferase Activity)
1.E+06
1.E+05
1.E+04
1.E+03
1.E+02
OV-3
SCC4
CHO
MCF7
T24
PC-3

B.

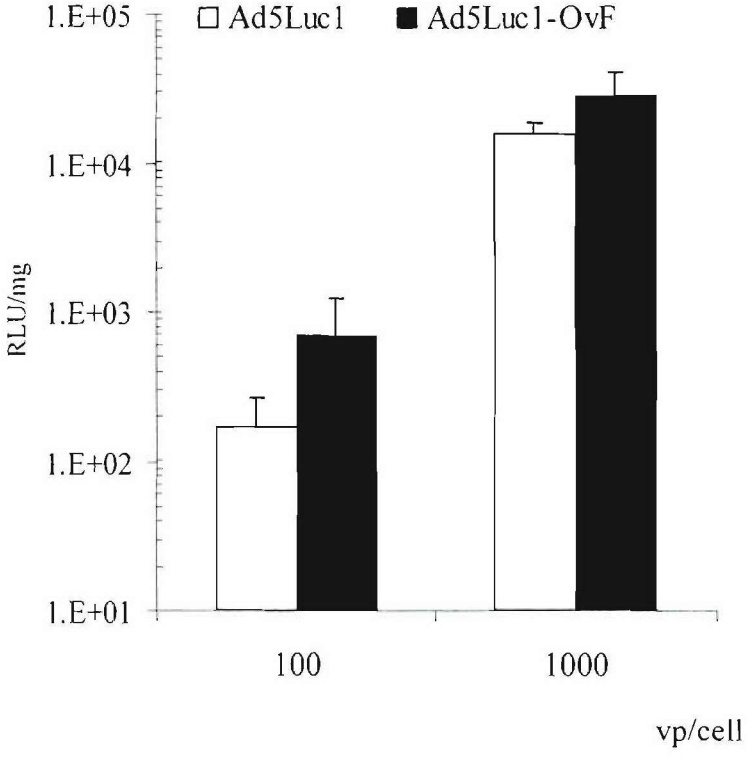
Ad5Luc1
Ad5Luc1-OvF
RLU/mg
1.E+05
1.E+04
1.E+03
1.E+02
1.E+01
100
1000
vp/cell

· Figure 3

A.

B.

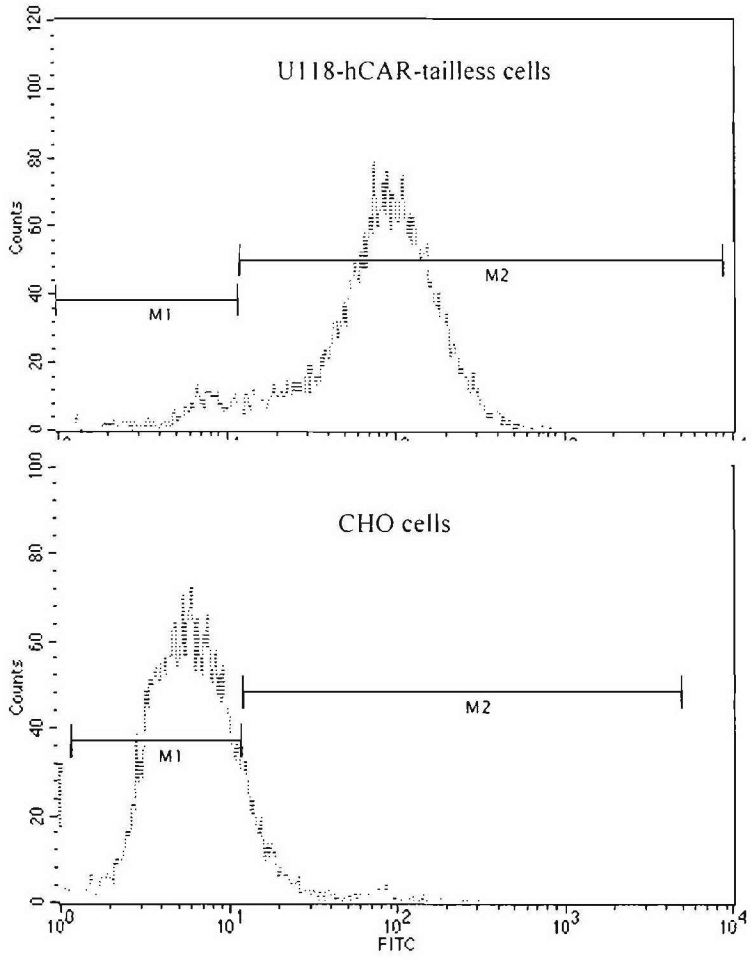
U118-hCAR-tailless cells
Counts
M1
M2
CHO cells
Counts
M1
M2
FITC

Figure 4

A.

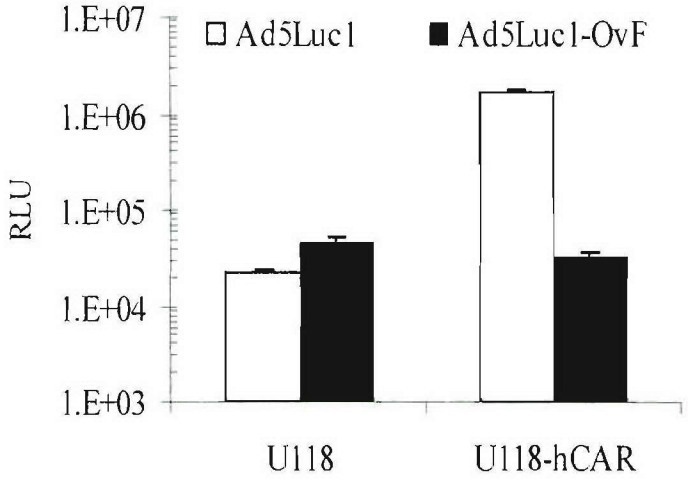
1.E+07
1.E+06
1.E+05
1.E+04
1.E+03
RLU
Ad5Luc1
Ad5Luc1-OvF
U118
U118-hCAR

B.

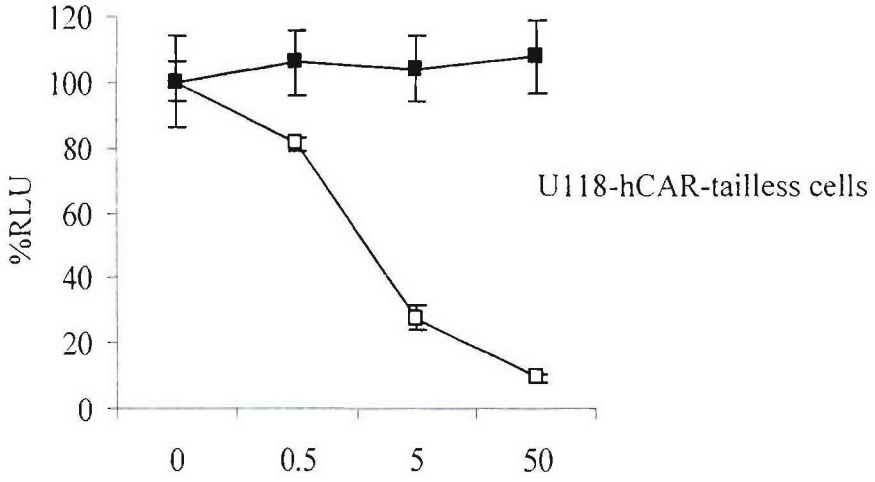
120
100
80
60
40
20
0
%RLU
U118-hCAR-tailless cells
0
0.5
5
50

C.

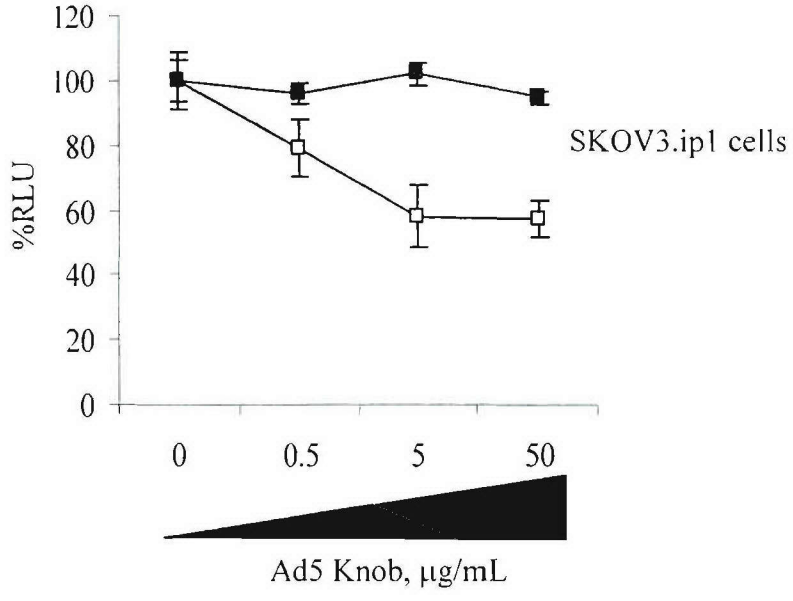
120
100
80
60
40
20
0
%RLU
SKOV3.ip1 cells
0
0.5
5
50
Ad5 Knob, µg/mL

Figure 5

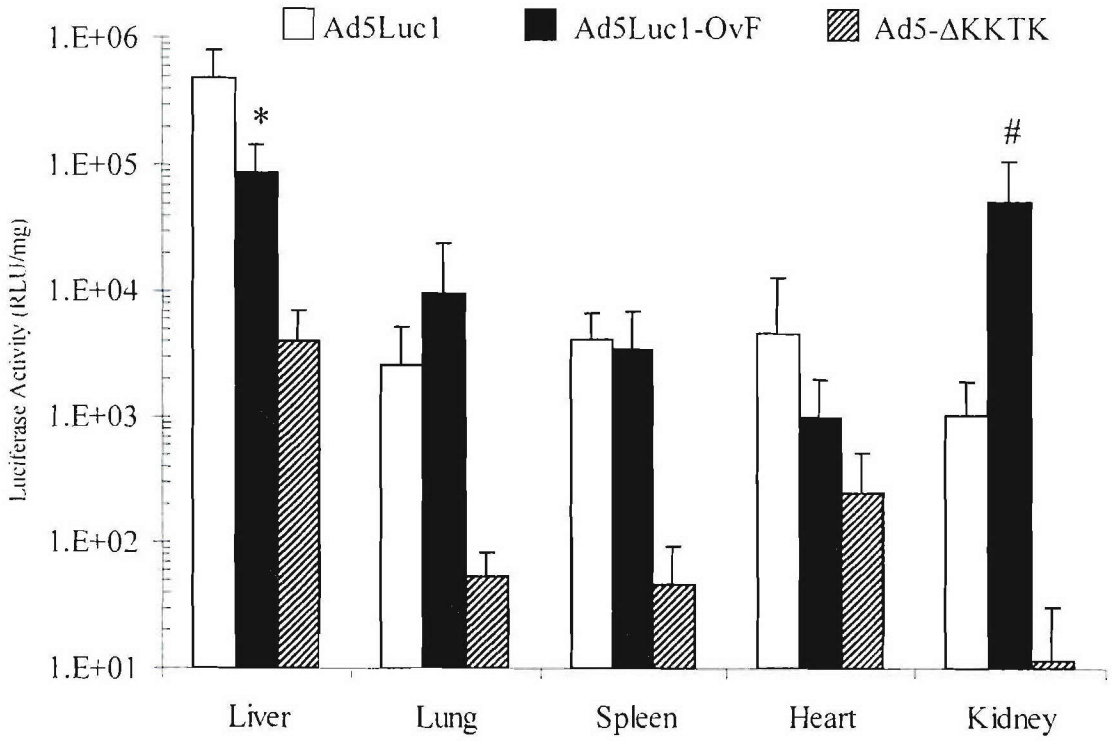
Ad5Luc1
Ad5Luc1-OvF
Ad5-ΔKKTK
Luciferase Activity (RLU/mg)
1.E+06
1.E+05
1.E+04
1.E+03
1.E+02
1.E+01
*
#
Liver
Lung
Spleen
Heart
Kidney

TABLE 1. Ad5Luc1-OvF luciferase gene expression in various cancer cell lines

Cell Line	Origin	CAR[a]	Fold increase in luciferase activity vs Ad5[b]	Reference
CHO	hamster ovary	L/N	22	Soudais et al., 2000
RD	rhabdomyosarcoma	L/N	1.5	Dmitriev et al., 1998; Cripe, et al., 2001
PC-3	prostate cancer	L/N	7.8	Okegawa et al., 2000
LNCaP	prostate cancer	M	5% of Ad5	Herning et al. 2004
T24	bladder cancer	L/N	9.8	Li et al., 1999
MCF7	breast cancer	L/N	9.2	Kawakami e
HeLa	cervical cancer	H	13% of Ad5	Bergelson, et al., 1997
LoVo	colon cancer	ND	60% of Ad5	
oLE	ovine normal stroma	ND	2.7	
JS8JSRV	ovine lung cancer	ND	5% of Ad5	
U118MG	glioma	L/N	2.2	Kim et al., 2003
U118 CAR-tailless	glioma	H	1% of Ad5	Kim et al., 2003
OV-3	ovarian cancer	ND	23	
OV-4	ovarian cancer	L/N	3.0	Hemminki et al., 2003b
HEY	ovarian cancer	L/N	6.5	Hemminki et al., 2003b
SKOV	ovarian cancer	ND	1	
SKOV3.ip1	ovarian cancer	L/N	5.0	Hemminki et al., 2003b
FaDu	pharynx cancer	L/N	21% of Ad5	Blackwell, et al., 1999
SCC-4	tongue cancer	L/N	9.7	Blackwell, et al., 1999
SCC-25	tongue cancer	M	9% of Ad5	Blackwell, et al., 1999
THLE-3	normal liver epithelial	ND	10% of Ad5	
Primary Cells				
Patient 1	ovarian cancer	ND	4	

[a] H, high levels of CAR; M, moderate; L/N, little or no CAR; ND, not determined. As determined by FACS analysis.

[b] 100 vp/cell, luciferase activity measured at 24 h post-infection.

ARTICLES

Dynamic Monitoring of Oncolytic Adenovirus In Vivo by Genetic Capsid Labeling

Long P. Le, Helen N. Le, Igor P. Dmitriev, Julia G. Davydova, Tatyana Gavrikova, Seiji Yamamoto, David T. Curiel, Masato Yamamoto

Background: **Conditionally replicative adenoviruses represent a promising strategy to address the limited efficacy and safety issues associated with conventional cancer treatment. Despite rapid translation into human clinical trials and demonstrated safety, the fundamental properties of oncolytic adenovirus replication and spread and host–vector interactions in vivo have not been completely evaluated.** ***Methods:*** **We developed a noninvasive dynamic monitoring system to detect adenovirus replication. We constructed capsid-labeled E1/E3-deleted and wild-type adenoviruses (Ad-wt) by fusing the minor capsid protein IX with red fluorescent proteins mRFP1 and tdimer2(12), resulting in Ad-wt-IX-mRFP1 and Ad-wt-IX-tdimer2(12). Virus DNA replication, encapsidation, cytopathic effect, thermostability, and binding to primary receptor (coxsackie adenovirus receptor) were measured in A549 lung adenocarcinoma cells and Chinese hamster ovary cells infected with Ad-wt-IX-mRFP1" using real-time quantitative polymerase chain reaction, cell viability (MTS) assay, and fluorescence microscopy. Athymic mice (n = 4) with A549-derived xenograft tumors were intratumorally inoculated with Ad-wt-IX-mRFP1, and adenovirus replication was dynamically monitored with a fluorescence noninvasive imaging system. Correlations between fluorescence signal intensity and viral DNA synthesis and replication were calculated using Pearson's correlation coefficient (r).** ***Results:*** **The red fluorescence label had little effect on viral DNA replication, encapsidation, cytopathic effect, thermostability, and coxsackie adenovirus receptor binding in either cell type". The fluorescent signal correlated with viral DNA synthesis and infectious progeny production both in vitro and in vivo (in A549 cells, r = .99 and r = .65; in tumors, r = .93 and r = .92, respectively). The replication efficiency of the labeled virus" in vivo was variable, and replication and viral spreading and persistence were limited, consistent with clinical observations.** ***Conclusions:*** **Genetic capsid labeling provides a promising approach for the dynamic assessment of oncolytic adenovirus function in vivo. [J Natl Cancer Inst 2006;98:1–13]**

Cancer is the second leading cause of disease-related mortality in humans after heart disease" despite technologic advances in clinical management *(1)*. Conventional tumor therapies, including surgery, radiotherapy, and chemotherapy, often have poor efficacy and may have undesirable side effects *(2–4)*. Oncolytic viral treatment (also known as virotherapy) has been proposed as a promising alternative to surgery, radiotherapy, and chemotherapy. Conditionally replicative adenoviruses represent a candidate agent in this endeavor and have the potential for transductional and transcriptional targeting *(5–8)*, and their rapid evaluation in clinical trials has demonstrated their safety. However, to date, conditionally replicative adenoviruses, when used as single agents, have not displayed the anticipated efficacy for cancer therapy *(9)*. Oncolytic adenovirus function in humans therefore needs to be carefully explored. Current clinical trial protocols and methods cannot provide the interval endpoint data necessary to fully study fundamental issues such as the extent of replication and spread, specificity, viral persistence, and host–vector interactions. The lack of tools to directly and dynamically observe the performance of conditionally replicative adenoviruses in vivo has been a major impediment in realizing the clinical utility of replicative adenoviral agents.

Current methods of vector detection include chemical labeling, DNA and RNA quantification or hybridization, immunohistochemistry, and reporter gene expression. Although these methods have been operative for certain in vitro and in situ studies of adenovirus biology and gene therapy, their limitations are evident when they are used in replicative vector systems. Most of these terminal assays only allow examination of a particular sample and of one moment in time. However, the adenovirus oncolytic mechanism revolves around the concept that the initial virus amplifies and spreads to eventually yield a tumor-wide therapeutic effect *(9–11)*. Such dynamics cannot be captured and represented by static analysis. The shortcomings of current vector detection methods are further complicated by the need to acquire multiple biopsies using an invasive procedure that is prone to sampling error and is concomitantly impractical for repeated monitoring of the entire tumor *(12–15)*. Reporter genes can only provide indirect and relative information with respect to virus replication and localization based on transgene expression.

The ideal approach for evaluating the replication and dissemination of oncolytic adenoviral agents should directly measure the

Affiliations of authors: Division of Human Gene Therapy (LPL, HNL, IPD, JGD, TG, SY, DTC, MY), Departments of Medicine, Pathology and Surgery and the Gene Therapy Center (IPD, DTC, MY), University of Alabama at Birmingham, Birmingham, AL

Correspondence to: David T. Curiel, MD, PhD, Division of Human Gene Therapy, 901 19th St. S., BMR2-508, Birmingham, AL 35294-2172 (e-mail: david.curiel@ccc.uab.edu) or Masato Yamamoto, MD, PhD, Division of Human Gene Therapy, 901 19th St. S., BMR2-410 Birmingham, AL 35294-2172 (e-mail: masato.yamamoto@ccc.uab.edu).

See "Notes" following "References."

DOI: 10.1093/jnci/djj022

viral mass that accrues from the initial administration without compromising replication capacity and be capable of noninvasive detection. To this end, we hypothesized that the detection of viral capsid proteins genetically fused with an imaging reporter would provide such an index of viral replication and localization. Previously, we established an adenovirus capsid labeling strategy by fusing the minor capsid protein IX with enhanced green fluorescent protein (EGFP) *(16)*. Herein, we expand the capsid labeling technology to develop red fluorescent protein (RFP)–labeled adenoviruses with conserved viral function to monitor adenoviral replication in vivo.

Methods

Cell Culture

Human embryonic kidney 293 (American Type Culture Collection [ATCC], Manassas, VA), human embryonic retinoblast 911 *(17)*, human lung adenocarcinoma A549 (ATCC), BALB/c mouse transformed liver BNL-1NG-A.2 (ATCC), and Chinese hamster ovary (CHO) (ATCC) cells were maintained according to the suppliers' protocols. The cells were incubated at 37 °C and 5% CO_2 under humidified conditions.

Recombinant Adenovirus Construction

All viruses were constructed by homologous recombination in *Escherichia coli (18)*. All parental plasmids have been previously described: pShuttle-cytomegalovirus (CMV) (AdEasy system; Qbiogene, Irvine, CA), pRSETB-mRFP1 and pRSETB-tdimer2(12) *(19)*, pSh1p1XNhe1 *(20)*, and pShuttle-wt-1X-EGFP [AQ5] *(21)*" Shuttle plasmids for the E1/E3-deleted (replication-deficient) vectors were constructed using restriction cloning as follows: pShuttle-E1-CMV-mRFP1 → pShuttle-CMV/BglII/HindIII + pRSETB-mRFP1/BamHI/HindIII; pShuttle-E1-CMV-tdimer2(12) → pShuttle-CMV/BglII/HindIII + pRSETB-tdimer2(12)/BamHI/HindIII; pShuttle-1X-mRFP1 → pSh1p1XNhe/BmtI/blunt + pRSETB-mRFP1/BamHI/EcoRI/blunt; pShuttle-1X-tdimer2(12) → pSh1p1XNhe/BmtI/blunt + pRSETB-tdimer2(12)/BamHI/EcoRI. All blunted fragments were generated with large Klenow fragment (New England Biolabs, Beverly, MA). pShuttle-wt-1X-mRFP1 was made by ligating pShuttle-1X-mRFP1/BspHI/MfeI with the BspHI/MfeI fragment from pShuttle-wt-1X-EGFP containing the wild-type E1 region; pShuttle-wt-1X-tdimer2(12) was similarly constructed. All E1/E3-deleted final genomes were made by recombining the above shuttle plasmids (linearized with PmeI) with pAdEasyDS, a modified pAdEasy plasmid that allows double-selection recombination [AQ6] (unpublished data). The wild-type vector", with the red fluorescent protein labels" 1X-mRFP1 and 1X-tdimer2(12), was recom- [AQ7] bined with pTG3602DS, a modified E1-deleted pTG3602 plasmid that also allows double-selection recombination. Clones were verified by digestion with restriction enzymes and 0.8% agarose gel electrophoresis. The viruses generated include E1/E3-deleted control vectors (with wild-type [wt] protein IX [p1X]) adenovirus (Ad)-E1-CMV-mRFP1 and Ad-E1-CMV-tdimer2(12), E1/E3-deleted Ad-1X-mRFP1 and Ad-1X-tdimer2(12) with p1X modifications, and wild-type E1/E3 Ad-wt-1X-mRFP1. We were unable to recover Ad-wt-1X-tdimer2(12). Therefore, Ad-wt-1X-mRFP1 served as a surrogate oncolytic replicative vector for our studies.

Virus Propagation and Purification

Replication-deficient viruses were propagated in E1-complementing 911 retinoblast cells, and Ad-wt-1X-mRFP1 was amplified in A549 lung cancer cells. Viruses were purified by double cesium chloride (CsCl) ultracentrifugation (AdEasy system; QBiogene) and were dialyzed against phosphate-buffered saline (PBS") containing 0.5 mM Mg^{2+}, 0.9 mM Ca^{2+}, and 10% glycerol. Final aliquots of virus were analyzed for viral particle titer (absorbance at 260 nm), transducing unit titer, and cytopathic effect unit titer. Based on a previously described protocol *(22)*, the transducing unit was determined by infecting 911 cells in 96-well plates with 1:10 serial dilutions of the virus and counting the number of red fluorescent cells 2 days after infection ($n = 3$). The same plate was assayed with an MTS viability assay (3-[4,5-dimethylthiazol-2-yl]-5-[3-carboxymethoxyphenyl]-2-[4-sulfophenyl]-2H-tetrazolium; Promega, Madison, WI) to determine the viral dilution that is cytotoxic to 50% of the cells. Three independent experiments were performed" Based on the number of [AQ9] cells seeded (15000/well), the cytopathic effect unit was calculated such that 1 unit is defined as the amount of virus that causes cytopathic effect in one 911 cell in 2 days *(23)*. All viruses were stored at –80 °C until use. [AQ8]

Characterization of Virus Gradient Fractions

For the fractionation studies, Ad-E1-CMV-mRFP1, Ad-E1-CMV-tdimer2(12), Ad-1X-mRFP1, and Ad-1X-tdimer2(12) were each propagated in 10 150-mm dishes of 911 cells. Cells were harvested by aspiration, and viruses were purified by double CsCl ultracentrifugation as described above, in which the top and bottom bands were retained in the same sample after two centrifugation steps, yielding one gradient from the 10 dishes. After the second centrifugation, fractions of 2 drops each (approximately 100 μL) were collected through a perforation at the bottom of the tube into a 96-well white opaque plate. Plates with the viral fractions were measured with a microplate fluorometer (Fluostar Optima; BMG Labtechnologies, Durham, NC) using a 560/10 nm excitation filter for all viruses, a 585/10 nm emission filter for the tdimer2(12) vectors, and a 605/10 nm emission filter for the mRFP1 viruses" To determine viral DNA content, a sample (10 μL) of each fraction was diluted in 90 μL of 0.5% sodium dodecyl sulfate in PBS and incubated at room temperature for 10 minutes to release the viral genomes. Absorbance at 260 nm was then measured for each sample (MBA 2000; Perkin Elmer, Shelton, CT) [AQ10]

Tracking of Red Fluorescent Adenovirus Infection

A549 cells (2.5×10^5 cells/well) were seeded in phenol red–free growth medium (Dulbecco's modified Eagle [DME]–5% fetal calf serum [FCS]) in six-well plates containing glass coverslips (one per well). The next day, cells were incubated for 1 hour at 4 °C with (two wells) or without (four wells) recombinant adenovirus serotype 5 fiber knob *(24)* (1 μg/mL) in 500 μL of phenol red-free DME medium containing 25 mM HEPES buffer. Ad-1X-mRFP1 or Ad-1X-tdimer2(12) (10000 viral particles/cell) were added to the infection solution to a total volume of 1 mL. The viruses were allowed to bind to the cells at 4 °C for 1 hour (cell binding and Ad5 knob block). Two wells with the added viruses were further incubated at 37 °C for 1.5 hours

quantified by TaqMan real-time quantitative PCR with E4 primers, as described above. The correlation coefficient (Pearson's r) was calculated with the CORREL function in Microsoft Excel, Office 2003 (Microsoft Corp., Redmond, WA).

Fluorescence-Based In Vivo Optical Imaging

pIX-mRFP1 fluorescence was detected noninvasively using a custom-built optical imaging system. Briefly, a cryogenically cooled, back-illuminated Princeton Instruments VersArray:1KB digital charge-coupled device camera (Roper Scientific, Trenton, NJ) with a liquid nitrogen autofill system was mounted on top of a light-tight enclosure. The camera was coupled with a 50-mm Nikkor *f*/1.2 lens (Nikon, Melville, NY) for image acquisition. Excitation light for fluorescence imaging was delivered by a Dolan-Jenner Fiber-Lite MH-100 metal halide light source equipped with a dual-fiberoptic gooseneck. Excitation and emission filter wheel assemblies were integrated with the light source and lens. Bandpass filters included 490/10 and 560/10 nm for excitation and 535/30 and 605/55 nm for emission (Chroma Technology, Rockinghan, VT).

A549 cells (7.5×10^6) were inoculated in the left and right flanks of athymic nude mice ($n = 6$)** (National Cancer Institute-Frederick Animal Production Area, Frederick, MD) to establish tumors. When the tumors reached 5–10 mm in diameter (in approximately 3 weeks), a single intratumoral injection of Ad-wt-IX-mRFP1 (10^{10} viral particles in 10 μL total volume of PBS) was performed for each tumor without deliberate spreading of the virus with the needle. Mice (up to three) were placed in the imaging chamber and maintained with 2% isoflurane gas anesthesia at a flow rate of approximately 0.5–1 L/min per mouse (Highland Medical Equipment, Temecula, CA). Images were acquired with WinView/32 software (Roper Scientific). To detect red fluorescence, images were captured at *f*/4 and *f*/2 with 2- and 5-second exposure times using two filter combinations: 560/605 and 490/605 (excitation/emission). The former filter setting applies to a red fluorescence signal and the latter configuration pertains to background autofluorescence. A bright-field image was also taken at *f*/16 for 1 second and at the lowest light level. Background subtraction was performed in WinView/32 after scaling the background image with a factor determined from areas surrounding tumors of individual mice *(27)*. The positive signal from background subtracted images was segmented and analyzed in ImageTool 3.0 (The University of Texas Health Science Center in San Antonio, TX) for integrated density (the product of mean intensity and signal area). Index color image overlays were created in Photoshop 7.0 (Adobe) using the segmentation or thresholding parameters determined in ImageTool.

In Vivo Correlation of pIX-mRFP1 Signal With Replication and Dynamic Monitoring

All** mice ($n = 6$) were imaged daily and analyzed using the above procedure. On day 6 after injection, the day after the maximal signal intensity was observed, four mice were killed. Dissected tumors were imaged in their anatomic position ex vivo and then frozen at –80 °C until use. The tumors were homogenized with the Mini-Beadbeater (BioSpect Products, Bartlesville, OK) and incubated with liver digest medium (4 μL/mg of tumor; Invitrogen, Carlsbad, CA) for 1 hour at 37 °C to further disrupt the tissue. Samples of the tumor homogenate (40 μL [or roughly 10 mg] for large tumors and 10 μL [or approximately 2.5 mg] for small tumors) were used for total DNA determination and viral DNA copy number as described above. The transducing unit titer and cytopathic effect unit titers were determined in the homogenate using the same methods described for purified virus. However, in this case, the cytopathic effect unit was determined 10 days after infection and would give higher values than the same assay read 2 days after infection. All results are presented as total values scaled for the entire tumor mass. The correlation coefficient (Pearson's r) was calculated with the CORREL function in Microsoft Excel. Two of the six original mice were maintained and imaged over the 30-day experiment. Images were processed and analyzed accordingly.

Comparison of In Situ Detection of pIX-mRFP1 Signal With Hexon Staining

Established A549 tumors injected with Ad-wt-IX-mRFP1 were excised on day 7 after injection and frozen in a dry ice–ethanol bath. Frozen tumor sections (5 μm) were fixed onto glass slides with 3% formalin, blocked with 1% BSA–PBS, and probed with a polyclonal goat anti-hexon antibody at approximately 20 μg/mL (1:200 dilution; Chemicon, Temecula, CA) for 1 hour at room temperature. The slides were then washed with 1% BSA–PBS and incubated with an Alexa Fluor 488–labeled secondary donkey anti-goat antibody (1:200 dilution; Molecular Probes, Eugene, OR). The slides were washed again with 1% BSA–PBS, and the cells were counterstained with Hoechst 33342 (Molecular Probes) and prepared for fluorescence microscopy as described above.

Statistical Analysis

All statistical analyses were performed with a two-sided single-factor analysis of variance test. P values <.05 were considered statistically significant.

Results

Incorporation of pIX-mRFP1 and pIX-tdimer2(12) Into Viral Particles

We initially constructed E1/E3-deleted viruses with carboxyl-terminal fusions of pIX with monomeric and tandem dimer red fluorescent proteins [mRFP1 and tdimer2(12), respectively] *(19)*. After standard CsCl double ultracentrifugation of the two vectors, we observed that the colors of the empty (top) and mature (bottom) viral bands were different from those obtained from purified conventional unlabeled vectors: Ad-IX-mRFP1 was purple and Ad-IX-tdimer2(12) was pink (Fig. 1, A, data not shown). The difference in color between these two vectors is probably due to the excitation and emission properties of the fluorescent proteins *(19)*. Applying our previously established approach *(21)*, we collected fractions of each viral gradient and analyzed each sample for red fluorescence and viral DNA content. Fluorescent peaks were detected for both the bottom and top bands of the two viruses, which coincided with the optical absorbance peaks of viral DNA (Fig. 1, B). Red fluorescent purified viral particles could be easily visualized using fluorescence microscopy for both vectors (Fig. 1, C).

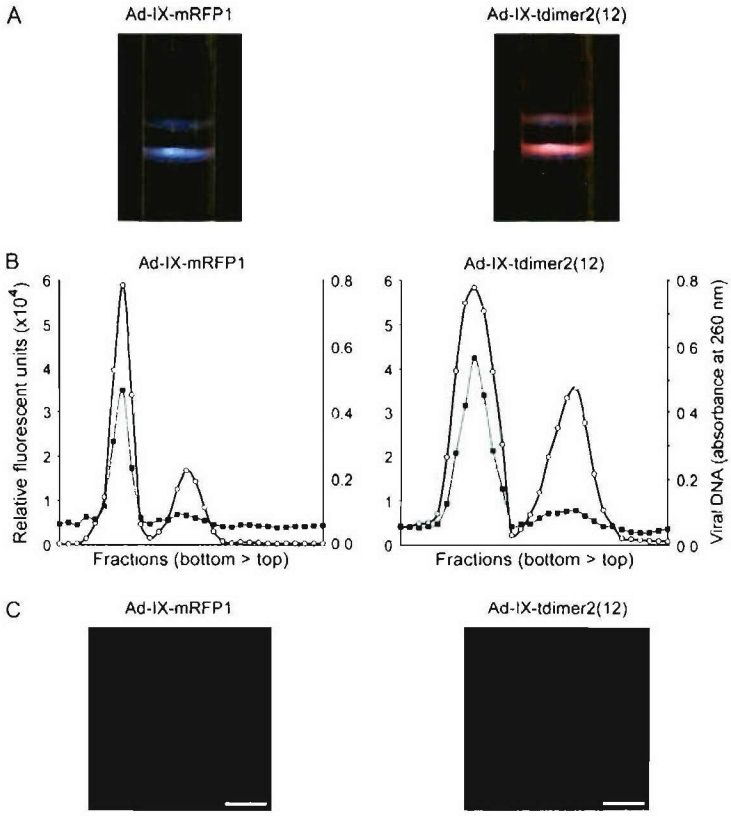

Fig. 1. Characterization of red fluorescent protein IX (pIX)–labeled adenovirus gradients. **A)** Images of Ad-IX-mRFP1 and Ad-IX-tdimer2(12) top and bottom virus bands after cesium chloride (CsCl) ultracentrifugation that were captured under normal ambient lighting. **B)** Fractions from Ad-IX-mRFP1 and Ad-IX-tdimer2(12) CsCl virus gradients were measured for red fluorescence (**open circles**) and viral DNA content (absorbance at 260 nm, **closed squares**). **C)** Also shown are the purified red fluorescent adenoviral particles visualized under fluorescence microscopy. **Bar** = 10 μm.

Tracking of Ad-IX-mRFP1

To examine the use of the red fluorescent adenoviruses**, we incubated A549 cells with Ad-** IX-mRFP1 at 4 °C for 1 hour to allow virus binding but not internalization. Fluorescence microscopy revealed distinct binding of Ad-** IX-mRFP1 particles to the plasma membrane (Fig. 2, A, cell binding). In another experiment, we allowed the viruses to bind to the cells at 4 °C** and then at 37 °C for 1.5 hours. After the incubation at 37 °C, numerous viruses were detected at the nuclear membrane or inside the nucleus (Fig. 2, A, nuclear trafficking). We also examined whether preincubation with recombinant Ad5 knob would mitigate virus binding. Indeed, few particles remained bound to the A549 cells after washing when knob blocking was implemented (Fig. 2, A, Ad5 knob block), suggesting that the pIX-mRFP1 fusion did not negatively affect the virus's interaction with its primary coxsackie adenovirus receptor. Similar results were also obtained for Ad-** IX-tdimer2(12) (data not shown).

Detection of Ad-wt-IX-mRFP1 in Tissue

To test the ability to detect red fluorescent virus in situ, we injected Ad-wt-IX-mRFP1 (10^{11} virus particles) into the tail veins of C57/BL6 mice. Twenty minutes after injection, the lungs, kidneys, liver, and spleen were surgically removed, frozen, and sectioned for microscopy. In the lungs, red particles were occasionally visualized around blood vessels and endothelial cells. Likewise, very few particles were detected in the kidneys. Numerous viral particles were seen in the liver, with accumulation being especially prominent in the sinusoids, where the Kupffer cells reside. Single particles (orange arrows, Fig. 2, B) were observed in the hepatocytes. This localization pattern in the liver closely resembles what we observed with Ad-wt-IX-EGFP *(16)*. A substantial amount of virus was also detected in the spleen, mostly in the marginal zones between the white and red pulp (Fig. 2, B).

DNA Encapsidation Efficiency of Red Fluorescent Viruses

Our goal was to establish genetic labeling of adenovirus with minimal perturbation of normal viral function to retain efficient oncolytic activity. One important function for viral replication is the DNA encapsidation efficiency of the red fluorescent adenoviruses. To analyze this function, we assayed lysates from 911 cells infected with the two red fluorescent adenoviruses and their respective E1-CMV expression vector controls for both total and encapsidated viral DNA copy number using TaqMan quantitative real-time PCR (Fig. 3, A, left and middle panels). The data revealed no differences in the total viral DNA replication of the two labeled vectors relative to their controls during 4 days of infection, except for total viral DNA comparison between the tdimer2(12) vectors on day 4 [Ad-E1-CMV-tdimer2(12) versus Ad-IX-tdimer2(12) at day 4, means = 5.50×10^6 versus 9.84×10^6, difference = 4.33×10^6, 95% confidence interval = 2.98×10^6 to 5.69×10^6]. Similarly, there were no differences in encapsidated viral DNA between the two labeled vectors and their controls during the first 3 days of infection. When the data were expressed as encapsidated viral

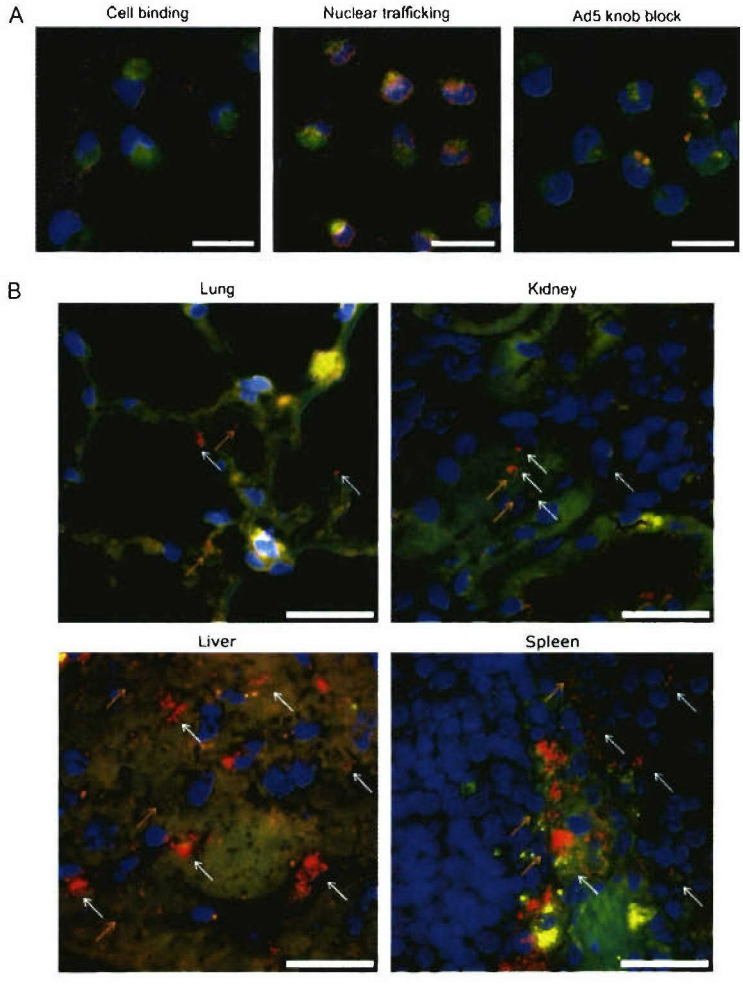

Fig. 2. Detection of Ad-IX-mRFP1 particles in vitro **A)** Tracking of adenovirus infection in cultured cancer cells A549 lung adenocarcinoma cells incubated with the respective red fluorescent adenoviruses were imaged using fluorescence microscopy to visualize virus binding (**left panel**) and nuclear trafficking (**middle panel**). In the **right panel**, A549 cells were blocked with recombinant Ad5 knob before the viruses were added. **Red**, Ad-IX-mRFP1; **blue**, Hoechst stain for nuclear DNA; **green**, cytoplasmic and nuclear autofluorescence; and **black/white**, phase-contrast image of the cells. Bar = 20 μm **B)** Detection of Ad-wt-IX-mRFP1 in tissues. Ad-wt-IX-mRFP1 particles were detected in the lung, kidney, liver, and spleen of a C57/BL6 mouse after intravenous injection with 10^{10} virus particles. **White arrows** designate clusters of fluorescent viral particles and **orange arrows** show single particles. **Bar** = 20 μm

DNA fraction, no differences were noted between the two labeled vectors and their controls (Fig. 3, A, right panel).

Cytopathic Effect of Red Fluorescent Adenoviruses

The red fluorescent adenoviruses were also evaluated with respect to their ability to induce a cytopathic effect in infected cells. |AQ22| This assay gauges viral function on a more comprehensive level" because the cytopathic effect is dependent not only on efficient transduction and virus replication but also on spread to neighboring cells. Any defect in the infection process would result in decreased cytotoxicity. 911 cells were infected with 0.5, 0.05, or 0.005 cytopathic effect units/cell of Ad-E1-CMV-mRFP1, Ad-IX-mRFP1, Ad-E1-CMV-tdimer2(12), and Ad-IX-tdimer2(12). Cell viability was measured every 2 days after infection for a total of 10 days. Under the various conditions examined, there were statistically significant differences noted at some time points and similarities at other time points between the labeled vectors and their controls" Overall, however, the differences were minor. |AQ23| Moreover, all four viruses achieved total oncolysis with similar kinetics in a dose-dependent manner (Fig. 3, B).

Thermostability of Red Fluorescent Adenoviruses

Adenovirus protein IX functions as a minor protein in capsid stabilization *(28,29)*. To test whether the fusion of red fluorescent proteins to pIX destabilizes the adenovirus capsid structure, we incubated the labeled viruses and their controls at 45 °C. After exposing the viruses to 45 °C for various time intervals, we determined the transducing unit to assess the presence of the remaining infectious virions that survived the temperature stress treatment. No statistically significant decrease in thermostability was detected for Ad-IX-mRFP1 and Ad-IX-tdimer2(12) compared with their controls Ad-E1-CMV-mRFP1 and Ad-E1-CMV-tdimer2(12) after 5 or 10 minutes at 45 °C" After 20 minutes of |AQ24| heat treatment, no infectious viruses remained for any of the four vectors (Fig. 4, A). |F4|

Coxsackie Adenovirus Receptor–Dependent Binding of Red Fluorescent Adenoviruses

We next evaluated the extent of the red fluorescent adenovirus interaction with the Ad5 primary coxsackie adenovirus

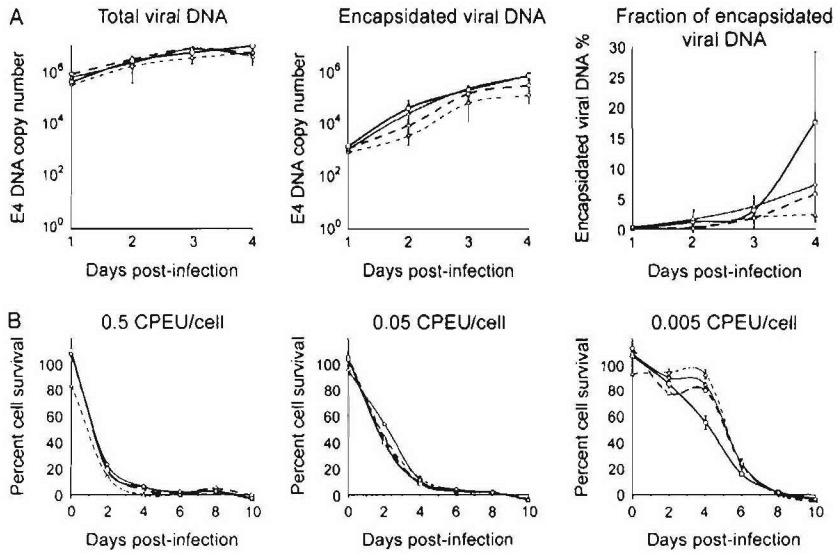

[AQ36] **Fig. 3.** "Viral DNA copy number for Ad-E1-CMV-mRFP1 (**open circles**), Ad-IX-mRFP1 (**open squares**), Ad-E1-CMV-tdimer2(12) (**open triangles**), and Ad-IX-tdimer2(12) (**open diamonds**) were quantified during infection of 911 [AQ37] cells over 4 days. Three independent experiments were performed" **Error bars** [AQ38] represent 95% confidence intervals". Comparison of total viral DNA over 4 days: Ad-E1-CMV-mRFP1 versus Ad-IX-mRFP1 ($P = .23$, $P = .40$, $P = .58$, and $P = .56$, for days 1, 2, 3, and 4, respectively) and Ad-E1-CMV-tdimer2(12) versus Ad-IX-tdimer2(12) ($P = 20$, $P = 11$, $P = .07$, and $P < .001$ for days 1, 2, 3, and 4, respectively). Comparison of encapsidated viral DNA over 4 days: Ad-E1-CMV-mRFP1 versus Ad-IX-mRFP1 ($P = .76$, $P = .35$, $P = 08$, and $P = .05$ for days 1, 2, 3, and 4, respectively), and Ad-E1-CMV-tdimer2(12) versus Ad-IX-tdimer2(12) ($P = 17$, $P = 12$, $P = 06$, and $P = .005$ for days 1, 2, 3, and 4, respectively). The results are also expressed as fraction of encapsidated viral DNA (encapsidated divided by total viral DNA) Comparison of encapsidated viral DNA fraction over 4 days: Ad-E1-CMV-mRFP1 versus Ad-IX-mRFP1 ($P = 36$, $P = .37$, $P = .08$, and $P = .14$ for days 1, 2, 3, and 4, respectively) and Ad-E1-CMV-tdimer2(12) versus Ad-IX-tdimer2(12) ($P = .29$, $P = 33$, $P = 27$, and $P = .06$ for days 1, 2, 3, and 4, respectively). **B)** Cytopathic effect of Ad-E1-CMV-mRFP1 (**open circles**), Ad-IX-mRFP1 (**open squares**), Ad-E1-CMV-tdimer2(12) (**open triangles**), and Ad-IX-tdimer2(12) (**open diamonds**) was determined in 911 cells every 2 days over 10 days after infection ($n = 5$). Cell viability was measured by an MTS (3-[4,5-dimethylthiazol-2-yl]-5-[3-carboxymethoxyphenyl]-2-[4-sulfophenyl]-2H-tetrazolium) assay and displayed as the percentage of noninfected cells. Comparison of Ad-E1-CMV-mRFP1 versus Ad-IX-mRFP1 over the respective days. 0.5 cytopathic effect unit (CPEU)/cell ($P = .05$, $P = 13$, $P < 001$, $P = 72$, $P < .001$, and $P < .001$), 0.05 CPEU/cell ($P = .51$, $P = .003$, $P = 33$, $P = .59$, $P = 11$, and $P = .11$); and 0 005 CPEU/cell ($P = 01$, $P = .004$, $P = 01$, $P = 03$, $P = .001$, and $P = .002$). P values for comparison of Ad-E1-CMV-tdimer2(12) versus Ad-IX-tdimer2(12) over the respective days. 0.5 CPEU /cell ($P < .001$, $P < 001$, $P < .001$, $P = 51$, and $P = .51$); 0 05 CPEU/cell ($P < 001$, $P < 001$, $P = 07$, $P = .06$, $P = .05$, and $P = .05$); and 0.005 CPEU/cell ($P < .001$, $P = .08$, $P = 003$, $P = .83$, $P = .78$, and $P = 71$). All P values were two-sided and were calculated by single-factor analysis of variance.

receptor. Coxsackie adenovirus receptor–deficient CHO cells were chosen as the negative control and high coxsackie adenovirus receptor–expressing A549 cells as the positive control. The viruses were incubated with A549 and CHO cells at 4 °C using vigorous agitation for 1 hour and were then washed to remove unbound viruses. TaqMan real-time quantitative PCR was used to quantify the number of bound virions. As expected, CHO cells showed minimal binding of all four vectors, similar to [AQ25] cell samples with no virus addition" A549 cells, however, demonstrated abundant binding of Ad-IX-mRFP1 and Ad-IX-tdimer2(12) that was equal to that of the control viruses Ad-E1-CMV-mRFP1 and Ad-E1-CMV-tdimer2(12). Similar to the tracking assay, binding was greatly attenuated when the A549 cells were initially incubated with recombinant Ad5 knob (Fig. 4, B).

Correlation of pIX-mRFP1 Signal With DNA Replication and Progeny Production In Vitro

To determine whether the fluorescence intensity of the label itself corresponds to the level of virus mass and replication, we constructed a pIX-mRFP1–labeled virus with intact E1 and E3 regions to serve as a surrogate oncolytic agent. In contrast, a wild-type pIX-tdimer2(12) virus could not be recovered", probably owing to compromise of the pIX function [AQ26] required in packaging full-length genomes *(30)*. As a result, we used Ad-wt-IX-mRFP1 to further investigate the genetic labeling system. We infected A549 and BNL-1NG-A.2 cells in vitro with various amounts of Ad-wt-IX-mRFP1 A549 cells are human lung adenocarcinoma cells that are frequently used to efficiently propagate replication-competent Ad vectors (possessing E1). BNL-1NG-A.2 cells are transformed BALB/c liver cells. Because human adenoviruses in general do not replicate productively in murine cells *(31)*, these two cell lines represent distinct substrates, the former being replication permissive and the latter being replication nonpermissive for human Ad5.

"Cell infection was monitored daily over 10 days by measur- [AQ27] ing the kinetics of red fluorescence resulting from Ad-wt-IX-mRFP1 replication. In BNL-1NG-A.2 cells, no increase in pIX-mRFP1 red fluorescence was detected relative to baseline levels under any of the conditions tested (Fig. 5, A, left panel). By contrast, strong, dose-dependent augmentation of [F5] red fluorescence signal with time was observed in A549 cells (Fig. 5, A, middle panel). These data support the concept that the pIX-mRFP1 signal can serve as an index of virus replication. Fluorescence microscopy of BNL-1NG-A.2 and A549 cells infected with Ad-wt-IX-mRFP1 corresponded to the quantitative

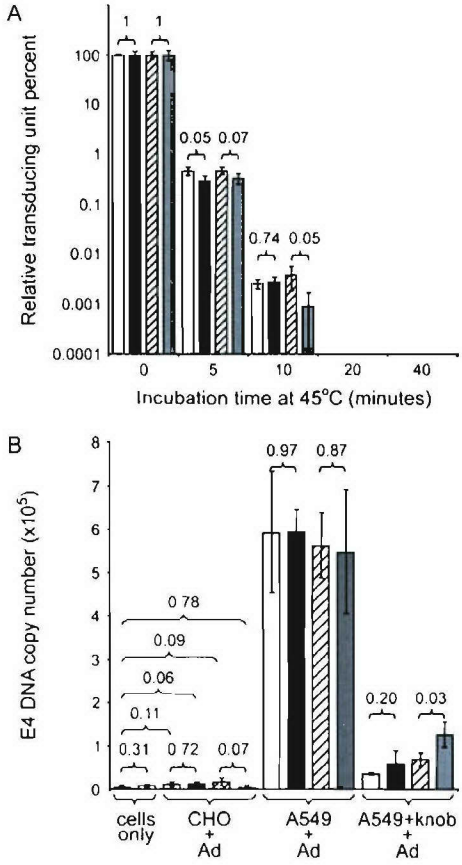

Fig. 4. Thermostability and coxsackie adenovirus receptor–dependent binding of red fluorescent adenoviruses **A)** Thermostabilities of Ad-E1-CMV-mRFP1 (**open bar**), Ad-IX-mRFP1 (**filled bar**), Ad-E1-CMV-tdimer2(12) (**hatched bar**), and Ad-IX-tdimer2(12) (**gray bar**) were determined at 45 °C for various times. Results are presented as the percentage of nontreated virus based on transducing unit titer. Three independent experiments were performed.** Error bars represent 95% confidence intervals.** *P* values (two-sided) calculated by analysis of variance are shown for comparison of the two groups indicated by the **brackets**. **B)** The coxsackie adenovirus receptor binding ability of red fluorescent adenoviruses was assessed in A549 (coxsackie adenovirus receptor positive) and Chinese hamster ovary (CHO) (coxsackie adenovirus receptor negative) cells. A549 cells were also blocked with recombinant Ad5 knob before incubation with the viruses. The **labels** below each set of bars indicate the various conditions tested. The extent of binding is represented as the number of bound genome copy number quantified by TaqMan real-time polymerase chain reaction. Three independent experiments were performed.** No virus was added to the "cells only" group. The vectors analyzed include Ad-E1-CMV-mRFP1 (**open bar**), Ad-IX-mRFP1 (**filled bar**), Ad-E1-CMV-tdimer2(12) (**hatched bar**), and Ad-IX-tdimer2(12) (**gray bar**). *P* values (two-sided) calculated by analysis of variance are shown for comparison of the two groups indicated by the **brackets**

fluorescence observations (data not shown). A red fluorescence signal was correlated with two parameters of virus replication over the 10-day infection depicted for 0.1 cytopathic effect unit/cell of Ad-wt-IX-mRFP1: viral DNA synthesis (r = .99) and transducing unit titer (r = .65). The poor correlation between fluorescence and transducing unit titer was much improved during the first 8 days, when cellular and medium conditions were suitable for active replication and progeny stability (r = .92) (Fig. 5, A, right panel).

Correlation of pIX-mRFP1 Signal With DNA Replication and Progeny Production In Vivo

The ultimate utility of our genetic capsid labeling system requires a correlation between fluorescence and viral mass in vivo** To establish such a correlation, we used a fluorescence based noninvasive optical imaging system to detect the replication of Ad-wt-IX-mRFP1 in vivo. Six** athymic nude mice with established A549 tumors in the left and right flanks were injected intratumorally with a single dose of Ad-wt-IX-mRFP1 and imaged daily for red fluorescence. After 6 days, tumors from four of the mice** were excised, imaged ex vivo, and homogenized. A portion of each tumor homogenate was used to measure viral DNA content, and the clarified supernatant of the remaining homogenate was used to quantify transducing unit titer and cytopathic effect unit titer.

An array of replication patterns in the different tumors were observed, despite the initial similarity in tumor sizes and viral treatment (Fig. 5, B). The variation in fluorescence intensity among the eight tumors allowed us to perform a correlative analysis of the underlying level of viral replication for a wide range of signals. Based on our hypothesis, we expected lower levels of adenovirus in tumors with weaker fluorescence and vice versa. The fluorescence-integrated densities (product of the mean intensity and segmented signal area) were strongly correlated with total viral genome copy number, transducing unit titer, and cytopathic effect unit titer in the tumors (Fig. 5, C, r = .93, r = .92, and r = .97, respectively). Likewise, associating the integrated densities observed in the ex vivo images with these same parameters of adenovirus detectionresulted in even stronger correlation (Fig. 6, A and B, r = .96, r = .97, and r = .97, respectively). We also conducted the same experiment with BNL-1NG-A.2 xenograft tumors (human Ad5 replication nonpermissive) as a negative control, which did not produce any red fluorescence signal (data not shown). In addition to strong correlation between fluorescence signal and viral replication, pIX-mRFP1 localization corresponded with the localization of hexon immunostaining (Fig. 7), a technique that is often used to detect adenovirus in participants of** clinical trials *(32,33)*.

Dynamic Monitoring of Red Fluorescent Ad-wt-IX-mRFP1 Replication In Vivo

We used the genetic adenovirus labeling system to dynamically monitor the replication and oncolysis of Ad-wt-IX-mRFP1 in vivo in two of the six mice with established A549 tumors on the left and right flanks for 30 days.** The images shown are for one representative mouse with a strong response to the virus over 30 days (Fig. 6). Initially, different virus behavior between the left and right tumors could be discerned, similar to that observed in the in vivo correlation experiment and other studies (data not shown). Similar to other mice, a peak in pIX-mRFP1 signal intensity was always detected several days following injection, after which the fluorescence appeared to decay over time. For example, the signal peaked at day 2 in the left tumor, whereas the same event occurred at day 4 in the right tumor (Fig. 8, A). We typically observed maximal signal between 2 and 6 days after injection (data not shown). After the signal peaked, it eventually disappeared completely (day 9 for the left tumor and day 20 for the right tumor; Fig. 8, A). Note that the occurrence of a second strong signal in the right tumor starting on day 6 appears to be

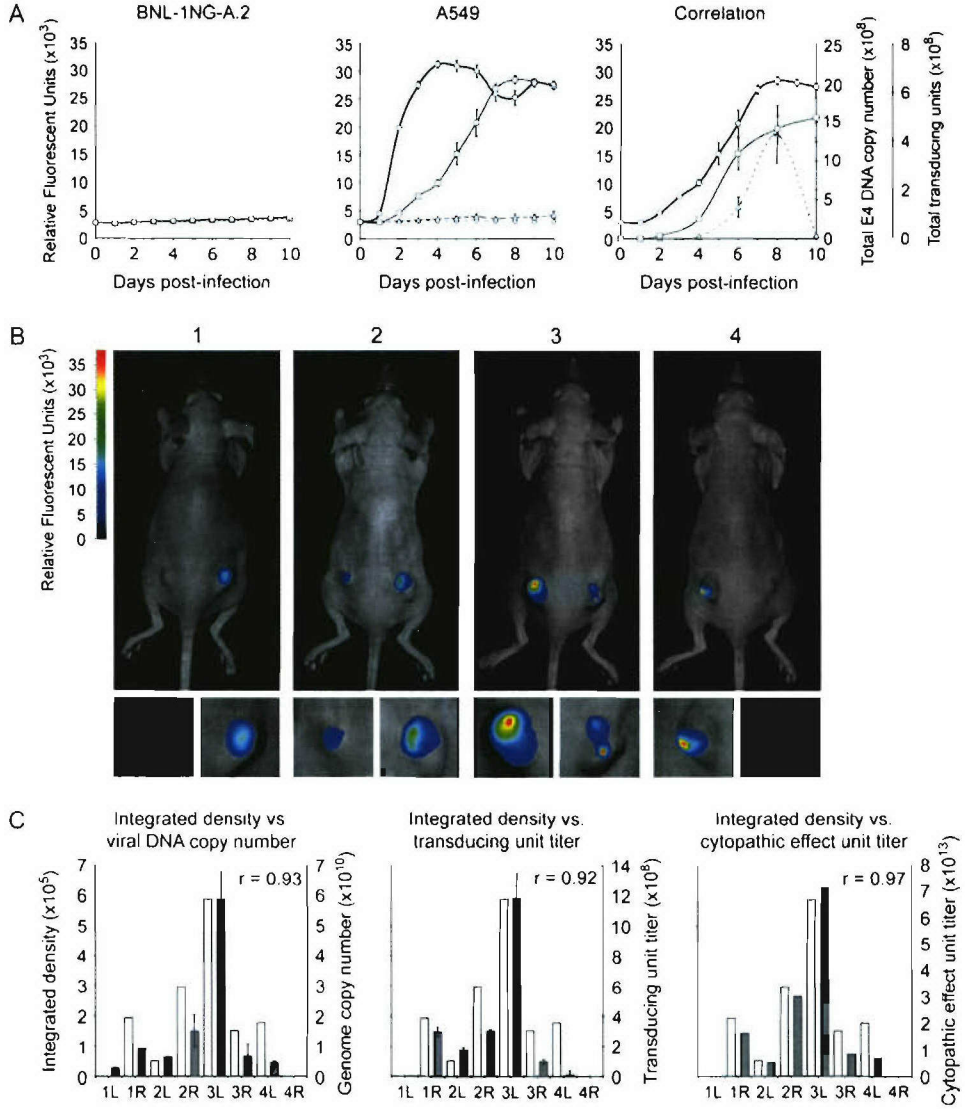

Fig. 5. In vitro and in vivo correlation of protein IX (pIX)-mRFP1 signal with replication. **A)** Ad-wt-IX-mRFP1 red fluorescent signal (relative fluorescent unit) was monitored in BNL-1NG-A.2 (replication nonpermissive) and A549 (replication permissive) cells over 10 days: 1 (**open circles**), 0.1 (**open squares**), 0.01 (**open triangles**), and 0.001 (**open diamonds**) cytopathic effect units. On days 1, 2, 4, 6, 8, and 10 after infection, samples were infected with 0.1 cytopathic effect unit/cell, and E4 viral DNA copy number (**open squares**) and transducing unit titer (**open triangles**) were determined. Also shown in the correlation panel is the red fluorescence curve of A549 cells infected with 0.1 cytopathic effect unit/cell (**open circles**). Pearson's correlation coefficient between red fluorescence and E4 viral DNA copy number, $r = .99$. Correlation coefficient between red fluorescence and transducing unit titer (days 1, 2, 4, 6, 8, and 10), $r = .65$. Correlation coefficient between red fluorescence and transducing unit titer (days 1, 2, 4, 6, and 8), $r = .92$. **Error bars** represent 95% confidence intervals." **B)** Noninvasive detection of pIX-mRFP1 signal. A549 tumors from four mice, 6 days after intratumoral injection with Ad-wt-IX-mRFP1, were imaged in vivo. Images shown are pseudocolored with the indicated index scale. Above the images are the mouse numbers. Below the whole body images are enlarged pictures of the left and right tumors of the respective mouse. **C)** Correlation of the in vivo pIX-mRFP1 signal with replication. E4 viral DNA copy number, transducing unit titer, and cytopathic effect unit titer were determined in tumor homogenates, as described in "Materials and Methods." In each graph, signal quantification from in vivo images (**open bars**: total integrated density) is displayed with the various virus detection measurements (**gray bars**: viral DNA copy number, transducing unit titer, and cytopathic effect unit infectious titer) and the correlation coefficients. The order in the charts corresponds to the tumors depicted in the in vivo images with the mouse number and left or right tumor indicated below each set of bars. The **left axis** in each chart represents the in vivo integrated density. **Error bars** represent 95% confidence intervals." [AQ42] [AQ43]

close to the injection site where granulation tissue eventually formed. Interestingly, the right tumor with the most intense pIX-mRFP1 signal regressed almost completely (day 20); however, it eventually relapsed after the pIX-mRFP1 signal abated, indicating little or no residual viral replication activity after 2 weeks to produce an ongoing antitumor effect. Quantification of the fluorescence signal intensity in the tumors of this mouse further highlights the transient behavior of Ad-wt-IX-mRFP1 replication

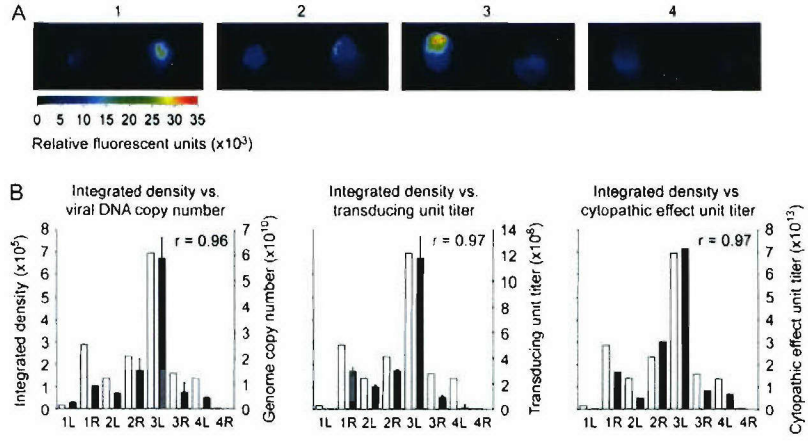

Fig. 6. Correlation of ex vivo protein IX (pIX)-mRFP1 signal with replication. **A)** Excised tumors from the same mice shown in Fig. 5, B, were imaged for red fluorescence in their respective anatomic positions. **B)** E4 viral DNA copy number, transducing unit titer, and cytopathic effect unit titer were determined in tumor homogenates. In each chart, signal quantification of ex vivo images (**open bars**: total integrated density) is displayed with the various virus detection measurements (**gray bars**: viral DNA copy number, transducing unit titer, and cytopathic effect unit titer) and the correlation coefficients. The order in the charts corresponds to the tumors depicted in the ex vivo images with the mouse number and left or right tumor indicated below each set of bars. The numbers above the ex vivo images correspond to the respective mouse shown in the in vivo correlation study (Fig. 5, B) [AQ44] **Error bars** represent 95% confidence intervals.**

in vivo (Fig. 8, B). These data show the feasibility of using this genetic capsid labeling system to dynamically monitor adenovirus replication in vivo and to capture the kinetic changes in this process.

Discussion

We have created a genetic capsid adenovirus labeling system by fusing the minor capsid protein IX with mRFP1 and tdimer2(12). The capsid fusion protein label was incorporated into virions to allow vector detection in tracking assays and in various tissues with high resolution. Modification of the pIX capsid protein with the red fluorescent proteins had a minimal effect on virus DNA replication, encapsidation, cytopathic effect, thermostability, and binding to its primary receptor coxsackie adenovirus receptor. pIX-mRFP1 signal represented the underlying level of adenovirus replication both in vitro and in vivo and correlated well with viral DNA synthesis and infectious progeny production. Furthermore, the localization of pIX-mRFP1 matched results obtained with the conventional hexon staining method used to detect the presence of adenovirus. We also successfully applied the genetic capsid labeling system to dynamically follow the kinetics of adenovirus replication in vivo.

The data we obtained in vivo demonstrate that this new imaging method to detect adenovirus replication greatly differs from conventional vector detection methods. With our method, the kinetics of viral mass and localization could be visualized in real time with a noninvasive procedure. Although our study was designed primarily to validate the basic utility of our system, we observed a number of important findings pertaining to adenovirus oncolytic function. In particular,** we found that adenovirus replication was highly variable from tumor to tumor, even [AQ33] in the same mouse. If this differential response is an inherent aspect of intratumoral injection techniques, then studies relying on methods such as tumor size measurements to gauge oncolysis function should be carefully revisited. The natural heterogeneity of tumor microarchitecture and host response to vectors can substantially impact the function of replicative vectors in vivo *(34)*. Therefore, a well-designed conditionally replicative adenovirus evaluation should embody tools that not only gauge tumor response to vectors but also simultaneously delineate vector function. Robust tumor regression should be attributed to oncolytic effect as a consequence of strong viral replication and spread. Indeed, our detection system showed that strong virus replication does lead to regression of the affected tumor (Fig. 8). Furthermore, we noted that weak replication or subsequent attenuation of replication allows the tumor to actively progress (Fig. 8). Without a noninvasive detection method, one that allows repeated monitoring of virus replication, failure or success in achieving a therapeutic effect would be difficult to determine.

What was not clearly ascertained with our adenovirus monitoring system was true spread of virus replication in the tumor, even though we attempted to use a minimal volume (10 μL) of injected virus and deliberately avoided moving the needle to distribute the virus in effect to create an initial small locus of

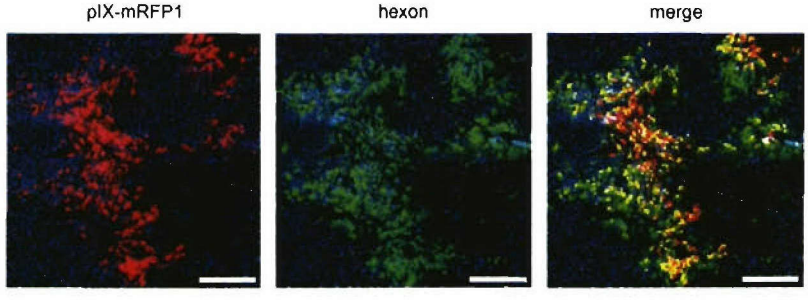

Fig. 7. Comparison of protein IX (pIX)-mRFP1 in situ localization with hexon staining. A frozen tissue section from an A549 tumor injected with Ad-wt-IX-mRFP1 (7 days after injection) was immunostained for adenovirus hexon protein, as described in "Materials and Methods." pIX-mRFP1 (**red**), hexon (**green**), and nuclear DNA (**blue**) signals were detected under fluorescence microscopy. In the overlay (**merge**), areas of **yellow** indicate overlap of red and green fluorescence. **Bar** = 100 μm

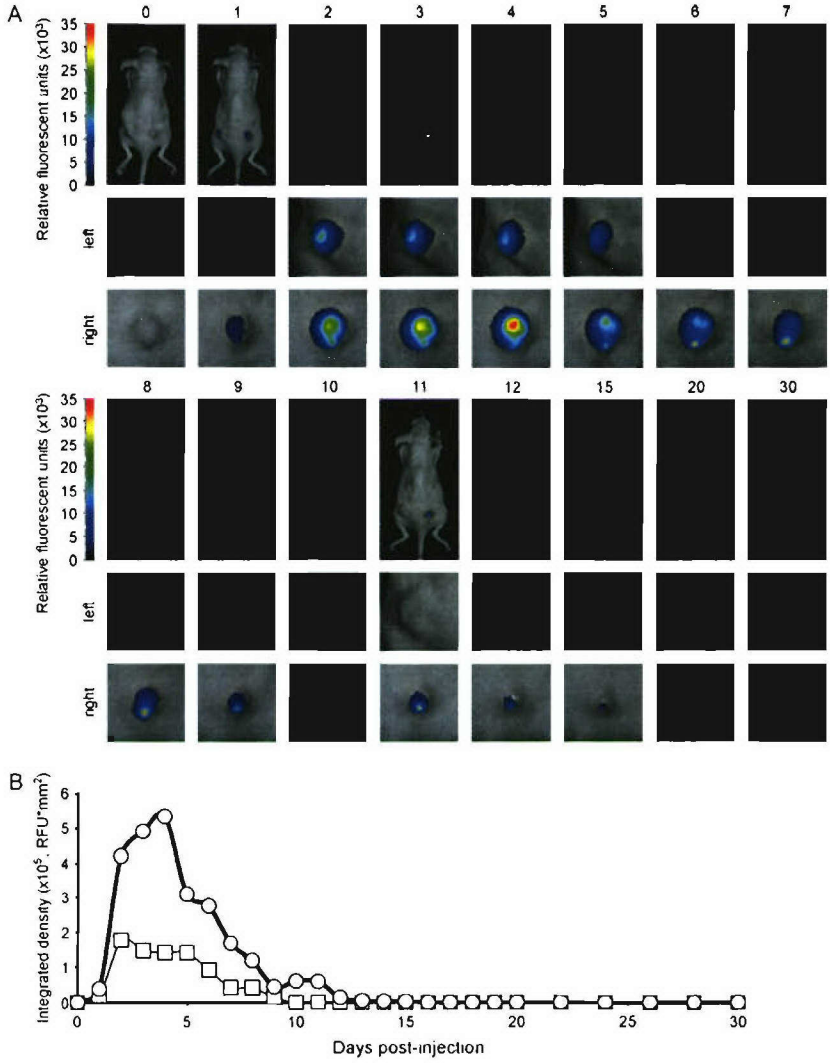

Fig. 8. Dynamic monitoring of Ad-wt-IX-mRFP1 replication in vivo. **A)** Established A549 flank tumors in nude mice (n = 2)** were injected intratumorally with Ad-wt-IX-mRFP1 (10^{10} virus particles in 10 μL). With a noninvasive fluorescence-based optical imaging system, viral replication and oncolysis were dynamically monitored in vivo over 30 days. The results are shown for one representative mouse as pseudocolored images with the indicated index scale. The number above each set of images corresponds to the day number after injection. The two images below the whole body image are enlarged pictures of the left and right tumors from each day. **B)** Time course dynamics of in vivo monitoring. Quantified Ad-wt-IX-mRFP1 signal (integrated density) from the left (**squares**) and right (**circles**) tumors of the mouse depicted in **A**. RFU = relative fluorescence units.

infection from which virus spread could be properly visualized. We have injected a similar amount and volume of virus (10^{10} virus particles, 10 μL) in mice with larger tumors (greater than 10 mm in diameter), and imaging also did not reveal the degree of spread expected from a replicative adenovirus (data not shown). A positive pIX-mRFP1 signal was not detected in the margins of the tumors, but the intense signal in the center of the tumor never spread far beyond the initial injection site. Our results are consistent with preclinical studies demonstrating the limited ability of oncolytic adenoviruses to spread intratumorally *(35)*, probably owing to confinement by surrounding necrotic and connective tissues *(36)*. The poor lateralization capability of adenovirus in tumors is also suggested by in situ viral DNA hybridization data from clinical trials that show a few focal patches of positive cells rather than gross, widespread presence of viral DNA *(12,13,15)*. For this very reason, most preclinical conditionally replicative adenovirus studies rely on much larger volumes for virus injection (50 or even 100 μL), apply multiple viral administrations, and practice intentional distribution of the virus to achieve widespread infection for an effective antitumor response**. Future studies should be devised to address this issue of virus lateralization and perhaps incorporate strategies to enhance dissemination of progeny virions. Our genetic capsid labeling system would provide the means to evaluate spreading of oncolytic adenoviruses in this respect.

The transient nature of virus replication detected in vivo in this study also raises questions regarding the persistence of adenovirus replication in subcutaneous tumors of athymic nude mice. We have routinely noticed this trend; i.e., a number of mice besides the ones used in this study showed attenuation of pIX-mRFP1 signal in a matter of weeks (data not shown). The short-lived intratumoral replication of adenovirus observed in our experiments corresponds with persistence data obtained in clinical trials. In patients, a peak in circulating viral DNA was typically detected several days after virus administration, indicative of active replication. Yet, over the course of a few weeks, a

substantial decrease to baseline followed, indicating clearance of the oncolytic agent *(14,37,38)*. Replicative adenovirus persistence in the tumor requires efficient infection of viable cells for replication as well as effective release and spread to neighboring cells for subsequent infection. Moreover, the virus has to elude the challenge mounted by the host immune system. Our adenovirus monitoring system offers the potential to study these host–vector interactions that are consequential for replicative adenovirus function. It is conceivable that in vivo clearance of the vector may have been due to immunogenicity of not only the native viral capsid proteins but also the red fluorescent protein used to label the exterior of the capsid. Further investigation is needed to determine the extent to which the exposed fluorescent label on the viral capsid contributes to the immune response directed against the vector.

Certain limitations are associated with the use of fluorescence imaging in our genetic capsid labeling system. The detection depth associated with current fluorescence-based optical imaging technology remains limited *(39)*. Additionally, the possibility of achieving tomographic data from fluorescence imaging for volumetric quantification is still under development and not widely available *(40)*. As a result, conventional fluorescence imaging is presently limited to application for superficial or accessible tumors and would not be adequate for accurate quantification of volumetric fluorescence signals. Other imaging ligands that may be more practical for deeper detection within tissue, such as luciferases *(41,42)* and herpes simplex virus thymidine kinase *(43,44)*, should be considered for genetic capsid labeling of adenovirus.

In summary, we have devised a genetic capsid labeling strategy that allows dynamic monitoring of oncolytic adenoviruses. This in vivo imaging system provides the means to study adenovirus replication, spread, persistence, and antitumor function for the purpose of addressing key issues that are fundamental to the design of replicative adenoviral agents for cancer therapy. Furthermore, capsid-labeled viruses will also have utility for vector targeting and adenovirus biology studies.

References

(1) Jemal A, Clegg LX, Ward E, Ries LA, Wu X, Jamison PM, et al. Annual report to the nation on the status of cancer, 1975–2001, with a special feature regarding survival. Cancer 2004;101:3–27.

(2) Chatelut E, Delord JP, Canal P. Toxicity patterns of cytotoxic drugs. Invest New Drugs 2003;21:141–8.

(3) Maduro JH, Pras E, Willemse PH, de Vries EG. Acute and long-term toxicity following radiotherapy alone or in combination with chemotherapy for locally advanced cervical cancer. Cancer Treat Rev 2003;29:471–88.

(4) Donnelly JG. Pharmacogenetics in cancer chemotherapy: balancing toxicity and response. Ther Drug Monit 2004;26:231–5.

(5) Krasnykh VN, Douglas JT, van Beusechem VW. Genetic targeting of adenoviral vectors. Mol Ther 2000;1(5 Pt 1):391–405.

(6) Wickham TJ. Ligand-directed targeting of genes to the site of disease. Nat Med 2003;9:135–9.

(7) Nettelbeck DM, Jerome V, Muller R. Gene therapy: designer promoters for tumour targeting. Trends Genet 2000;16:174–81.

(8) Glasgow JN, Bauerschmitz GJ, Curiel DT, Hemminki A. Transductional and transcriptional targeting of adenovirus for clinical applications. Curr Gene Ther 2004;4:1–14.

(9) Kirn D, Martuza RL, Zwiebel J. Replication-selective virotherapy for cancer: Biological principles, risk management and future directions. Nat Med 2001;7:781–7.

(10) Chiocca EA. Oncolytic viruses. Nat Rev Cancer 2002;2:938–50.

(11) Everts B, van der Poel HG. Replication-selective oncolytic viruses in the treatment of cancer. Cancer Gene Ther 2005;12:141–61.

(12) Nemunaitis J, Ganly I, Khuri F, Arseneau J, Kuhn J, McCarty T, et al. Selective replication and oncolysis in p53 mutant tumors with ONYX-015, an E1B-55kD gene-deleted adenovirus, in patients with advanced head and neck cancer: a phase II trial. Cancer Res 2000;60:6359–66.

(13) Khuri FR, Nemunaitis J, Ganly I, Arseneau J, Tannock IF, Romel L, et al. A controlled trial of intratumoral ONYX-015, a selectively-replicating adenovirus, in combination with cisplatin and 5-fluorouracil in patients with recurrent head and neck cancer. Nat Med 2000;6:879–85.

(14) Nemunaitis J, Khuri F, Ganly I, Arseneau J, Posner M, Vokes E, et al. Phase II trial of intratumoral administration of ONYX-015, a replication-selective adenovirus, in patients with refractory head and neck cancer. J Clin Oncol 2001;19:289–98.

(15) Galanis E, Okuno SH, Nascimento AG, Lewis BD, Lee RA, Oliveira AM, et al. Phase I-II trial of ONYX-015 in combination with MAP chemotherapy in patients with advanced sarcomas. Gene Ther 2005;12:437–45.

(16) Le LP, Everts M, Dmitriev IP, Davydova JG, Yamamoto M, Curiel DT. Fluorescently labeled adenovirus with pIX-EGFP for vector detection. Mol Imaging 2004;3:105–16.

(17) Fallaux FJ, Kranenburg O, Cramer SJ, Houweling A, Van Ormondt H, Hoeben RC, et al. Characterization of 911: a new helper cell line for the titration and propagation of early region 1-deleted adenoviral vectors. Hum Gene Ther 1996;7:215–22.

(18) He TC, Zhou S, da Costa LT, Yu J, Kinzler KW, Vogelstein B. A simplified system for generating recombinant adenoviruses. Proc Natl Acad Sci U S A 1998;95:2509–14.

(19) Campbell RE, Tour O, Palmer AE, Steinbach PA, Baird GS, Zacharias DA, et al. A monomeric red fluorescent protein. Proc Natl Acad Sci U S A 2002; 99:7877–82.

(20) Dmitriev IP, Kashentseva EA, Curiel DT. Engineering of adenovirus vectors containing heterologous peptide sequences in the C terminus of capsid protein IX. J Virol 2002;76:6893–9.

(21) Le LP, Dmitriev IP, Davydova JG, Yamamoto M, Curiel DT. Fluorescently labeled adenovirus with pIX-EGFP for vector detection. Mol Imaging 2004;2:105–16.** |AQ35|

(22) Alemany R, Suzuki K, Curiel DT. Blood clearance rates of adenovirus type 5 in mice. J Gen Virol 2000;81(Pt 11):2605–9.

(23) O'Carroll SJ, Hall AR, Myers CJ, Braithwaite AW, Dix BR. Quantifying adenoviral titers by spectrophotometry. Biotechniques 2000;28: 408–10, 412.

(24) Short JJ, Pereboev AV, Kawakami Y, Vasu C, Holterman MJ, Curiel DT. Adenovirus serotype 3 utilizes CD80 (B7.1) and CD86 (B7.2) as cellular attachment receptors. Virology 2004;322:349–59.

(25) Buil C. IRIS: An astronomical images processing software version 5.10. Available at: http://www.astrosurf.org/buil/us/iris/iris.htm. [Last accessed May 8, 2004.]

(26) Yamamoto M, Davydova J, Wang M, Siegal GP, Krasnykh V, Vickers SM, et al. Infectivity enhanced, cyclooxygenase-2 promoter-based conditionally replicative adenovirus for pancreatic cancer. Gastroenterology 2003;125:1203–18.

(27) Troy T, Jekic-McMullen D, Sambucetti L, Rice B. Quantitative comparison of the sensitivity of detection of fluorescent and bioluminescent reporters in animal models. Mol Imaging 2004;3:9–23.

(28) Colby WW, Shenk T. Adenovirus type 5 virions can be assembled in vivo in the absence of detectable polypeptide IX. J Virol 1981;39:977–80.

(29) Rosa-Calatrava M, Grave L, Puvion-Dutilleul F, Chatton B, Kedinger C. Functional analysis of adenovirus protein IX identifies domains involved in capsid stability, transcriptional activity, and nuclear reorganization. J Virol 2001;75:7131–41.

(30) Ghosh-Choudhury G, Haj-Ahmad Y, Graham FL. Protein IX, a minor component of the human adenovirus capsid, is essential for the packaging of full length genomes. EMBO J 1987;6:1733–9.

(31) Eggerding FA, Pierce WC. Molecular biology of adenovirus type 2 semipermissive infections. I. Viral growth and expression of viral replicative functions during restricted adenovirus infection. Virology 1986;148:97–113.

(32) DeWeese TL, van der Poel H, Li S, Mikhak B, Drew R, Goemann M, et al. A phase I trial of CV706, a replication-competent, PSA selective oncolytic adenovirus, for the treatment of locally recurrent prostate cancer following radiation therapy. Cancer Res 2001;61:7464–72.

(33) Wadler S, Yu B, Tan JY, Kaleya R, Rozenblit A, Makower D, et al. Persistent replication of the modified chimeric adenovirus ONYX-015 in both tumor

and stromal cells from a patient with gall bladder carcinoma implants. Clin Cancer Res 2003;9:33–43.

(34) Wang Y, Hallden G, Hill R, Anand A, Liu TC, Francis J, et al. E3 gene manipulations affect oncolytic adenovirus activity in immunocompetent tumor models. Nat Biotechnol 2003;21:1328–35.

(35) Ganly I, Kirn D, Eckhardt G, Rodriguez GI, Soutar DS, Otto R, et al. A phase I study of Onyx-015, an E1B attenuated adenovirus, administered intratumorally to patients with recurrent head and neck cancer. Clin Cancer Res 2000;6:798–806.

(36) Sauthoff H, Hu J, Maca C, Goldman M, Heitner S, Yee H, et al. Intratumoral spread of wild-type adenovirus is limited after local injection of human xenograft tumors: virus persists and spreads systemically at late time points. Hum Gene Ther 2003;14:425–33.

(37) Freytag SO, Khil M, Stricker H, Peabody J, Menon M, DePeralta-Venturina M, et al. Phase I study of replication-competent adenovirus-mediated double suicide gene therapy for the treatment of locally recurrent prostate cancer. Cancer Res 2002;62:4968–76.

(38) Reid T, Warren R, Kirn D. Intravascular adenoviral agents in cancer patients: Lessons from clinical trials. Cancer Gene Ther 2002;9:979–86.

(39) Weissleder R, Ntziachristos V. Shedding light onto live molecular targets. Nat Med 2003;9:123–8.

(40) Ntziachristos V, Schellenberger EA, Ripoll J, Yessayan D, Graves E, Bogdanov A Jr, et al. Visualization of antitumor treatment by means of fluorescence molecular tomography with an annexin V-Cy5.5 conjugate. Proc Natl Acad Sci U S A 2004;101:12294–9.

(41) Wu JC, Sundaresan G, Iyer M, Gambhir SS. Noninvasive optical imaging of firefly luciferase reporter gene expression in skeletal muscles of living mice. Mol Ther 2001;4:297–306.

(42) Bhaumik S, Gambhir SS. Optical imaging of *Renilla* luciferase reporter gene expression in living mice. Proc Natl Acad Sci U S A 2002;99:377–82.

(43) Tjuvajev JG, Avril N, Oku T, Sasajima T, Miyagawa T, Joshi R, et al. Imaging herpes virus thymidine kinase gene transfer and expression by positron emission tomography. Cancer Res 1998;58:4333–41.

(44) Gambhir SS, Bauer E, Black ME, Liang Q, Kokoris MS, Barrio JR, et al. A mutant herpes simplex virus type 1 thymidine kinase reporter gene shows improved sensitivity for imaging reporter gene expression with positron emission tomography. Proc Natl Acad Sci U S A 2000;97:2785–90.

Notes

We thank Dr. Roger Y. Tsien (University of California at San Diego) for providing the mRFP1 and tdimer2(12) constructs. This work was supported with grants from the National Institutes of Health (RO1CA083821, RO1CA94084, RO1DK063615-01, and 1P20CA101955), Department of Defense (W81XWH-04-1-0025, W81XWH-05-1-0035, and DAMD17-03-1-0104), and the Medical Scientist Training Program of the University of Alabama at Birmingham.

Manuscript received May 25, 2005; revised October 17, 2005; accepted December 15, 2005.

AUTHOR QUERIES

[AQ1] Au: correct?

[AQ2] Au: correct?

[AQ3] Au: Ad-wt-IX-mRFP1?

[AQ4] Au: ok?

[AQ5] Au: Please state the sources.

[AQ6] Au: provide designation

[AQ7] Au: Correct?

[AQ8] Au: provide components

[AQ9] Au: Correct? or was one performed in triplicate?

[AQ10] Au: vectors?

[AQ11] Au: Correct? or the experiments were performed in triplicate?

[AQ12] Au: or? They were each added to different groups of cells, correct?

[AQ13] Au: as meant?

[AQ14] Au: per style, please report x g instead of rpm

[AQ15] Au: Correct?

[AQ16] Au: Correct?

[AQ17] Au: for what?

[AQ18] Au: wt?

[AQ19] Au: wt?

[AQ20] Au: how long?

[AQ21] Au: wt?

[AQ22] Au: than what?

[AQ23] Au: (data not shown)?

[AQ24] Au: (data not shown)?

[AQ25] Au: (data not shown)?

[AQ26] Au: as meant?

[AQ27] Au: new para?

[AQ28] Au: edits ok?

[AQ29] Au: Correct?

[AQ30] Au: Correct?

[AQ31] Au: as meant?

[AQ32] Au: omitted sentences of methods.

[AQ33] Au: ok?

[AQ34] Au: ref?

[AQ35] Au: Please confirm correct article information per PubMed citation.

[AQ36] Au: Please add a title

[AQ37] Au: Correct?

[AQ38] Au: Correct?

[AQ39] Au: Correct?

[AQ40] Au: Correct?

[AQ41] Au: Correct?

[AQ42] Au: Correct?

[AQ43] Au: Correct?

[AQ44] Au: Correct?

[AQ45] Au: Correct?